Phototrophic Chloroflexus-like bacteria and their role in hypersaline microbial mats

Ami Bachar

12/03/2009

Phototrophic *Chloroflexus*-like bacteria and their role in hypersaline microbial mats

Dissertation

zur Erlangung des Doktorgrades

der Naturwissenschaften

- Dr. rer. nat. -

Dem Fachbereich Biologie/Chemie

der Universität Bremen vorgelegt von

Ami Bachar

Bremen

2009

Die vorliegende Arbeit wurde in der Zeit von Februar 2004 bis April 2006 am Max-Planck Institut für Marine Mikrobiologie in Bremen erstellt.

1. Gutachter: Prof. Dr. Bo Barker Jørgensen
2. Gutachter: Prof Dr. Ulrich Fischer

Weitere Prüfer:

Prof. Dr. Friederike Koenig

Dr. Henk M. Jonkers

Tag des Promotionskolloquiums: 12 / 03 / 2009

Name: Ami Bachar Ort, Datum: 20/11/2008, Israel

Anschrift: 31 Rambam St. Petach-Tiqwa (49542), Israel

ERKLÄRUNG

Hiermit erkläre ich, dass ich die Arbeit mit dem Titel:

Phototrophic *Chloroflexus*-like bacteria and their role in hypersaline microbial mats

selbstständing verfasst und geschrieben habe und auβer den angegebenen Quellen keine weiteren Hilfsmittel verwendet habe.

Ebenfalls erkläre ich hiermit eidesstattlich, dass es sich bei den von mir abgegebenen Arbeiten um 3 identische Exemplare handelt.

_____

(ünterschrift)

Table of Content

Acknowledgments:

I would like to thank Dirk de-Beer for accepting me for this PhD program in MPI-Bremen and helping with easy acclimation. Enoma Omoregie is much appreciated for his extensive scientific support, ideas and discussions as well as teaching and guiding me in the molecular sections of this work. L. Polerecky and D. de-Beer are thanked for their significant scientific donation as well as external lessons in life. This work would not have been possible without the good help of the technicians of the microsensor group and especially Gabi Eickert. I would like to thank all those who took practical part of the different projects: E. Omoregie, L. Polerecky, D. de-Beer, R. de-Wit, K. Vamvakopoulos, J. Fischer, M. Grinstein, R. Schoon and B.B. Jørgensen. Many thanks to my MPI colleagues and friends who helped me survive the cold weather of north Germany: Carsten Schwermer, Susanne Hink, Gunter Wegner, Raid Abed Armin Gieseke, Miriam Weber and others. The administration and all MPI-Bremen supporting forces are thanked. I would like to thank Galit Ofer, Adv. for the endless support and love. I thank my family and especially my mom and dad for all they gave and let me take the patience and the inspiration, respectively. Vered and Iol Zelyuk are much appreciated for escorting me during my entire study time.

Henk Jonkers is an equal partner of this work, a friend and a leader of all the science I was privileged to do in the MPI-Bremen. Thank you very much for the guidance, the freedom, the internal and external support and for making all this possible. I am forever in your debt.

Summary

Chloroflexus-like bacteria (CLB) are filamentous anoxygenic phototrophic bacteria possessing BChl*a* and sometimes BChl*c* as major photosynthetic pigments. Their ecological function in nature is still largely unknown due to their unique versatile physiology that allows both photoautotrophy, photoheterotrophy and heterotrophy under different conditions. This physiological flexibility increases the ability to compete with other bacteria, probably one reason why they are often encountered as quantitative important microbial mat community members. Most CLB characterized so far originate from hyperthermal lakes and indeed most knowledge regarding the *In situ* behavior of CLB is from thermophilic species. Nevertheless, CLB are known to populate other marine and hypersaline environments as well as other aquatic ecosystems, though knowledge about them is scarce.

In this work CLB from the natural hypersaline athalassic Lake Chiprana (NE Spain) were investigated with respect to eco-physiological properties and phylogenetic diversity to determine their ecological role in this specific environment. For the first time, aerobic respiration of hypersaline CLB community members was assessed by a novel *In situ* method, using near-infrared (NIR) light of 740 nm and oxygen microsensor techniques. These studies revealed that CLB respire oxygen when NIR light is absent but immediately switch to anoxygenic photosynthesis upon its presence. It was concluded that CLB play a major role in microbial mat community aerobic respiration in the absence of NIR light, as a switch to NIR light illumination resulted under some conditions to a 50% increase in oxygen in the mat. The effect of NIR light illumination and the role of CLB in mat community aerobic respiration was further quantified and mathematically modeled.

In addition to NIR light dependent functional properties also structural, i.e. spatial, properties of CLB in the mat were investigated in order to better understand its impact on mat community physiology. FISH studies confirmed that members of the *Roseiflexus* and *Chloroflexus* genera were confined to the upper photic zone of the mat in close proximity to

cyanobacteria at a depth of ~2-4 mm. In this specific depth zone which is fully oxygenated during the day, CLB may profit from cyanobacterial organic excretion products while facing no competition with the strict anaerobic green sulfur bacteria as occurs in deeper parts of the mat. Further 16S rRNA gene clone library and photopigment analysis revealed that members of the genera *Oscillochloris* and *Candidatus* Chlorothrix also occurred in deeper mat layers where they probably depend less on excreted photosynthates but more on the presence of free sulfide produced by sulfate-reducing bacteria.

A further 16S rRNA gene clone library study in which four hypersaline mats from three different continents were compared revealed a number of unique environmental CLB sequences (< 97% homology) in each mat suggesting a relatively high as well as endemic species diversity. As in all four mats, however, the majority of retrieved sequences were most closely related to the previously isolated species *Candidatus* Chlorothrix halophila, it was concluded that this bacteriochlorophyll *c*-producing species is pandemic and dominates the Chloroflexaceae community in hypersaline microbial mats.

The overall conclusion of these studies is that despite the fact that CLB phylogeny as well as *In-situ* physiology needs still further elucidation, these bacteria play a significant and important role community carbon cycling and should therefore be given more consideration in future microbial mat studies.

Zusammenfassung

Die *Chloroflexus*-ähnlichen Bakterien (CLB) sind faserartige, anoxygene, phototrophe Bakterien, die BCHl*a* und gelegentlich auch BChl*c* als photosynthetische Hauptpigmente beinhalten. Ihre ökologische Funktion in der Natur ist immer noch weitgehend ungeklärt. Dies liegt vor allem an der beweglichen Physiologie, die sowohl Photoautotrophie, Photoheterotrophie als auch Heterotrophie unter mehreren Bedingungen zulässt. Diese physiologische Flexibilität unterstützt ihre Fähigkeit, mit anderen Bakterien zu konkurrieren. Möglicherweise ist dies der Grund, warum sie oft als quantitativ wichtige Mitglieder mikrobischer Populationen angesehen werden. Die meisten CLB, die bisher charakterisiert wurden, besitzen ihren Ursprung in hyperthermalen Seen und tatsächlich stammt das meiste Wissen bezüglich ihres *In situ*-Verhaltens aus thermosphilischen Spezies. Obwohl das Wissen über die CLB recht spärlich ist, sind sie dafür bekannt, dass sie Meeresgegenden, hypersaline Umgebungen und andere Wasserökosysteme besiedeln.

In dieser Arbeit wurden die CLB aus dem natürlichen, hypersalinen und thalassischen See Ciprana (NE Spanien) mit dem Interessensschwerpunkt auf öko-physiologische und phylogenetische Unterschiede untersucht , um ihre ökologische Rolle in der spezifischen Umgebung zu bestimmen. Die aerobische Atmung hypersaliner CLB Mattenpopulationen wurde erstmals durch eine neue *In- situ* Methode unter Benutzung von Nah-infrarotlicht mit 740nm und O_2 Mikrosensortechniken gemessen. Die Untersuchungen ergaben, dass CLB dann Sauerstoff aufnimmt wenn kein NIR- Licht vorhanden ist, sobald es aber vorhanden ist, wechselt es sofort zur anoxygenischen Photosynthese über. Zusammenfassend ließ sich sagen, dass die CLB in Abwesenheit von NIRlicht, eine wesentliche Rolle in der aerobischen Atmung mikrobischer Mattenpopulationen spielen, wo hingegen das Anschalten des NIR-Lichtes unter einigen Umständen dazu führte, dass der Sauerstoff in der Matte um 50% angestiegen ist. Der Einfluss des NIR- Lichts und die Rolle der CLB in der aerobischen Atmung der Mattenpopulation wurde weiter gemessen und mathematisch abgebildet.

Zusätzlich zu den von NIR -Licht abhängigen Funktionseigenschaften wurden auch strukturelle, d.h. räumliche Eigenschaften von CLB innerhalb der Matte untersucht, um ihren Einfluss auf die Physiologie der Mattenpopulation besser zu verstehen. Die FISH-Untersuchungen haben bestätigt, dass Mitglieder der *Roseiflexus* und *Chloroflexus* Gattungen auf die obere photische Zone der Matte beschränkt wurden. In dieser Tiefenzone, welche während des gesamten Tages mit Sauerstoff angereichert ist, könnte das CLB von canyobakteriellen, organischen Ausscheidungsprodukten profitieren und steht dabei außer Konkurrenz mit den streng anaerobischen, grünen Sulfurbakterien, die in tieferen Teilen der Matte auftauchen. Weitere 16S rRNA Genklon Bibliothek und eine Photopigmentanalyse ergaben, dass Mitglieder der Gattungen *Oscillochloris* und *Candidatus Clorothrix* auch in tieferen Lagen der Matte auftauchen, wo sie wohl weniger von der ausgeschiedenen Photosythates abhängen, eher aber von der Gegenwart freier Sulfide, die von Sulfat reduzierenden Bakterien produziert wurden.

Eine weitere Untersuchung der 16S rRNA Genklon Bibliothek, in der vier hypersaline Matten aus drei verschiedenen Kontinenten verglichen wurden, brachte in jeder Matte eine Anzahl an einzigartigen, ökologischen CLB Sequenzen (<97%) zum Vorschein, die sowohl eine relativ hohe als auch standortheimische Speziesvielfalt vermuten lassen. Obwohl in allen vier Matten die Mehrheit der erneuerten Sequenzen am ehesten mit den zuvor isolierten *Candidatus Chlorothrix halophila* verwandt sind, ließ sich abschließend sagen, dass diese bakteriochlorophyll *c* -produzierende, Spezies pandemisch ist und die *Chloroflexaceae* Population in hypersalinen, mikrobischen Matten dominiert.

Die Schlussfolgerung dieser Untersuchungen ist, dass abgesehen von der Tatsache, dass die CLB Phylogenie und auch die *In-situ* Physiologie zwar immer noch weitere Klärung benötigen, dieses Bakterium eine bezeichnende und wichtige Rolle in der Population des Kohlenstofffluss besitzt und den mikrobischen Matten daher in künftigen Untersuchungen weitere Beachtung geschenkt werden sollte.

Prologue:

Photosynthetic microbial mats are remarkable complete self-sustaining ecosystems on a millimeter scale, yet they have substantially affected environmental processes on a planetary scale (27). This microbial warp-and-woof thread like structure is the residence of many species across a range of microniches, due to a chemical and physical gradient stratification (27). This phenomenon called microbial mat, a biogenic sediment of free living and aggregated bacteria, dissolved and non-dissolved organic matter, and mineral precipitations is, one of the steepest gradient habitat as a function of distance. Over few hundred micrometers complete shifts from aerobic to anaerobic, from light to dark and from sulfide free and supersaturation of oxygen to sulfide saturation occur – these essential characteristics shape a complex interconnected matrix of organisms.

The microbial mats, as other ecosystems, are influenced by its surrounding and have been studied extensively in terms of ecology, physiology, medical, industrial etc. With modern scientific tools scientists have increased the resolution of observations and hence have obtained a better and more detailed understanding of the structural and functional aspects of the modern mat. The combination of microsensors with molecular tools allows an even greater resolution and understanding of this complex system. In this PhD thesis my colleagues and I have applied different methods in order to elucidate the function of *Chloroflexus*-like bacteria (CLB) inhabiting a hypersaline microbial mat from Lake Chiprana (NE Spain).

CLB from the hypersaline lake Chiprana were chosen as the main objective of this work, in order to obtain a better understanding of their physiology and ecology in a hypersaline complex system. During this study we developed and used methods to characterize the functional role of environmentally important but difficult to culture bacteria.

In this introduction chapter I would like to highlight the main objective of my work - *Chloroflexus*-like bacteria – and what is known about them and their ecophysiology in mats and in culture.

Microbial mats: habitat for CLB

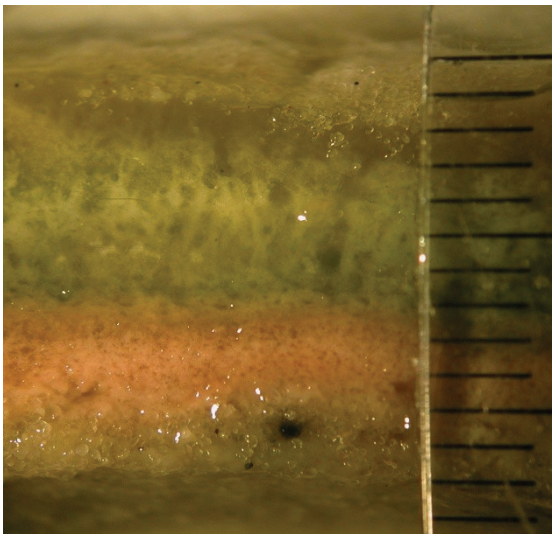

Fig. 1: Developed microbial mat with various visible layers: top bright diatom layer, below a green cyanobacterial layer. Beneath colorless mixed with green color – probably due to CLB and cyanobacteria. Below a reddish layer of purple bacteria is seen, and finally a black bottom layer. The different colors are due to different major pigment in the habituated

Cyanobacteria dominated microbial mats are conspicuous along the shallow littoral zone in "Lake Chiprana", the single enduring hypersaline natural inland lake of western Europe, located in the Ebro river basin in north-eastern Spain (29). This doctorate deals with *Chloroflexus*-like bacteria (CLB) from this lake and hence, a synopsis of cyanobacterial microbial mats is presented below. Microbial mats are highly productive (44), highly compact, and highly diverse communities (73). They are amongst most visibly conspicuous of layered communities (Fig. 1). Microbial mats can be found all over the world and typically flourish under extreme environmental conditions such as very high or low temperatures, high osmotic pressure and extreme pH (9, 14, 15, 55, 77, 87, 124).

Population distribution, of phototrophic members in phototrophic mats, is governed by light availability, diffusive flux and local production of substrates and metabolites. Light is significantly reduced by the water column and pigmented microorganisms at the surface of the mat (56, 57). It is attenuated exponentially, however, with different attenuation coefficients for different wavelengths. The pigmented microorganisms in different depth layers of the mat affect light attenuation coefficients: for instance, in a dense cyanobacterial layer the main pigment will be Chlorophyll *a*, what absorbs maximally at 440 and 667 nm, and hence those particular wavelengths attenuation coefficients will be augmented. This way, according to specific characteristic pigments of different bacterial populations, light is attenuated. For example, in a layer enriched in purple sulfur bacteria the light attenuation coefficient of 800 nm, corresponding to the maximum absorption of Bacteriochlorophyll (BChl) *a*, will rise significantly. In a CLB and/or green sulfur bacteria (Chlorobiaceae) rich layers, the attenuation coefficient of 740 nm, corresponding to BChl*c*, is increasing. This way, according to light fields measured *In-situ* with microsensors[1] one can try and typify the main microbial population inhabiting the measured spot. Visible light usually penetrates merely into the upper

[1] see chapters 3+4

millimeters, and mainly near infrared (NIR) and light of even longer wavelengths penetrate deeper into the mat. This is one of the reasons of the lamination in mats. Organisms that produce Chl*a* (green layer) use visible light for photosynthesis and are situated on top of BChl*a* (purple and green layers), which use light of longer wavelengths.

The vertical distribution of microorganisms in the microbial mat is not trivial since this is likely related to various yet unknown bacterial processes and lifestyles. While one bacterium may be considered, for example, an obligate anaerobe in culture, it may be detected *In-Situ* "unexpectedly" in an oxygen supersaturated area (54). Highly structured biogenic sediments such as microbial mats are stratified according to chemical (e.g. oxygen, sulfide and pH), physical (e.g. light, heat), biological (e.g. predation, competition) and sometimes anthropogenic (e.g. pollution, irrigation) means, resulting potentially in a wide variety of microniches on a micrometers scale. See figure 2 for a simplified schematic orientation of microbial groups that contribute to the visible lamination in mats.

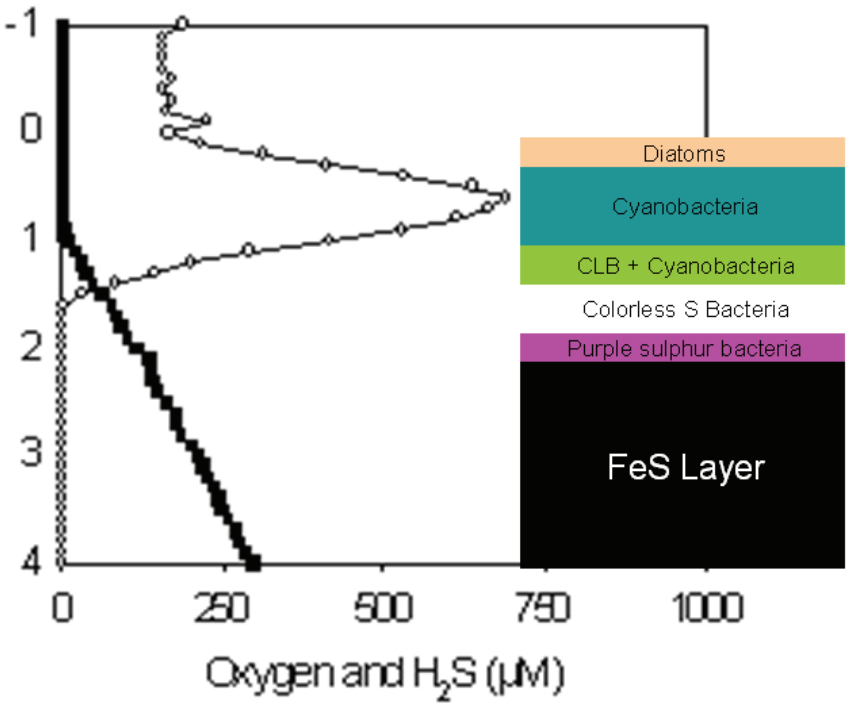

Fig. 2: Simplified scheme (not in scale) of the possible orientation of microbial mat organisms in relation to O_2 and H_2S gradients in the light as measured in Lake Chiprana. Organisms that do not contribute to the visible lamination of the mat are not considered. Black line represents H_2S (µM) and empty circles represent O_2 (µM). Numbers on the vertical axis indicate depth (mm). Microsensor measurements of this scheme are represented in chapter 2 of this thesis.

In lake Chiprana microbial mats the upper layer is frequently dominated by diatoms (eukaryotic algae), whereas *Microcoleus chthonoplastes* and other filamentous cyanobacteria as well as CLB dominate deeper layers (18). Several parameters affect the spatial distribution of these microorganisms. Diatoms for example, are sensitive to sulfide and hence are located at

the upper most part of the mat where sulfide is less abundant; the more sulfide tolerant cyanobacteria can migrate to lower depth zones where light is still available; motile CLB can migrate up and down according to light and nutrient availabilities. Although both CLB and Chlorobiaceae possess BChlc and/or d, the bulk of BChl*c/d* present in the oxygen saturated surface layer of the mat can be likely attributed to CLB rather than Chlorobiaceae, since the latter are not oxygen tolerant. Denaturing gradient gel electrophoresis analysis of "most probable number" dilution cultures[2] from distinct Chiprana mat layers, showed that various phylotypes of anoxygenic phototrophic, aerobic heterotrophic, colorless sulfur, and sulfate reducing bacteria were present (55) and microscopic observations supported the observed high biodiversity. A recent study of another hypersaline microbial mat revealed the presence of 752 different phylotypes according to 16S rRNA survey (73) – most certainly high diversity and complexity.

In Lake Chiprana several distinct mat types were observed: some dominated by a top layer of diatoms and some lacking diatoms, some 1-cm thick and some 1-mm thick, some multicolored and some monocolored – all dominated by various microbes. Mats are inhabited by aerobic and anaerobic autotrophic and heterotrophic bacteria, Archaea, and eukaryotes and all these usually show typical zonation patterns within the mat (131). At the oxic upper region of the mat one can usually find a layer of diatoms above a layer of cyanobacteria – those are the oxygenic phototrophs of the mat that produce very high (up to 5 times air concentration) oxygen levels. These oxygenic phototrophs are considered nutrient limited (18) and hence secrete organics fixed via photosynthesis (photosynthates); organics that may act as energy and/or carbon source for (photo) heterotrophic bacteria such as CLB. Heterotrophs would eventually also need nutrients for growth and in case the mat is indeed nutrient limited, heterotrophic growth will be limited as well. Thus, excreted photosynthates (with low or no N/P content) may serve heterotrophic consumers as "junk-food" (31) for respiration (energy acquisition), rather than for growth. Different species may develop different mechanisms for nutrient acquisition what may result in different nutrient affinities.

As depth increases toward the oxic-anoxic boundary layer, populations of CLB and colorless sulfur bacteria amass[3]. Organisms in the oxic zone must evidently be oxygen tolerant and can, in some cases such as CLB, use oxygen for respiration i.e. energy production. Among the oxygen tolerant organisms are the obligate and facultative aerobic heterotrophs, nitrifiers and methanotrophs. At the photic anoxic zone, where oxygen is depleted, Chlorobiaceae and purple sulfur bacteria, using light for photosynthesis while avoiding oxygen, start to thrive. The latter two populations share similar photopigment properties with CLB located among or above

[2] a technique used to estimate numbers of viable bacteria
[3] see chapter 4 for CLB spatial distribution at Lake Chiprana

them what may result in competition for light. When light is depleted further down in the mat, a black FeS-rich layer is often visible. In the anoxic zone of the mat one will be able to find fermenting bacteria, denitrifiers and methanogens. Sulfate reducing bacteria are considered to be distributed throughout the entire microbial mat as evidence of many oxygen tolerant species have been presented in mats (8, 16, 19, 54, 55, 125, 138)

Most laminated mats are constituted of oxygenic cyanobacteria and/or diatoms as main autotrophs (24, 94, 118) as well as populations of heterotrophic consumers. The proportion between number of oxygenic and anoxygenic phototrophs in the photic zone is variable and in one study, for example, was determined to be 3:2 (80). The contribution to the primary production was found to vary from ~22% (53) to 95% (67) for the two groups. Phototrophic mats, including the hypersaline cyanobacterial mats of this study, are characterized in general by intense oxygen production in the photic surface layer during the daylight hours, and by highly active sulfate reduction throughout the oxic and anoxic parts of the mat (19, 105). As the sum of aerobic and anaerobic mineralization rates are often reported to be comparable to primary production rates, the overall net biomass accretion rate in mats is low (19).

Food webs will always depend on primary producers as the base of the pyramid, providing organic carbon as carbon and energy sources for higher trophic levels. In a microbial system these boundaries get blurred since several organisms are capable of more than one type of metabolism. Examples for these are CLB, capable of exploiting different modes of energy generation (photo- and chemotrophically) and different carbon (organic and inorganic) sources.

Nutrient cycles in mats

In this thesis the anoxygenic phototrophic filamentous CLB are mainly considered. These CLB are part of the phylum Chloroflexi (20, 96) and were formerly named the green nonsulfur bacteria (93, 117). Its phototrophic members are largely placed within the Family Chloroflexaceae, which is comprised of five Genera: *Chloroflexus*, *Chloronema*, *Oscillochloris*, *Heliothrix* and *Roseiflexus.* In addition to those there are also non-phototrophic (e.g. *Herpetosiphon*) as well as non-filamentous (e.g. *Dehalococcoides*) members of the phylum Chloroflexi, as determined by 16S rRNA. CLB have been observed and reported to occur in marine and hypersaline microbial mats (26, 95, 121, 133) as well as sulfidic and nonsulfidic hot springs (7, 12, 22, 39, 86, 137). These different Chloroflexaceae species have similar metabolic characteristics and hence similar nutrient demands.

Carbon cycle and heterotrophy:

Microorganisms need C for biomass production (heterotrophs need organic C, autotrophs inorganic C) and some need organic C additionally as a source for energy generation during respiration. Versatile are the bacterial ways to acquire energy and most bacteria use organic compounds both to obtain C building blocks and for energy generation. One important ecological role of heterotrophic bacteria is mineralization of organic compounds, i.e. "returning" elements to the environment. Oxygen is a common terminal e^- acceptor, but there are others, such as SO_4^{2-}, NO_3^-. A specific type of heterotrophy is fermentation, in which an organic compound is partly oxidized and partly reduced. Usually fermenting bacteria are anaerobes, since oxygen is not required for growth and/or might be toxic for them. At Lake Chiprana carbon was found to be efficiently cycled within the mat (75) and it was estimated that 14% of the mats gross photosynthetic production and 49% of the mats net photosynthetic production diffused out of the mat in the form of low molecular mass fatty acids (55) which may be available for heterotrophic activity.

CLB are known to be flourishing at organic-rich ecosystem and their part in community C-cycling may be significant. The usage of organic compounds as C source and light as energy source was proven to support photoheterotrophic growth of cultured *Chloroflexus* and *Roseiflexus* (96) species. In Chiprana CLB and Chlorobiaceae seem not to be N/P limited (18) contrary to oxygenic phototrophs – which probably are nutrient limited, as nutrient addition did

not result in CLB related pigment concentration changes. It may be that growth of CLB is controlled by other factors then N/P availability (e.g. S availability). CLB, contrary to the nutrient limited cyanobacteria, on the other hand may balance its growth using a combination of photosynthesis, respiration and heterotrophy to maintain community growth and succession – an ability that may further increase nutrient limitation due to community growth. Why Chlorobiaceae and Chloroflexaceae are not nutrient limited like the cyanobacteria is still to be answered; it can perhaps be due to a better nutrient affinity then cyanobacteria.

Since cyanobacteria are abundant, it can therefore be assumed that organic compounds excreted by them are not limiting heterotrophs as well as CLB as carbon or energy source for heterotrophic growth in the light. Hence there is, perhaps, no competition between CLB and other heterotrophs. In other words: Due to the excretion of organic C by cyanobacteria in the form of extracellular polymeric substance, CLB are likely not carbon limited (75).

During autotrophy CLB use inorganic C for growth but then need in addition reduced inorganic sulfur compounds and/or H_2 as e^- donor for the C fixation pathways. These reduced inorganics are not abundant at supersaturating oxygen concentrations in the photic zone of mats and autotrophy or heterotrophy in CLB may thus depend on the oxygenation state of the mat (127). Sulfate reduction was demonstrated all over mats as mentioned above, thus sulfides must be produced here as well. To what extend local sulfate reduction in the oxic zone of mats supports autotrophic C fixation of CLB? This remains largely to be investigated, as at oxygen supersaturating conditions, chemical oxidation of reduced sulfur compounds may be a fast process. Under such conditions CLB may even combine photoauto- and photoheterotrophy, thus using inorganic and organic C compounds simultaneously as C source. Sulfide was detected in dimly lit photic zones of mats and hence the possibility of CLB autotrophy was suggested in the morning and evening (107). Relation between inorganic C fixation and organic C oxidation of CLB to time of day was suggested as well (127): CLB are thought to be mainly photoheterotrophic, using cyanobacterial metabolites as carbon sources, however, stable carbon isotopic composition of CLB lipids suggests photoautotrophic metabolism. It may be that CLB fix inorganic carbon only during certain times of the day. During the morning, inorganic C fixation was light dependent and it was calculated that CLB fixed inorganic C at least to the same degree as cyanobacteria.

<u>Oxygen dynamics in mats and (an) aerobic respiration:</u>

Diurnal cycle of oxygen and relationship with microbial photosynthesis in cyanobacterial sediment was described before (61). The latter reference showed that in a

cyanobacterial mat, oxygen fluctuation is a common element in mats: from daybreak to darkness, the sun provides an energetic flux that allows oxygenic and anoxygenic photosynthesis. This light energy, efficiently harvested by oxygenic phototrophs (i.e. cyanobacteria and diatoms), is partially converted to organic C compounds (via photosynthesis) that hold the energy within it. In result, $CO_2 + H_2O$ are converted to organic C + O_2. Oxygen rises in cyanobacterial mats as a function of light intensity, oxygen concentration (due to Rubisco sensitivity to the O_2/CO_2 ratio) and diffusion limitation in the mat, until a point in which light and oxygen concentration starts to inhibit photosynthesis. Therefore, oxygen concentration can be generally described as accumulating from dawn to noon (when light + accumulated O_2 cause photoinhibition) and again accumulating when light intensity and O_2 concentration are no longer inhibiting photosynthesis. As the sun goes down, oxygenic photosynthesis rate, and hence oxygen concentration, decrease as light decrease through evening until night finally falls. At night oxygen is rapidly consumed from the mat interior. The only measurable oxygen flux into the mat is the oxygen diffusing from the water column into the mat.

Using oxygen as terminal e^- acceptor for respiration is very efficient due to its low reduction potential. Concerning CLB, respiration is yet another way of energy generation (78, 97, 98) and serves as a complementary energy acquisition system when light is not available for photosynthesis. In brief, in prokaryotes the electron transport system (ETS) of photosynthesis has common components with the ETS of respiration. Due to this, ETS can be used to generate energy in the light (photosynthesis) or to generate energy during respiration, or maybe even both at the same time. In case both light and oxygen are available, it was shown that CLB favor photosynthesis over respiration (127). Potentially if pigments are synthesized at night, CLB can use these during the day, also at high O_2 levels, as demonstrated to occur in purple sulfur bacteria. It is predicted (107, 127) that oxygen respiration of CLB occurs mainly at hours of darkness - if oxygen is available. It may be also possible that CLB prefer respiration under high oxygen concentrations since oxygen inhibits photopigment synthesis and may even interrupt the photosynthetic ETS. Not much is known about this interplay of oxygen and anoxygenic photosynthesis and literature is poor regarding this subject with respect to CLB.

S-cycle:

Sulfide appears to support photoautotrophy in marine and hypersaline CLB (103). Sulfate reduction is an energetically poor process in which H_2S is produced. Some of the δ-

Proteobacteria (e.g. *Desulfotomaculum*) are known sulfate-reducing bacteria (SRB). They are usually anaerobes; some are heterotrophs, using organic C as energy source, and some autotrophs, using hydrogen as e^- donor for CO_2 reduction. In Lake Chiprana SRB have been found throughout the entire mat at the oxic and anoxic zones (55). Different types of bacteria that compete with CLB for it use produced sulfide. Among those are:

Chemolithotrophs, organisms that gain energy from oxidizing inorganic compounds. Many of them (e.g. colorless sulfur bacteria) use sulfide and hydrogen as e^- donors, both for energy generation and C fixation. They often inhabit oxic-anoxic interfaces; using sulfide and/or hydrogen (the latter may be produced by fermenting bacteria) while still having some oxygen around. Some of the chemolithotrophs are also sulfur oxidizers (e.g. *Beggiatoa*). Generally inorganic sulfur, intermediate oxidation product of sulfide, is stored and eventually further oxidized in steps to sulfate. Some can use nitrate as terminal e^- acceptor instead of oxygen to oxidize sulfide (e.g. *Beggiatoa* spp; *Thiobacillus denitrificans*).

Other sulfide competitors are the phototrophic sulfide oxidizing bacteria: Phototrophic purple (non) sulfur bacteria are anoxygenic phototrophs mainly located in the lower layer of the microbial mat. They harvest infrared light of above 800 nm due to their BChl*a* based photosynthetic reaction center (RC). As they use sulfur components as e^- donor, they may compete for it with CLB. In a microbial mat such as the one I studied, hydrogen sulfide is a limiting factor in the light in the photic zone and hence CLB may compete for it with purple bacteria. Furthermore purple (non) sulfur bacteria can use organics as C source and/or oxygen as e^- acceptor and hence may become competitors for those as well (92).

Green sulfur bacteria (Chlorobiaceae) are known to be capable of very low light intensity photoacclimation (79) and hence, in order to reduce competition, are likely to be found below the CLB in mats. Furthermore, contrary to CLB, Chlorobiaceae are obligate anaerobes and are probably not to be found at the upper photic-oxic zone due to oxygen toxicity.

The process of sulfate reduction is providing CLB of reduced sulfur – an e^- donor for the photosynthetic reaction in which CO_2 is fixed as well as for the generation of energy. If an inorganic e^- donor is not available, respiration is taking place in the process of energy production, using organics as substrate (e^- source). If an inorganic e^- donor is available under dark conditions, it may be oxidized to supply energy (i.e. chemolithotrophy). Hence, the availability of light and reduced sulfur components will reduce oxygen consumption by CLB – since photosynthesis is a preferable process over heterotrophy. Sulfate and thiosulfate are used by CLB as a source for sulfur biosynthesis (68, 70) as well as S containing amino acids.

CLB as nutrient (C/S/O) competitors

The vertical distribution of CLB in microbial mats is not well described. At chapter 4 I investigate spatial distribution of CLB. The spatial distribution is very important with respect to the availability of substrate. Since CLB are able to make energetic profit both from oxygen and sulfides, it may be preferable for them to be situated at the oxic-anoxic zone of the mat, where oxygen and H_2S co-occurs. There, competition by Chlorobiaceae is reduced since Chlorobiaceae are considered oxygen phobic. Competition by obligate aerobes over oxygen is also reduced at this boundary layer, as O_2 concentration is low. Usually the reddish layer of purple bacteria is found below the oxic-anoxic boundary layer, in which case the competition over oxygen and local H_2S production is diminished between CLB and purple bacteria. This interface of H_2S and oxygen may still be illuminated by long wavelengths that support photosynthesis. In this case, it is most favorable for CLB to be located at the oxic-anoxic boundary layer: H_2S and light are available for photosynthesis, oxygen is available for respiration but not at a high concentration (what inhibits pigment synthesis). Furthermore, the proximity to the cyanobacterial layer above contributes to a better accessibility to their excreted organics.

Phototrophic *Chloroflexus*-like bacteria

In general, the oxygenic and anoxygenic photosynthetic bacteria can be placed into five phylogenic groups: the [1]purple bacteria (sulfur and nonsulfur), the [2]heliobacteria, the [3]green sulfur bacteria (Chlorobiaceae), the [4]Chloroflexaceae (i.e. CLB) and the [5]cyanobacteria (117). The Chloroflexaceae are phylogenetically distant from any other photosynthetic group (93). The phylum that accommodates the Family Chloroflexaceae has been named the "Chloroflexi" after the genus *Chloroflexus*, the most thoroughly studied genus in this group (20).

All members of the Family Chloroflexaceae (phylum Chloroflexi) are [a] gram-negative [b] filamentous [c] gliding bacteria [d] lacking a lipopolysaccharide-containing outer membrane and [e] contain L-ornithine instead of the diaminopimelic acid in the peptidoglycan membrane. All of them also [f] possess bacteriochlorophyll (BChl) *a*. Table 1 summarizes general and specific characteristics of the different Chloroflexaceae members.

Other than by phylogeny, the five genera within the Chloroflexaceae Family can be divided to subgroups: the genera *Chloroflexus*, *Oscillochloris* and *Chloronema* are chlorosome-bearing organisms. Chlorosomes are the light-harvesting organelles and are also found in the Chlorobiaceae (green sulfur bacteria). These photosynthetic complexes contain at least a few thousand BChl*a/c* and/or *d* molecules (34). The so far described species that belong to the genera *Heliothrix* and *Roseiflexus* of the Chloroflexaceae are chlorosome-less.

Table 1: Characteristics of members of the Family Chloroflexaceae

Genus	*Chloroflexus*		*Oscillochloris*		*Chloronema*		*Heliothrix*	*Roseiflexus*
Species	*aurantiacus*	*aggregans*	*trichoides*	*chrysea*	*giganteum*	*spiroditum*	*oregonensis*	*castenholzii*
Cell diameter (um)	0.7-1.2	1-1.5	1-1.5	4.5-5.5	2-2.5	1.5-2	1.5	0.8-1
Gas vesicles	-	-	+	+	+	+	-	-
Optimal temp. (°C)	55	55	29	15	10	10	48	50
Chlorosomes	+	+	+	+	+	+	-	-
Bacteriochlorophylls	a + c		a + c		a + c + d		a	a
Absorption max. *In-vivo (nm)*	740, 808, 868	740, 808, 869	748, 852	?	720	?	795, 865	801, 878
Carotenoids	β + γ		β + γ	not detected			γ-like	
O_2 respiration	+	+	-	?	-	?	?	+
Photoautotrophy	+	-	+	?	+	?	?	-
Photoheterotrophy	+	+	+	?	?	?	+	+
Gram-staining	-	-	+	+	?	?	?	-
Comments					sheath	spiral	granules	no granules
Position in mat	below cyanobacteria		?	?	planktonic		above cyanos	below cyanos
Sulfide environment	low & high conc.		high conc.		low conc.		low conc.	high conc.
Found at	hot springs		freshwater mats		freshwater		hot springs	
Color	greenish		yellowish		green		reddish	red-brown

- Data taken from the review of "The family of Chloroflexaceae" (Hanada and Pierson 2002) at the on-line version of "The prokaryotes"
- Reference: C. *aurantiacus*: (45, 97, 98), C. *aggregans*: (46), Oscillochloris: (43, 62-64), Chloronema: (30, 42), Heliothrix: (100, 101), Roseiflexus: (47, 123)

Photoheterotrophy is apparently a common feature of all CLB, although still unproven for *Chloronema*. It is still unclear whether all genera in the Family Chloroflexaceae are capable of respiration with oxygen. Two species (O. trichoides and C. giganteum) are considered not to be able to respire with oxygen.

Bacteriochlorophylls (*a-e, g*) are bacterial photosynthetic pigments different from each other in their chemical composition and hence light absorption characteristics (Table 2). BChl*c/d* are chlorins[4]; the other BChl's (*a, b, e, g*) are bacteriochlorins, with two reduced pyrrole rings. It can generally be said that purple bacteria possess BChl*a/b* as main photosynthetic pigments, Chlorobiaceae and CLB possess BChl*c/d* but also *a* as main photosynthetic pigments while Heliobacteria possess BChl*g* as its main photosynthetic pigment. In the context of pigmentation, the presence of BChl*e* is perhaps one distinguished characteristic of Chlorobiaceae from CLB, since only the latter are considered lacking BChl*e*.

Table 2: Major absorption maxima of (bacterio) chlorins in whole cells and in the dissolved state, and fluorescence maxima of whole cells of phototrophic prokaryotes (91)

Absorption spectra of chlorins (nm)

Pigment	Whole cell	Acetone extraction	Fluorescence maxima (cell)
BChl*a*	375, 590, 805, 830-911	358, 579, 771	907-915
BChl*b*	400, 605, 835-850, 986-1035	368, 407, 582, 795	1040
BChl*c*	457-460, 745-755	433, 663	775
BChl*d*	450, 715-745	425, 654	763
BChl*e*	460-462, 710-725	459, 648	738
BChl*g*	375, 419, 575, 788	365, 405, 566, 762	Not detected
Chl*a*	670-675	435, 663	680-685
Chl*b*	Not detected	455, 645	(In acetone - 652)
Chl*d*	714-718	400, 697	(In acetone - 745)

Heliothrix and *Roseiflexus* are chlorosome-less and contain BChl*a* and γ carotenes as photosynthetic pigment. Due to their photosynthetic pigments, while *Heliothrix* and *Roseiflexus* are cherry in color, the rest of the family is olive colored. Chlorosome-containing CLB has as well γ carotene but also β, which are both presented in chlorosomes and

[4] heterocyclic aromatic ring consisting, at the core, of 3 pyrroles and one reduced pyrrole coupled through 4 methine linkages

cytoplasmic membrane[5]. *Oscillochloris* and *Chloronema*, contrary to the rest of the Chloroflexaceae Family, contain gas vesicles, though only *Chloronema* is known to be planktonic.

In the presence of oxygen, thermophilic mat-inhabiting CLB exhibit a carroty-color whereas they are olive-colored under anoxic conditions (23). The carroty-color is the result of the enhanced carotenoid biosynthesis under oxic conditions.

Cell structure (presence of chlorosomes) and photosynthetic pigments (BChl*c/d*) of certain members of the CLB resemble Chlorobiaceae (109), but their metabolism is similar to that of the purple nonsulfur bacteria. There are strong structural and functional similarities between *C. aurantiacus* and purple bacteria: Their photochemical reaction center is very similar (11, 102, 112); the intermediate e^- acceptor in both is bacteriopheophytin *a* (11, 65); the arrangement of the chromophores appears to be similar (132), as well as the two subunits of the reaction center (89, 90, 113). The BChl*a* antenna of the two groups is also similar, but *C. aurantiacus* has in addition also chlorosomes (thus lacking in purple bacteria) that funnels light to the reaction center. The reaction center (RC) – a protein that is the site of the light reactions of photosynthesis - has BChl*a* and is composed of two subunits (smallest RC known).

Known *Chloroflexus*-like bacteria species

A description of the five established and recently proposed sixth respective CLB genera from the Family Chloroflexaceae follows

***Chloroflexus*:** the two isolated species of this genus (C. *aurantiacus* and C. *aggregans*) are thermophiles, i.e. capable of growth from 30-72 ^{o}C (99). *Chloroflexus* species are generally found in mats below a thin top layer of cyanobacteria, which presumably provide organic C, what can be used as carbon and/or energy source, and oxygen, what can be used as electron acceptor during aerobic respiration in the dark (6, 14, 127). C. *aurantiacus* can grow heterotrophically by aerobic respiration, photoheterotrophically (using light as energy source to incorporate organic compounds), and photoautotrophically - using light to fix inorganic C (96). It appears that some of the organic substrates are fermentation products (acetate, propionate, butyrate, lactate, and ethanol) produced, for example, by cyanobacteria (4). The main photopigment BChl*c* of *C. aurantiacus* absorbs *In-vivo* at 740 nm, and BChl*a,* produced in

[5] Carotenoids are helping pigments for the photosynthetic apparatus. There are over 600 known compounds of this family and can be apportioned to 5 subgroups (α, β, γ, δ and ε) according to their compound formulation

lower amounts, absorbs at 802 and 865 nm. Both pigments are contained in chlorosomes that line the cytoplasmic membrane (109). The two *Chloroflexus* species are narrow (<1.2 μm) olive/carroty filaments with gliding motility and undefined length. Although two *Chloroflexus* species isolated from mats are in pure culture, other presumable *Chloroflexus* species have been observed in microbial mats. Occasionally, layers of *Chloroflexus* species are reported to be positioned above the cyanobacterial layers (observed in the hypersaline lake Chiprana and at sulfide rich hot spring ponds) (55, 60) in contrast to what was observed in hot spring mats where the isolated species originated from, in which *Chloroflexus* were positioned underneath the cyanobacterial layers. *Chloroflexus* species may position themselves according to oxygen tolerance and/or photopigment composition (light quality and quantity), but whether or not the exact position of CLB – above or below cyanobacteria – is crucially affecting its physiology is yet unknown. As *Chloroflexus* species are motile organisms, they can presumably choose their preferred position according to environmental conditions (e.g. light and e^- donors).

Filamentous chlorosome-containing *Chloroflexus*-like species, with BChl*a/c/d*, from marine and hypersaline environments have been observed as well (26, 40, 55, 76, 95, 103, 120, 133), but none were isolated in pure culture. It is uncertain whether these are truly *Chloroflexus* species (or even part of the Chloroflexi Phylum) and not other chlorosome-containing genera until isolates will be characterized based on phylogeny. The absorption spectra *In-vivo* of these uncultured presumably *Chloroflexus* species is around 755 nm (due to BChl*c/d*) and they are assumed to be able to respire with oxygen (103). These are usually olive-colored and may be as slim as 0.5 μm but also, sometimes, wider then 2μm. The mesophilic uncultured assume-to-be-*Chloroflexus* species are usually in sheaths (103).

Chloronema: Within this genus there are two known species: C. *giganteum* and C. *spiroideum*. They are obligate anaerobic phototrophs, and found to be the dominant planktonic CLB (30) from some fresh waters lakes characterized by high ferrous iron content and various sulfide concentrations (40). They were found below the aerobic precinct of the lakes photic zone, amid purple and Chloroflexi bacteria. *Chloronema* species are about 1.5-2.5 μm wide and possess gas vesicles for buoyancy and chlorosomes containing BChl*a/d* (30) and some strains also have *c* (36) with γ carotene as main carotenoid. The *In-vivo* absorption spectrum is 720 nm due to BChl*d* - the most important pigment in Chloronema species. At Lake Chiprana, sulfide concentration of the lower anoxic water column may go up to 7 mM and an inspection of this lake did not yield any planktonic CLB, but rather Chlorobiaceae (135).

Oscillochloris: Within this genus there are two known species: O. *trichoides* and O. *chrysea.* Species of this genus have been observed in freshwater microbial mats characterized by high sulfide and/or dissolved organic carbon concentrations, in which they seem to be associated with various bacteria and algae species (41). These are wide (1- 5 μm), rapidly gliding, blonde/olive, *Oscillatoria*-like filaments containing gas vesicles and chlorosomes (43). The *In-vivo* absorption spectra are at 748 and 852 nm due to BChl*c* and *a* respectively. Although the two known species of this genus where found in freshwater systems, one cannot utterly rule out the possibility of finding a hypersaline adapted species from the *Oscillochloris* genus in mat types such as the ones from Lake Chiprana.

Heliothrix oregonensis is the only known species of the genus *Heliothrix*. It is a chlorosome-less CLB containing BChl*a* (sole photosynthetic pigment) from alkaline, sulfide depleted hot springs (101), though one clone library study from soil environment also yielded *Heliothrix* related sequences (51). In one study it was found above a cyanobacterial stratum in the fully oxic zone of the upper mat, where light intensities are high (21). It is aerotolerant and photoheterotrophic (101). Filaments are narrow and short (1.5 and 10 μm respectively). Contrary to *Roseiflexus* [see below], *Heliothrix* contains large amounts of polyhydroxybutyrate granules (101) and has *In-vivo* absorption maxima at 795 and 865 nm due to BChl*a*. Carotene properties are similar to those of *Roseiflexus*. It is hard to predict whether or not one will encounter this organism or closely related species in a hypersaline microbial mat such as those from Lake Chiprana.

Roseiflexus *castenholzii* is the only known species of the genus *Roseiflexus*. It is another chlorosome-less CLB containing BChl*a* (sole photosynthetic pigment) from hot springs (47). The carotenoids were derivatives of keto-γ-carotene but also non-oxidized carotenoids (123) and it lacks of β-carotene, typical for chlorosome bearing CLB. Recently it was shown that the RC complex appeared to enclose three molecules of BChl's and three molecules of bacteriopheophytin, as in the RC preparation from C. *aurantiacus* (139). Although *Roseiflexus* is phylogenetically related to *C. aurantiacus*, the arrangement of its *puf* genes, which code for the light-harvesting proteins and the RC subunits, was dissimilar to that of C. *aurantiacus* and similar to that in purple bacteria (139). It is phylogenetically different from *Heliothrix* and *Roseiflexus* and was in contrast to *Heliothrix* found below the cyanobacterial stratum in the mat. By light microscopy it is difficult to distinguish between these two species, the only apparent difference is the potential of *Heliothrix* to produce polyhydroxybutyrate granules (47, 101). Data on stable isotopic composition indicate that

Roseiflexus can grow photoautotrophically (47). *Roseiflexus* is narrower then *Heliothrix* (< 1 μm) and the *In-vivo* absorption maxima are at 801 and 878 nm due to BChl*a* - slightly different than the *In-vivo* BChl*a* absorption maxima of *Heliothrix*. Differences between BChl*a* *In-vivo* spectra varieties of the two genera are small and can be due to small structural differences such as the presence or absence of methyl-groups. CLB containing BChl*a* where observed in hypersaline microbial mats (25) and might be related to *Roseiflexus*. In Chapter 4 the application of previously designed fluorescent *In-situ* hybridization (FISH) probes specific for *Roseiflexus* will be described. The positive signals obtained from it indicate that *Roseiflexus*-like species represent part of the CLB community in Lake Chiprana microbial mats.

Candidatus Chlorothrix halophila [6] is suggested as a hypersaline genus of the Chloroflexaceae Family (66), although not yet in pure culture. It is a green, chlorosome-containing filament of 2-2.5μm in diameter and undefined length with no gas vesicles. It has an *In-vivo* absorption maxima of 753 and 800-900nm due to BChl*c* and *a* – respectively. This gram variable bacterium showed tolerance to high concentration of sulfides (up to 100μm) and its optimal temperature for growth was determined between 35 to 38 ^{o}C. As a hypersaline bacterium, *C. halophila* may grow at 50-120 ppt at which photoautotrophy is detected when sulfides are present. As appose to *Chloroflexus* sp., *C. halophila* does not possess the appropriate enzymes for the 3-hydroxy propionate pathway. The phylogenetic relationship of C. *halophila* to the rest of the CLB indicates distance consistent with that separating other genera within this group from each other (ca. 85%).

CLB in hypersaline mats: Other studies on hypersaline environments (70-140 ppt) report observations of olive CLB species as well, occasionally associated with other bacteria (e.g. *Beggiatoa*, cyanobacteria, purple sulfur bacteria) (26, 72, 73, 76, 116, 119, 133). These associations are considered mutually beneficial. CLB-cyanobacteria association is an example for a mutual benefit: while CLB may use organic excretions of cyanobacteria, the cyanobacteria may benefit from CLB as sulfide oxidizing bacteria since sulfides are inhibitory for most cyanobacteria. CLB may also benefit from being located near sulfate-reducing bacteria: while the latter may provide CLB e- donors for photosynthesis (e.g. sulfides), CLB on the other hand may reduce the oxygen pressure that is toxic for some sulfate-reducing bacteria. In one study, members of the Chloroflexi phylum formed most of the rRNA of clones in a gene library. This study challenges the general belief that cyanobacteria dominate phototrophic

[6] Genus not represented in table 1 since no axenic culture was yet achieved.

microbial mats (73); however, as cyanobacteria have less easily extractable rRNA per biomass, results may have been biased.

CLB identification by light/fluorescence microscopy: The filamentous CLB lack, unlike cyanobacteria, Chl*a* and phycobiliproteins and hence will not fluoresce in the visible red light spectrum under blue (450-495 nm) excitation light while emitted light is incised with a filter for wavelengths below 520 nm. The filamentous *Beggiatoa* for example could be easily distinguished from CLB by the presence of elemental sulfur inclusions. Several filamentous sulfate-reducing bacteria (SRB) species (e.g. *Desulfonema*) known to occur in hypersaline mats are usually colorless and not fluorescent, contrary to CLB which usually have a green-yellow-red color and exhibit fluorescence in the near infrared region (35), what can potentially be visualized using a near infrared light-sensitive camera system connected to the microscope.

Photosynthesis and carbon metabolism in CLB

All known oxygenic photosynthetic bacteria are cyanobacteria, while anoxygenic photosynthetic bacteria belong to the purple (non) sulfur bacteria, green sulfur bacteria (Chlorobiaceae), Chloroflexaceae (e.g. CLB) or the heliobacteria. All photosynthetic organisms contain their photosynthetic RC bound within the membrane, which may be invaginations of the cytoplasmic membrane (purple bacteria), thylakoid membranes (cyanobacteria), specialized antenna structures called chlorosomes (Chlorobiaceae and Chloroflexaceae) or the cytoplasmic membrane itself (heliobacteria). Some contain more specialized light-harvesting structures e.g. phycobilisomes in cyanobacteria allowing increased light utilization efficiency.

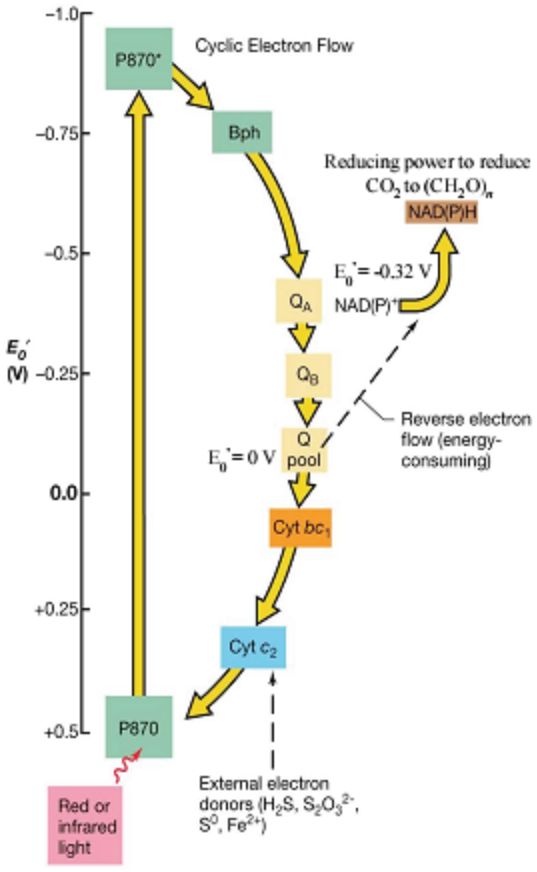

Fig 3: Cyclic electron flow (photophosphorylation) and reversed electron flow in the photosystem of purple bacteria and CLB, needed for ATP and NAD[P]H generation respectively. Taken from "The biology of microorganisms" (Madigan and Martinko, 2005).

Anoxygenic photosynthesis is very different from oxygenic photosynthesis: anoxygenic phototrophs, contrary to cyanobacteria, have only one photosystem. Anoxygenic phototrophs use their sole photosystem for both ATP (energy) and NAD[P]H (reducing equivalents needed to reduce CO_2 during autotrophic growth) production. ATP is produced by a process known as 'cyclic electron flow' (Fig 3) while NAD[P]H production can be directly light driven (green sulfur bacteria, Heliobacteria), or indirectly by the ATP consuming process known as 'reverse electron flow' (purple bacteria, CLB).

ATP (energy) production in CLB:

In the cyclic electron flow (cyclic photophosphorylation) in the photosystem of CLB and purple (non)sulfur bacteria an e^- is exited with light and is transported through a sequence of e^- carriers. ATP synthesis during photosynthetic e^- flow occurs as a result of the formation of a proton motive force (ΔP), generated by proton extrusion during e^- transport and the activity of ATPase in coupling the dissipation of ΔP to ATP formation. Cyclic photophosphorylation resembles respiration in that e^- flow through the membrane establishes ΔP, the former however, does not consume electrons, as they travel a closed route (Fig. 3). The e^- donor for the e^- flow must also be highly reduced, usually H_2S or H_2. The e^- is transferred enzymatically from the substrate to the cytochrome. For autotrophic growth reducing power NAD[P]H is also needed, so that CO_2 can be reduced to the level of cell material. For this, electrons from the quinone pool are used. However, as the electro-potential of the quinone is insufficiently negative to reduce $NAD[P]^+$ directly, electrons must be forced against the thermodynamic gradient (backwards) to reduce $NAD[P]^+$ to NAD[P]H. This energy requiring process is called 'reversed electron flow' and is driven by the energy generated by ΔP.

An e^- in a "special pair" of BChl molecules, P870, is promoted to an excited state, and is then transferred to a bacteriopheophytin – a metal-free BChl (10); a menaquinone[7] and a putative cytochrome bc_1 complex[8]. All these steps take place within the cytoplasmic membrane. In the concluding step, the e^- is returned from the membrane-bound cytochrome via the periplasm to the RC through a blue copper protein (Auracyanin; not shown in Fig 3). Auracyanin, one of the e^- chain components, is an analogues protein of plastocyanin and azurin present in cyanobacteria and proteobacteria respectively (5). The primary e^- acceptor is cytochrome C_{554} (33) but there are other b and c type cytochromes.

[7] Membrane-diffusible e^- carrier - quinone, also shared for respiration process
[8] Similar to the cytochrome bf complex of oxygenic photosynthesis

In oxygenic photosynthesis, two photosystems (II+I) are used to generate ATP and NAD[P]H: after water is split in PSII (P680), the e^- is transferred to PSI (P700).

The two different RC (II and I) can generate ΔP by both noncyclical e^- flow from PSII to I, and cyclic e^- flow from ferredoxin of PSI to the cytochrome and back again (Fig 4). Reducing power, NAD[P]H is produced in PSI when electrons from ferredoxin are transferred via flavoproteins to $NAD(P)^+$.

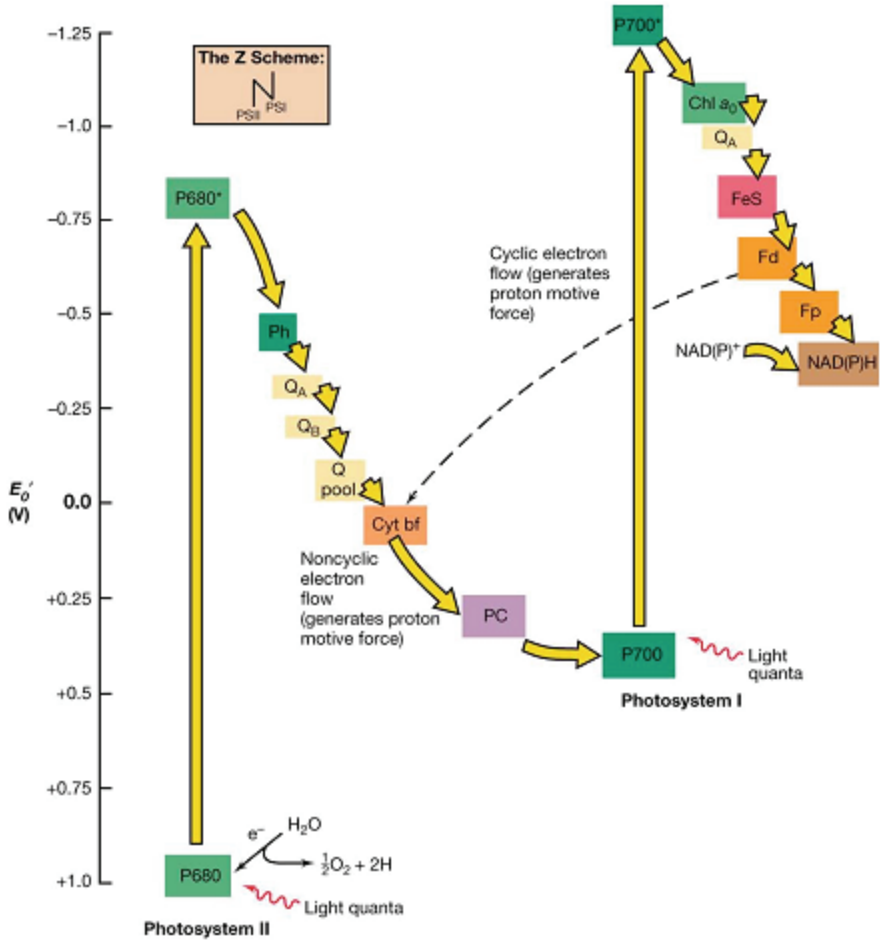

Fig 4: The "Z-scheme". Showing the reduction potentials and e^- flow during oxygenic photosynthesis. Light energy drives e^- flow uphill by the special-pair pigments, P680 and P700,. Ph = pheophytin a, e^- acceptor of P680; $Q_{A/B}$ = plastoquinone tightly bound to PSII; Chl a_o = chlorophyll a, the primary e^- acceptor of PSI; Q_A = phylloquinone; FeS and Fp are iron sulfur clusters; and Fd = a ferredoxin. $NAD[P]^+$ is reduced by a hydride ion donated by the $FADH_2$ prosthetic group of ferredoxin-$NAD[P]^+$ oxidoreductase. Two photons of light must be absorbed for an e^- to follow the entire Z-scheme. Adapted from "The biology of microorganisms" (Madigan and Martinko, 2005).

Photosynthesis can thus be divided into two different types of reactions: The light reaction[1], in which light energy is trapped and converted into reducing equivalents and ATP, and the so-called dark reaction[2] of biosynthetic organic carbon production.

[1]*Light reaction*: $2\ H_2X + 2\ R_{ox} + light \rightarrow 2X + 2\ R_{red}\cdot H^+ + \Delta P$

$ADP + P_i + \Delta P \rightarrow ATP + H_2O$

Where R is a reduced/oxidized component (e.g. plastoquinone) and ΔP is the proton motive force.

[2]*Dark reaction*: $CO_2 + ATP + 2\ R_{red}\cdot H^+ + H_2O \rightarrow <CH_2O> + ADP + P_i + 2\ R_{ox}$

SUM: $CO_2 + 2\ H_2X \rightarrow CH_2O + H_2O + 2X$

After NAD[P]H is formed, C fixation in *C. aurantiacus* proceeds by carboxylation of acetyl-CoA and via hydroxypropionyl-CoA as an intermediate and yields glyoxylate as the end product [hydroxypropionate cycle; (32, 48, 122) Fig. 5]. Glyoxylate is further assimilated into cell material with tartronate semialdehyde and 3-phosphoglycerate as intermediates (81).

Autotrophic carbon metabolism in CLB:

Autotrophic CO_2 fixation in eukaryotes is represented solely by the Calvin cycle, though in prokaryotes there are several pathways of autotrophic CO_2 fixation: [1]the Calvin cycle; [2]the reverse tricarboxylic acid cycle; [3]acetogenesis; and [4]the hydroxypropionate pathway (Fig. 5) of which the latter is used by *C. aurantiacus.*

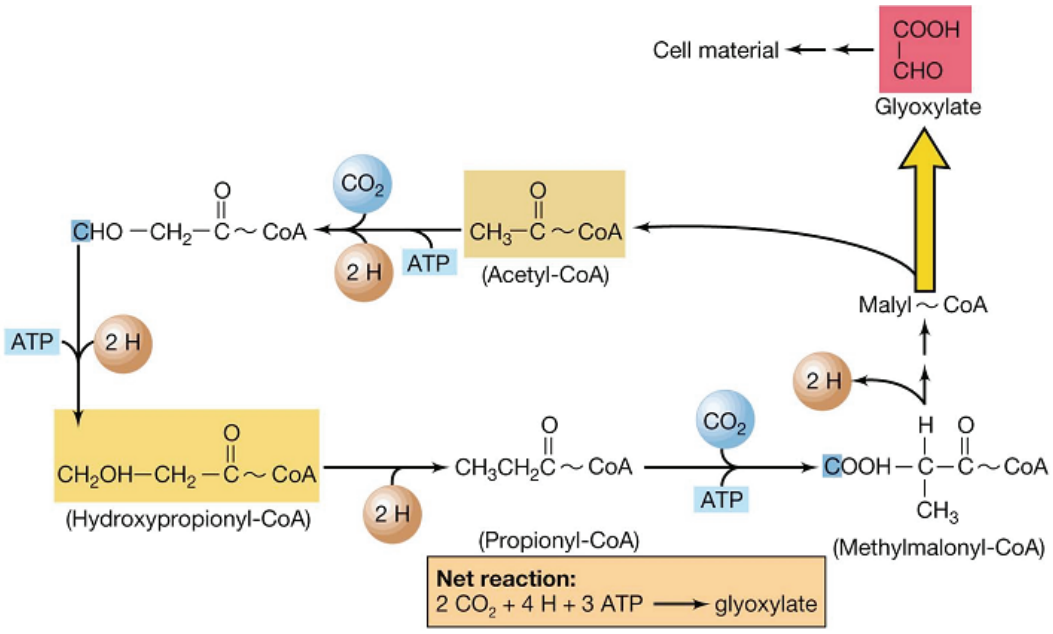

Fig. 5: The 3-hydroxypropionate-carbon fixation pathway: acetyl-CoA is carboxylated and reductively converted via 3-hydroxypropionate to propionyl-CoA. Propionyl-CoA is carboxylated and converted via succinyle-CoA and CoA transfer to malyl-CoA. Malyl-CoA is cleaved to acetyl-CoA and glyoxylate. In so doing, the first CO_2 acceptor molecule acetyl-CoA is regenerated, completing the cycle and the net CO_2 fixation product glyoxylate is released. This cycle represents the 4th autotrophic pathway in nature and is designated the 3-hydroxypropionate cycle. Taken from "The biology of microorganisms" (Madigan and Martinko, 2005).

In 1986 it was discovered that C. *aurantiacus* had a previously undescribed pathway for CO_2 fixation (50): instead of the Calvin cycle or the reductive tricarboxylic acid cycle, one strain of C. *aurantiacus* grown with H_2 as e^- donor, showed that acetyl-CoA was an important intermediate (49). It was carboxylated to pyruvate, reduced and phosphorylated to triose phosphate. This novel C fixation pathway is named after the 3-hydroxypropionate intermediate used for regeneration of acetyl-CoA (48). Each twirl of the cycle results in the net fixation of two CO_2 molecules, forming one molecule of glyoxylate: acetyl-CoA (2C) integrates 1 CO_2 molecule to form malonyl-CoA (3C); with the donation of 2[H] molecules an aldehyde is formed (3C); further investment of 2[H] will form the 3-hydroxypropionate intermediate (3C), and eventually with addition of 2[H] a propionyl-CoA (3C) is formed. Another CO_2 molecule is subsequently added and succinyl-CoA (4C) is formed. Now, after $2CO_2$ molecules integrated, a series of enzymatic processes will modify the 4C molecule and eventually cut it to glyoxalate (2C) and acetyl-CoA (2C). The product (glyoxalate, $C_2H_2O_3$) is an organic building block available for cellular components and is this way formed. This proposed pathway also seems to operate in the branch of archaebacteria comprising autotrophic *Acidianus, Sulfolobus,* and *Metallosphaera* species (17, 52, 81, 85).

Other than autotrophic photosynthesis, growth in CLB (not known for *Chloronema* sp.) can be supported by numerous organic substrates, which can act as carbon source during photo-heterotrophy. In fact C. *aurantiacus* grows preferably by photo-heterotrophy (99) and cyanobacteria are assumed to provide the required organic substrates (115). Moreover, also energy generation in the dark can be supported by aerobic respiration on many organics but also inorganic substrates (78) as well as by fermentation of sugars (69). The two different C acquisition methods (i.e. organic and inorganic) yield different isotopic fractionations due to enzymatic selectivity towards the lighter isotope in inorganic carbon fixation. This, for example, results in an isotopic fractionation ratio of -29 ‰ in most oxygenic phototrophs (RuBisCo-mediated), while in anoxygenic phototrophs a ratio of -11‰ (84) was found. Stable C isotopic composition of typical *C. aurantiacus* lipids (111, 127, 130) suggests that it is autotrophic in sulfidic mats according to its high $^{12/13}C$ ratio: -13 ‰ (128, 129), comparable with inorganic C fixation via the 3-hydroxypropionate pathway (50, 130).

For autotrophic growth (CO_2 fixation) anoxygenic phototrophs like CLB need reducing equivalents (NAD[P]H) and thus a suitable e^- donor (e.g. sulfide or other reduced sulfur components) to generate these. When such e^- donors are however not available, CLB may switch from autotrophy to heterotrophy (i.e. use organic- instead of inorganic carbon as carbon source for growth). Previous studies have shown that C. *aurantiacus* in culture grows rather well photoheterotrophically and even prefers it over photoautotrophic growth (7, 39, 78, 97) and there is some verification that it does so as well in nature (4, 6, 108, 127). Exposure of *C.*

aurantiacus to aerobic conditions and high light intensity resulted in increase of carotenoids (110) and gradual loss of BChl's (98).

Lake Chiprana:

"La Salada de Chiprana" (41°14’20N 0°10’55W) is a 31 ha, hypersaline (ca. 78 ppt) lake at the Ebro basin in Saragossa (Aragon, NE Spain). A few centuries ago there was a non permanent shallow lake there but due to irrigation and agriculture, a permanent lake (5.6 m deep) was formed (126). Lake Chiprana has non-marine characteristics with magnesium (0.32 M) and sulfate (0.5 M) as main ions (55), originating from the rocks surrounding the area. With no human interference, the lake naturally is balanced by evaporation (up to 1.5m per year), some rain (about 350mm per year) and its ground water inflow. In recent years, due to irrigation, the lake started to get a new fresh water source (Laguna de las Roces) through a linking channel. At one of the field trips to the lake, our group observed a periodical (days) fresh water (<5 ppt) flow into the lake at an area we called area #10 – on which we took microbial mats and experimented with. The spot where fresh water reached Lake Chiprana was characterized by a very compact mat (1-mm thick photosynthetic layer), mainly composed of green cyanobacteria and *Chloroflexus*-like bacteria. This fresh water inflow naturally reduces salinity of the lake, but also led to eutrophication at the early 1990's. The effect was destructive to the present microbial mats and by 1994, in order to preserve the lakes ecology, it was declared protected area (at the Ramsar convention) and a management plan has been developed in order to protect it. Strong fluctuations of salinity have been observed in the lake (74, 134). Microbial mats cover the lake bottom from shore down to 1.5m depths. It was shown before that Lake Chiprana's microbial mats are highly productive and nutrient limited (75), and therefore excretes an extensive amount of dissolved organic matter to the surrounding water (55). That same study analyzed the structure and function of Chiprana's species rich microbial mat community. In general, the biology of the lake is far from being fully understood. In recent years the Microsensor Research Group from the Max-Planck-Institute for Marine Microbiology, Bremen started an extensive biological research program of the lake focusing mainly on C cycling, microbial calcification mechanisms and the *In-situ* eco-physiology of *Beggiatoa* and *Chloroflexus*-like bacteria. Much of the biological processes of this lake are yet to be revealed.

Goals of research:

In this PhD study a series of research questions and objectives concerning CLB have been treated (diversity; depth distribution in relation to physicochemical gradients; *In-situ* physiology; importance for community oxygen and C cycling). Not much is known of the *In-situ* physiology of hypersaline CLB – uncultured bacteria with an extensive abundance in the field. The work can be departmentalized to 4 main subjects:

- Developing a method to assess CLB ecological importance in the microbial mat oxygen and carbon cycle; test and support it with several scientific tools. NIR light has been used here for the first time to distinguish CLB from total community oxygen consumption in the mat. Since CLB are able to switch between oxygen respiration and anoxygenic photosynthesis for energy generation, NIR light is artificially added, as it appeared to inhibit CLB respiration. Development of the method and results concerning CLB diversity are discussed in chapter 2 "Diversity and function of *Chloroflexus*-like bacteria in a hypersaline microbial mat: phylogenic characterization and impact on oxygen cycling"
- Detailed quantification of CLB respiration in the microbial mat in relation to total community respiration and the modeling of the "NIR light/dark shift" method. This is a further and detailed investigation of the previous chapter in which the effect of NIR light on the microbial mats oxygen fluxes are shown. Here the VIS/NIR light technique is applied as a tool to quantify CLB respiration based on a modified version of the traditional "light dark shift technique" originally described by Revsbech et al. (106). Since CLB respire oxygen in the absence of NIR light, illumination with it will stop (or at least reduce) CLB oxygen consumption. This change will allow us to provide a budget of CLB respiratory rate and estimate their role in community carbon cycling. Subject is presented and discussed in chapter 3: "Quantification of respiration by *Chloroflexus*-like bacteria in a hypersaline microbial mat"
- Characterization of *Chloroflexus*-like bacteria distribution in the microbial mat will be discussed in chapter 4: "Spatial distribution of *Chloroflexus*-like bacteria in a hypersaline artificial microbial mat". Previous observations on CLB in a thick (ca. 1 cm) artificial mesocosm microbial mat revealed the notion of a CLB specific layer – as observed in the literature. Here, with various tools, I show CLB spatial distribution and functional importance as a function of depth. Local respiration rates are achieved; again, using the VIS/ NIR light technique and compared with the spatial distribution of pigments, light absorption and CLB related sequences.

- In chapter 5 in a biogeography study, the community compositions of *Chloroflexus*-like bacteria from hypersaline microbial mats from three continents (Asia, Europe and America) are compared through 16S rRNA analysis. The main objective was to find out whether distant (different continents) but environmentally comparable (hypersaline phototrophic microbial mat) communities support related (cosmopolitan) dominant members. Results are furthermore compared to the CLB communities from hot spring microbial mats, which are environmentally unrelated (fresh, hot water) but home to the most studied CLB species *Chloroflexus aurantiacus*.
- Finally at the end of the thesis a general discussion highlights once more the major results and discusses future possibilities to further clarify the role of culture-resisting but environmentally important CLB in nutrient cycling using *In-situ* techniques

Methods used in this research

The main questions were addressed by state of the art tools, which will be explained in more detail below:

a) Microsensors (O_2/H_2S/light) where employed throughout all 4 studies. In order to determine oxygen availability and quantification of oxygenic photosynthesis rates an oxygen microsensor was used. For the characterization of the anoxic part of the mat sulfide (and pH) microsensors were employed to determine the availability of sulfide, a potential e^- donor for CLB anoxygenic photosynthesis. A light microsensor was used to determine light fields and wavelengths attenuation in the mat in order to infer pigment distribution and vertical zonation of phototrophic microorganisms.
b) Several clone libraries where constructed for phylogenic investigation
c) Pigments where analyzed with HPLC
d) Bacteria where detected with microscopy and upon FISH application in order to reveal possible distinct spatial distribution of CLB species
e) DGGE was applied for functional analysis – the spatial distribution of CLB species in the mat.
f) 2 field trips to Lake Chiprana allowed *In-Situ* measurements of some parameters measured in the lab.

Microsensors: are probing devices with high spatial resolution due to their small measuring tip (<20 μm). They can record chemical and physical gradients and therefore have been extensively employed in microbial mats and many other microenvironments. Microsensors are highly reliable and useful tools, although tend to break under the hands of a disoriented (caffeine-deprived) scientist. In this research I have used them to measure fluxes of oxygen and sulfide and calculate photosynthesis and respiration rates. Furthermore I used light microsensors to measure light fields within the microbial mats layers. Field and lab work gave reproducible results generally fast and easily and gave a backbone for further investigation finding out *In-situ* physiology of CLB. For detailed microsensors application and overview, reader is referred to available publications in the literature (28, 38, 71). In my work I used oxygen, sulfide and light microsensors. Fiberoptic microprobes were described (59) and the downwelling spectral radiance was measured, approaching the mats surface from below. The incident radiance spectra were measured in the water column as soon as the sensor broke out of the sediment surface. Measured irradiance is then calculated for each wavelength at every depth. Backscattered light is measured from the mat surface downwards. The reader can read about my usage of this sensor at chapters' 3+4. Oxygen microsensor with respect to photosynthesis in mats was described (106) in a study in which measurements where compared to inorganic ^{14}C assimilation in the light. Methods (105) and sensors (104) where improved over time. The limiting factor of this method is the diffusion speed of oxygen, restricting the resolution of this method to 100μm. To learn about the diffusive boundary layer of sediments and oxygen micro-gradients over a microbial mat, the reader is referred to reference (58). The reader can read about my usage of this sensor at chapters 2-4. Sulfide microsensor was only used to characterize the chemical fluxes of sulfide at the mat (chapter 2). Mass transfer theoretical background and the diffusive boundary layer are large issues at sediment biology and where described, among others, in a book by Boudreau & Jørgensen (13). During my work at the microsensor department at the MPI I experimented with several microsensor types at different occasions. I find this tool very useful and reliable.

FISH: is a cytogenetic technique, which can be used to detect and localize DNA sequences on chromosomes. It uses fluorescent probes (dyes linked to oligonucleotide sequences), which bind only to those parts of the chromosome with which they show a high degree of sequence similarity. In my study (chapter 4) I applied CLB specific probes (86) to an intact microbial mat in order to visualize the abundance and location of these bacteria. Probes targeted the *Roseiflexus* (5'CGCATTGTCGGCGCCATT'3) and *Chloroflexus* (5'CGCATTGTCGTGGCCATT'3) genus. Disadvantages of this method are mainly non-specific bindings of the probe to substrates. For more details about FISH, reader is referred to the review publications available (3, 88)

HPLC: High Performance Liquid Chromatography is a form of column chromatography used frequently in biochemistry and analytical chemistry. HPLC is used to separate components of a mixture based on a variety of chemical interactions, usually of a non-covalent nature, between the analyte and the chromatography column. The end result is that chemical compounds which start mixed in a single sample injected into the instrument are eluted at different times. These peaks, each representing a different chemical species, may be collected as separate purified compounds or more often simply detected to determine their presence or quantity. In my study I used HPLC to determine pigments composition quantitatively and qualitatively as well as spatial distribution of pigments in microbial mats. Disadvantage of the method are the methodologically induced allomers in the sample and method related artifacts (such as pH) that affect the chemical form of the analyte. Furthermore, in a complex system such as microbial mats, one can never be sure from which bacteria comes a specific compound solely by HPLC analysis: CLB produce BChl*c*, like Chlorobiaceae, and BChl*a*, like purple (non) sulfur bacteria, and for example β-carotene, like cyanobacteria. Although a general picture of pigmentation can be obtained, further investigation must be added in order to answer questions of species distribution and quantification. For more details about HPLC, reader is referred to the review publications available (2)

Cloning of any DNA sequence is comprised of the following four steps: amplification, ligation, transfection, and screening/selection. In the beginning, the DNA fragment of interest needs to be amplified and many copies are produced. Amplification is commonly achieved by means of PCR. Afterwards, a ligation procedure is employed whereby the amplified fragment is inserted into a vector. The vector (frequently circular) is linearised by means of restriction enzymes, and incubated with the section of interest under proper conditions that allow for ligation to occur. Following ligation the vector with the insert is transfected to cells. Most commonly electroporation is employed, although a number of alternative techniques are available. Ultimately the transfected cells are cultured. Modern cloning vectors include selectable antibiotic resistance markers, which allow only for cells in which the vector has been transfected to grow. However this selection step does not guarantee that the DNA insert is present in the vector. This can be accomplished by means of blue/white screening and/or PCR, possibly followed by DNA sequencing. In my study I constructed several clone libraries of CLB from different microbial mats in order to determine diversity within the mat (manuscript 2) and biogeography of CLB in microbial mats from around the world (manuscript 5). For CLB diversity study in the Chiprana mat I used specific primers, which allegedly amplify 16S rRNA genes of all members of the phylum Chloroflexi. These primers yield relatively short (ca. 400bp) sequences (37) but reveal the diversity of the different phylotypes of CLB [GNSB-941F 5'AGCGGAGCGTGTGGTTT'3 and GNSB-1340R

5’CGCGGTTACTAGCAAC’3] and other members of the phylum Chloroflexi. For biogeography of CLB from different hypersaline environments I used primers, which yield longer sequences, which enable a better classification of the different Chloroflexaceae phylotypes. Primers used CCR344F (ACGGGAGGCAGCAGCAAG) and CCR1338R (ACGCGGTTACTAGCAACT) (86) resulted in ca. 1000bp rRNA gene sequence lengths. I did not use general 16S rRNA bacteria primers because diversity within a microbial mat is huge resulting in a small chance of obtaining CLB sequences. When I tried to apply general 16S rRNA primers, many non-CLB bacterial sequences were obtained and in order to get several CLB representatives, thousands of colonies would have been needed to be sequenced. Furthermore, clones of CLB related sequences may have been low in number and biogeographic questions of these bacteria would have been hard to answer. Disadvantages of this method are well described in the literature and the main disadvantage may be the bias of the PCR product toward specific groups of organisms. For more details about cloning, reader is referred to the review publications available (116, 136)

DGGE: Denaturing gradient gels are used to detect polymorphisms in 16S rRNA gene fragments. The small (200-700 bp) genomic restriction fragments are run on a low to high denaturant gradient acrylamide gel; initially the fragments move according to molecular weight, but as they progress into higher denaturing conditions, each (depending on its sequence composition) reaches a point where the DNA begins to melt. The partial melting severely retards the progress of the molecule in the gel, particularly due to the presence of an added DGGE clamp to one end of the primer, and a mobility shift is observed. It is the mobility shift that can differ for slightly different sequences (depending on the sequence, as little as a single bp change can cause a mobility shift). In my research I used this method to assess the presence of possibly different phylotypes of CLB as a function of depth in the microbial mat (chapter 4). Disadvantage of this method is its reliability: some would claim that there are no advantages today for DGGE over regular cloning (that has become cheap and fast in recent years). In contrast, the technique of DGGE yields a relatively fast overview if many samples are available: instead for building many clone libraries, one can satisfy a survey with DNA extraction and one step PCR run on a gradient gel. Depending on the question (and resources), one should choose its working tools. For more details about DGGE, reader is referred to the review publications available (1, 82, 83, 114).

Reference:

1. **Abed, R. M. M., N. M. D. Safi, J. Koster, D. de Beer, Y. El-Nahhal, J. Rullkotter, and F. Garcia-Pichel.** 2002. Microbial diversity of a heavily polluted microbial mat and its community changes following degradation of petroleum compounds. Applied and Environmental Microbiology **68:**1674-1683.

2. **Airs, R. L., J. E. Atkinson, and B. J. Keely.** 2001. Development and application of a high resolution liquid chromatographic method for the analysis of complex pigment distributions. Journal of Chromatography A **917:**167-77.

3. **Amann, R. I.** 1995. *In situ* identification of micro-organisms by whole cell hybridization with rRNA- targeted nucleic acid probes. Molecular Microbiology and Ecology Management **4:**543–554.

4. **Anderson, K. L., T. A. Tayne, and D. M. Ward.** 1987. Formation and fate of fermentation products in hot spring cyanobacterial mats. Applied and Environmental Microbiology **53:**2343-2352.

5. **Baker, E. N.** 1988. Structure of azurin from Alcaligenes denitrificans refinement at 1.8A resolution and comparison of the two crystallographically independent molecules. Journal of molecular biology **203:**1071-95.

6. **Bateson, M. M., and D. M. Ward.** 1988. Photoexcretion and fate of glycolate in a hot spring cyanobacterial mat. Applied and Environmental Microbiology **54:**1738-1743.

7. **Bauld, J., and T. D. Brock.** 1973. Ecological studies of *Chloroflexus*, a gliding photosynthetic bacterium. Archiv Für Mikrobiologie **92:**267-284.

8. **Baumgartner, L. K., R. P. Reid, C. Dupraz, A. W. Decho, D. H. Buckley, J. R. Spear, K. M. Przekop, and P. T. Visscher.** 2006. Sulfate reducing bacteria in microbial mats: changing paradigms, new discoveries. Sedimentary Geology **185** 131–145.

9. **Bebout, B. M., H. W. Paerl, K. M. Crocker, and L. E. Prufert.** 1987. Diel Interactions of oxygenic photosynthesis and N2 fixation (Acetylene-reduction) in a marine microbial mat community. Applied and Environmental Microbiology **53:**2353-2362.

10. **Becker, M., V. Nagarajan, D. Middendorf, W. W. Parson, J. E. Martin, and R. E. Blankenship.** 1991. Temperature-dependence of the initial electron-transfer kinetics in photosynthetic reaction centers of *Chloroflexus aurantiacus*. Biochimica et Biophysica Acta **1057:**299-312.

11. **Blankenship, R. E., L. J. Mancino, R. Feick, R. C. Fuller, J. Machnicki, H. A. Frank, C. Kirmaier, and D. Holten.** 1984. Primary photochemistry and pigment composition of reaction centers isolated from the green photosynthetic bacterium *Chloroflexus aurantiacus*, p. 203–206. *In* C. Sybesma (ed.), Advances in Photosynthesis Research. M. Nijhoff/Dr. W. Junk, The Hague The Netherlands.

12. **Boomer, S. M., D. P. Lodge, B. E. Dutton, and B. Pierson.** 2002. Molecular characterization of novel red green nonsulfur bacteria from five distinct hot spring communities in Yellowstone National Park. Applied and Environmental Microbiology **68:**346-355.

13. **Boudreau, B. P., and B. B. Jørgensen.** 2001. The Benthic Boundary Layer: Transport Processes and Biogeochemistry Oxford University, New York.

14. **Brock, T. D.** 1978. Thermophilic microorganisms and life at high temperatures. Springer-Verlag, New York.

15. **Brunberg, A. K., E. Nilsson, and P. Blomqvist.** 2002. Characteristics of oligotrophic hardwater lakes in a postglacial land-rise area in mid-Sweden. Freshwater Biology **47:**1451-1462.

16. **Buhring, S. I., M. Elvert, and U. Witte.** 2005. The microbial community structure of different permeable sandy sediments characterized by the investigation of bacterial fatty acids and fluorescence in situ hybridization. Environmental Microbiology **7:**281-93.

17. **Burton, N. P., T. D. Williams, and P. R. Norris.** 1999. Carboxylase genes of Sulfolobus metallicus. Archives of Microbiology **172:**349-353.

18. **Camacho, A., and R. De Wit.** 2003. Effect of nitrogen and phosphorus additions on a benthic microbial mat from a hypersaline lake. Aquatic Microbial Ecology **32:**261-273.

19. **Canfield, D. E., and D. J. Des Marais.** 1993. Biogeochemical cycles of carbon, sulfur, and free oxygen in a microbial mat. Geochimica et Cosmochimica Acta 57:3971–3984.

20. **Castenholz, R. W.** 2001. Class I: "Chloroflexi", p. 427. *In* D. R. Boone, R. W. Castenholz, and G. M. Garrity (ed.), Bergey's Manual of Systematic Bacteriology, 2 ed, vol. 1. Springer-Verlag, New York.

21. **Castenholz, R. W.** 1988. The green sulfur and nonsulfur bacteria of hot springs, p. 243–255. *In* J. M. Olson, J. G. Ormerod, J. Amesz, E. Stackebrandt, and H. G. Trüper (ed.), Green Photosynthetic Bacteria. Plenum Press New York, NY.

22. **Castenholz, R. W.** 1973. The possible photosynthetic use of sulfide by the filamentous phototrophic bacteria of hot springs. Limnology and Oceanography **18:**863–876.

23. **Castenholz, R. W., and B. K. Pierson.** 1995. Ecology of thermophilic anoxygenic phototrophs. *In* R. E. Blankenship, M. T. Madigan, and C. E. Bauer (ed.), Anoxygenic Photosynthetic Bacteria. Kluwer.

24. **Cohen, Y., and E. Rosenberg.** 1989. Microbial mats: physiological ecology of benthic microbial communities. American Society for Microbiology, Washington, DC.

25. **D'Amelio, E. D., Y. Cohen, and D. J. Des Marais.** 1987. Association of a new type of gliding, filamentous, purple phototrophic bacterium inside bundles of *Microcoleus chthonoplastes* in hypersaline cyanobacterial mats. Archives of Microbiology **147:**213-20.

26. **D'Amelio, E. D., Y. Cohen, and D. J. Des Marais.** 1989. Comparative functional ultrastructure of two hypersaline submerged cyanobacterial mats: Guerrero Negro, Baja California Sur, Mexico, and Solar Lake, Sinai, Egypt, p. 97-103. *In* Y. Cohen and E. Rosenberg (ed.), Microbial mats physiological ecology of benthic microbial communities. American Society for Microbiology, Washington, D.C.

27. **D'Amelio, E. D., Y. Cohen, and D. D. Marais.** 1989. Comparative functional ultrastructure of two hypersaline submerged cyanobacterial mats: Guerrero Negro, Baja California Sur, Mexico, and Solar Lake, Sinai, Egypt, p. 97-103. *In* Y. Cohen and E. Rosenberg (ed.), Microbial mats physiological ecology of benthic microbial communities. American Society for Microbiology, Washington, D.C.

28. **De Beer, D.** 1999. Use of microelectrodes to measure *in situ* microbial activities in biofilms, sediments and microbial mats. *In* A. D. L. Akkermans, J. D. v. Elsas, and F. J. d. Bruin (ed.), Molecular Microbial Ecology Manual Kluwer.

29. **De Wit, R., L. I. Falcon, and C. Charpy-Roubaud.** 2005. Heterotrophic dinitrogen fixation (acetylene reduction) in phosphate-fertilized *Microcoleus chthonoplastes* microbial mat from the hypersaline inland lake 'la Salada de Chiprana' (NE Spain). Hydrobiologia **534:**245-253.

30. **Dubinina, G. A., and V. M. Gorlenko.** 1975. New filamentous photosynthetic green bacteria containing gas vacuoles. Microbiology **44:**452–458.

31. **Dubinsky, Z., and P. L. Jokiel.** 1994. Ratio of energy and nutrient fluxes regulates symbiosis between zooxanthellae and corals. Pacific Science **48:**313-324.

32. **Eisenreich, W., G. Strauss, U. Werz, G. Fuchs, and A. Bacher.** 1993. Retrobiosynthetic analysis of carbon fixation in the phototrophic eubacterium Chloroflexus aurantiacus. European Journal of Biochemistry **215**:619-32.

33. **Freeman, J. C., and R. E. Blankenship.** 1990. Isolation and Characterization of the Membrane-Bound Cytochrome C-554 from the Thermophilic Green Photosynthetic Bacterium Chloroflexus-Aurantiacus. Photosynthesis Research **23:**29-38.

34. **Frigaard, N.-U., and D. A. Bryant.** 2006. Chlorosomes: antenna organelles in photosynthetic green bacteria. *In* J. M. Shively (ed.), Inclusions in prokaryotes. Springer, Berlin.

35. **Fukui, M., A. Teske, B. Assmus, G. Muyzer, and F. Widdel.** 1999. Physiology, phylogenetic relationships, and ecology of filamentous sulfate-reducing bacteria (genus *desulfonema*). Archives of Microbiology **172:**193-203.

36. **Gich, F., R. L. Airs, M. Danielsen, B. J. Keely, C. A. Abella, J. Garcia-Gil, M. Miller, and C. M. Borrego.** 2003. Characterization of the chlorosome antenna of the filamentous anoxygenic phototrophic bacterium Chloronema sp. strain UdG9001. Archives of Microbiology **180:**417-26.

37. **Gich, F., J. Garcia-Gil, and J. Overmann.** 2001. Previously unknown and phylogenetically diverse members of the green nonsulfur bacteria are indigenous to freshwater lakes. Archives of Microbiology **177:**1-10.

38. **Gieseke, A., and D. De Beer.** 2004. Use of microelectrodes to measure in situ microbial activities in biofilms, sediments, and microbial mats. *In* A. D. L. Akkermans and D. v. Elsas (ed.), Molecular Microbial Ecology Manual. Kluwer, Dordrecht.

39. **Giovannoni, S. J., N. P. Revsbech, D. M. Ward, and R. W. Castenholz.** 1987. Obligately phototrophic Chloroflexus: primary production in anaerobic hot spring microbial mats. Archves of Microbiology **147:**80–87.

40. **Gorlenko, V. M.** 1988. Ecological niches of green sulfur and gliding bacteria, p. 257–267. *In* J. M. Olson, J. G. Ormerod, J. Amesz, E. Stackebrandt, and H. G. Trüper (ed.), Green Photosynthetic Bacteria. Plenum Press, New York

41. **Gorlenko, V. M.** 1989. Genus "Oscillochloris" p. 1703–1706. *In* J. T. Staley, M. P. Bryant, N. Pfennig, and J. G. Holt (ed.), Bergey's Manual of Systematic Bacteriology. Williams and Wilkins, Baltimore, MD.

42. **Gorlenko, V. M., and B. K. Pierson.** 2001. Genus II: Chloronema, p. 437–438. *In* D. R. Boone, R. W. Castenholz, and G. M. Garrity (ed.), Bergey's Manual of Systematic Bacteriology, 2 ed, vol. 1. Springer-Verlag press, New York

43. **Gorlenko, V. M., and T. A. Pivovarova.** 1977. On the belonging of blue green alga Oscillatoria coerulescens Gicklhorn, 1921 to a new genus of Chlorobacteria Oscillochloris nov. gen., vol. 3. Izv. Akad., Nauk SSSR.

44. **Guerrero, R., and J. Mas.** 1989. Multilayered Microbial Communities in Aquatic Ecosystems: Growth and Loss Factors, p. 37-51. *In* C. Y and R. E (ed.), Microbial Mats, Physiological Ecology of Benthic Microbial Communities. ASM, Washington DC.

45. **Halfen, L. N., B. K. Pierson, and G. W. Francis.** 1972. Carotenoids of a gliding organism containing bacteriochlorophylls. Archives of Mikrobiology **82:**240–246.

46. **Hanada, S., A. Hiraishi, K. Shimada, and K. Matsuura.** 1995. *Chloroflexus aggregans* sp. nov., a filamentous phototrophic bacterium which forms dense cell aggregates by active gliding movement. International Journal of Systematic Bacteriology **45:**676-81.

47. **Hanada, S., S. Takaichi, K. Matsuura, and K. Nakamura.** 2002. *Roseiflexus castenholzii* gen. nov., sp. nov., a thermophilic, filamentous, photosynthetic bacterium that lacks chlorosomes. International Journal of Systematic and Evolutionary Microbiology **52:**187-93.

48. **Holo, H.** 1989. *Chloroflexus aurantiacus* Secretes 3-Hydroxypropionate, a Possible Intermediate in the Assimilation of CO2 and Acetate. Archives of Microbiology **151:**252-256.

49. **Holo, H., and D. Grace.** 1987. Polyglucose Synthesis in *Chloroflexus aurantiacus* Studied by C-13-Nmr - Evidence for Acetate Metabolism by a New Metabolic Pathway in Autotrophically Grown Cells. Archives of Microbiology **148:**292-297.

50. **Holo, H., and R. Sirevag.** 1986. Autotrophic Growth and CO_2 Fixation of *Chloroflexus aurantiacus*. Archives of Microbiology **145:**173-180.

51. **Ibekwe, A. M., S. K. Papiernik, J. Gan, S. R. Yates, C. H. Yang, and D. E. Crowley.** 2001. Impact of fumigants on soil microbial communities. Applied and Environmental Microbiology **67:**3245- 57.

52. **Ishii, M., T. Miyake, T. Satoh, H. Sugiyama, Y. Oshima, T. Kodama, and Y. Igarashi.** 1996. Autotrophic carbon dioxide fixation in Acidianus brierleyi. Archives of Microbiology **166:**368-371.

53. **Javor, B. J., and R. W. Castenholz.** 1984. Productivity studies of microbial mats, Laguna Guerrero Negro, Mexico, p. 149-170. *In* Y. Cohen, R. W. Castenholz, and H. H. O. (ed.), Microbial mats: Stromatolites. Alan R. Liss, New York.

54. **Jonkers, H. M., I. O. Koh, P. Behrend, G. Muyzer, and D. de Beer.** 2005. Aerobic organic carbon mineralization by sulfate-reducing bacteria in the oxygen-saturated photic zone of a hypersaline microbial mat. Microbial Ecology **49:**291-300.

55. **Jonkers, H. M., R. Ludwig, R. De Wit, O. Pringault, G. Muyzer, H. Niemann, N. Finke, and D. De Beer.** 2003. Structural and functional analysis of a microbial mat ecosystem from a unique permanent hypersaline inland lake: 'La Salada de Chiprana' (NE Spain). Fems Microbiology Ecology **44:**175-189.

56. **Jørgensen, B. B.** 1989. Light penetration, absorption and action spectra in cyanobacterial mats, p. 123–137. *In* Y. Cohen and E. Rosenberg (ed.), Microbial mat: Physiological ecology of benthic microbial communities. American Society for Microbiology Washington.

57. **Jorgensen, B. B., Y. Cohen, and D. J. Des Marais.** 1987. Photosynthetic action spectra and adaptation to spectral light distribution in a benthic cyanobacterial mat. Applied and Environmental Microbiology **53:**879-86.

58. **Jorgensen, B. B., and D. J. Des Marais.** 1990. The diffusive boundary layer of sediments: oxygen microgradients over a microbial mat. Limnology and Oceanography **35:**1343-55.

59. **Jorgensen, B. B., and D. J. Desmarais.** 1986. A Simple Fiberoptic Microprobe for High-Resolution Light Measurements - Application in Marine Sediment. Limnology and Oceanography **31:**1376-1383.

60. **Jørgensen, B. B., and D. C. Nelson.** 1988. Bacterial zonation, photosynthesis, and spectral light distribution in hot spring microbial mats of Iceland. Microbial Ecology **16:**133–147

61. **Jorgensen, B. B., N. P. Revsbech, T. H. Blackburn, and Y. Cohen.** 1979. Diurnal Cycle of Oxygen and Sulfide Microgradients and Microbial Photosynthesis in a Cyanobacterial Mat Sediment. Applied and Environmental Microbiology **38:**46-58.

62. **Keppen, O. I., O. I. Baulina, and E. N. Kondratieva.** 1994. *Oscillochloris trichoides* neotype strain DG-6. Photosynthesis Research **41:**29–33.

63. **Keppen, O. I., O. I. Baulina, A. M. Lysenko, and E. N. Kondrat'eva.** 1993. New green bacterium belonging to family Chloroflexaceae. Mikrobiologiya **62:**179–185.

64. **Keppen, O. I., T. P. Tourova, B. B. Kuznetsov, R. N. Ivanovsky, and V. M. Gorlenko.** 2000. Proposal of Oscillochloridaceae fam. nov. on the basis of a phylogenetic analysis of the filamentous anoxygenic phototrophic bacteria, and emended description of Oscillochloris and *Oscillochloris trichoides* in comparison with further new isolates. International Journal of systematic and evolutionary microbiology **50, 4:** 1529-37.

65. **Kirmaier, C., D. Holten, R. Feick, and R. E. Blankenship.** 1983. Picosecond measurements of the primary photochemical events in reaction centers isolated from the facultative green photosynthetic bacterium *Chloroflexus aurantiacus*: Comparison with the purple bacterium *Rhodopseudomonas sphaeroides*. FEBS Letters **158:**73–78.

66. **Klappenbach, J. A., and B. K. Pierson.** 2004. Phylogenetic and physiological characterization of a filamentous anoxygenic photoautotrophic bacterium ' Candidatus Chlorothrix halophila' gen. nov., sp. nov., recovered from hypersaline microbial mats. Archives of Microbiology **181:**17-25.

67. **Kompantseva, E. I., D. Y. Sorokin, V. M. Gorlenko, and B. B. Namsaraev.** 2005. The phototrophic community found in Lake Khilganta (an alkaline saline lake located in the southeastern Transbaikal Region). Microbiology **74:**352-361.

68. **Kondrateva, E. N., and E. N. Krasilnikova.** 1988. Utilization of Thiosulfate by *Chloroflexus-Aurantiacus*. Microbiology **57:**291-294.

69. **Krasil'nikova, E. N., and E. N. Kondrat'eva.** 1987. Growth of *Chloroflexus aurantiacus* under anaerobic conditions in the dark and the metabolism of organic substrates. Microbiology **56:**281–285.

70. **Krasilnikova, E. N.** 1986. Atp Sulfurylase Activity in Chloroflexus-Aurantiacus and Other Photosynthesizing Bacteria as a Function of Temperature. Microbiology **55:**418-421.

71. **Kühl, M.** 2005. Optical microsensors for analysis of microbial communities. Methods in Enzymology **397:**166-99.

72. **Lefebvre, O., N. Vasudevan, K. Thanasekaran, R. Moletta, and J. J. Godon.** 2006. Microbial diversity in hypersaline wastewater: the example of tanneries. Extremophiles **10**:505-513

73. **Ley, R. E., J. K. Harris, J. Wilcox, J. R. Spear, S. R. Miller, B. M. Bebout, J. A. Maresca, D. A. Bryant, M. L. Sogin, and N. R. Pace.** 2006. Unexpected diversity and complexity of the Guerrero Negro hypersaline microbial mat. Applied and Environmental Microbiology **72:**3685-95.

74. **Lopez-Bermudez, F., A. Romero-Diaz, J. Martinez-Fernandez, and J. Martinez-Fernandez.** 1998. Vegetation and soil erosion under a semi-arid Mediterranean climate: a case study from Murcia (Spain). Geomorphology **24:**51-58.

75. **Ludwig, R., O. Pringault, R. de Wit, D. de Beer, and H. M. Jonkers.** 2006. Limitation of oxygenic photosynthesis and oxygen consumption by phosphate and organic nitrogen in a hypersaline microbial mat: a microsensor study. FEMS Microbiology and Ecology **57:**9-17.

76. **Mack, E. E., and B. K. Pierson.** 1988. Preliminary characterization of a temperate marine member of the Chloroflexaceae, p. 237–241. *In* J. M. Olson, J. G. Ormerod, J. Amesz, E. Stackebrandt, and H. G. Trüper (ed.), Green Photosynthetic Bacteria. Plenum Publishing, New York, NY.

77. **Madigan, M. T., D. O. Jung, C. R. Woese, and L. A. Achenbach.** 2000. Rhodoferax antarcticus sp nov., a moderately psychrophilic purple nonsulfur bacterium isolated from an Antarctic microbial mat. Archives of Microbiology **173:**269-277.

78. **Madigan, M. T., S. R. Petersen, and T. D. Brock.** 1974. Nutritional Studies on Chloroflexus, a Filamentous Photosynthetic, Gliding Bacterium. Archives of Microbiology **100:**97-103.

79. **Manske, A. K., J. Glaeser, M. M. Kuypers, and J. Overmann.** 2005. Physiology and phylogeny of green sulfur bacteria forming a monospecific phototrophic assemblage at a depth of 100 meters in the Black Sea. Applied and Environmental Microbiology **71:**8049-60.

80. **Martinez-Alonso, M., J. Mir, P. Caumette, N. Gaju, R. Guerrero, and I. Esteve.** 2004. Distribution of phototrophic populations and primary production in a microbial mat from the Ebro Delta, Spain. International Microbiology **7:**19-25.

81. **Menendez, C., Z. Bauer, H. Huber, N. Gad'on, K. O. Stetter, and G. Fuchs.** 1999. Presence of acetyl coenzyme A (CoA) carboxylase and propionyl-CoA carboxylase in autotrophic Crenarchaeota and indication for operation of a 3-hydroxypropionate cycle in autotrophic carbon fixation. Journal of Bacteriology **181:**1088-1098.

82. **Muyzer, G.** 1999. DGGE/TGGE a method for identifying genes from natural ecosystems. Current Opinions in Microbiology **2**:317-322.

83. **Muyzer, G., and E. C. d. Waal.** 1994. Determination of the genetic diversity of microbial communities using DGGE analysis of PCR-amplified 16S rDNA **NATO ASI Series:**207–214.

84. **Nisbet, E. G., and M. R. Fowler.** 2003. The Early History of Life, p. 1-39. *In* W. H. Schlesinger (ed.), Biogeochemistry, vol. 8. Elsevier Pergamon.

85. **Norris, P. R., and A. Nixon.** 1989. Acidophilic, mineral-oxidizing bacteria: the utilization of carbon dioxide with particular reference to autotrophy in Sulfolobus, p. 24–43. *In* D. C. M. S, D. J. C, and W. R. A. D (ed.), Microbiology of extreme environments and its potential for biotechnology. Elsevier, London, United Kingdom.

86. **Nubel, U., M. M. Bateson, V. Vandieken, A. Wieland, M. Kühl, and D. M. Ward.** 2002. Microscopic examination of distribution and phenotypic properties of phylogenetically diverse Chloroflexaceae-related bacteria in hot spring microbial mats. Applied and Environmental Microbiology **68:**4593-4603.

87. **Olendzenski, L. C.** 1999. Growth, fine structure and cyst formation of a microbial mat ciliate: *Pseudocohnilembus pusillus* (Ciliophora, scuticociliatida). Journal of Eukaryotic Microbiology **46:**132-141.

88. **Oliveira, A. M., and C. A. French.** 2005. Applications of fluorescence in situ hybridization in cytopathology: a review. Acta Cytologica **49:**587-94.

89. **Ovchinnikov Yu, A., N. G. Abdulaev, B. E. Shmuckler, A. A. Zargarov, M. A. Kutuzov, I. N. Telezhinskaya, N. B. Levina, and A. S. Zolotarev.** 1988. Photosynthetic reaction centre of *Chloroflexus aurantiacus*. II Primary structure of M-subunit. FEBS Letters **232:**364-8.

90. **Ovchinnikov Yu, A., N. G. Abdulaev, A. S. Zolotarev, B. E. Shmukler, A. A. Zargarov, M. A. Kutuzov, I. N. Telezhinskaya, and N. B. Levina.** 1988. Photosynthetic reaction centre of *Chloroflexus aurantiacus*. I. Primary structure of L-subunit. FEBS Letters **231:**237-42.

91. **Overmann, J., and F. Garcia-Pichel.** 2000. The phototrophic way of life: Pigments and Light-harvesting Complexes *In* Dworkin (ed.), The Prokaryotes: an evolving electronic resource for the microbiology community, 3.2 ed. Springer-Verlag, New York.

92. **Overmann, J., and N. Pfennig.** 1992. Continuous Chemotropic Growth and Respiration of Chromatiaceae Species at Low Oxygen Concentrations. Archives of Microbiology **158:**59-67.

93. **Oyaizu, H., B. Devrunner-Vossbrinck, L. Mandelko, J. A. Studier, and C. R. Woese.** 1987. The green non-sulfur bacteria: a deep branching in the eubacterial line of descent. System. Applied Microbiology **9:**47–53.

94. **Paerl, H. W., J. L. Pinckney, and T. F. Steppe.** 2000. Cyanobacterial-bacterial mat consortia: examining the functional unit of microbial survival and growth in extreme environments. Environmental Microbiology **2:**11-26.

95. **Palmisano, A. C., S. E. Cronin, E. D. D'Amelio, E. Munoz, and D. J. Des Marais.** 1989. Distribution and survival of lipophilic pigments in a laminated microbial mat community near Guerrero Negro Mexico, p. 138-152. *In* Y. Cohen and E. Rosenberg (ed.), Microbial Mats: Physiological Ecology of Benthic Microbial Communities. American Society for Microbiology, Washington, DC.

96. **Pierson, B. K., and R. W. Castenholz.** 2005. The Family Chloroflexaceae. *In* Dworkin (ed.), The Prokaryotes: an evolving electronic resource for the microbiology community, 3 ed. Springer-Verlag, New York.

97. **Pierson, B. K., and R. W. Castenholz.** 1974. A phototrophic gliding filamentous bacterium of hot springs, *Chloroflexus aurantiacus*, gen. and sp. nov. Archives of Microbiology **100:**5–24.

98. **Pierson, B. K., and R. W. Castenholz.** 1974. Studies of pigments and growth in Chloroflexus aurantiacus, a phototrophic filamentous bacterium. Archives of Microbiology **100:**283–305.

99. **Pierson, B. K., and R. W. Castenholz.** 1995. Taxonomy and physiology of filamentous anoxygenic phototrophs, p. 31–47. *In* M. T. M. R. E. Blankenship, and C. E. Bauer (ed.), Anoxygenic Photosynthetic Bacteria. Kluwer Academic Publishers, Dordrecht, The Netherlands.

100. **Pierson, B. K., S. J. Giovannoni, and R. W. Castenholz.** 1984. Physiological Ecology of a Gliding Bacterium Containing Bacteriochlorophyll a. Applied and Environmental Microbiology **47:**576-584.

101. **Pierson, B. K., S. J. Giovannoni, D. A. Stahl, and R. W. Castenholz.** 1985. *Heliothrix oregonensis*, gen. nov., sp. nov., a phototrophic filamentous gliding bacterium containing bacteriochlorophyll a. Archives of Microbiology **142:**164-7.

102. **Pierson, B. K., and J. P. Thornber.** 1983. Isolation and spectral characterization of photochemical reaction centers from the thermophilic green bacterium Chloroflexus aurantiacus strain J-10-fl. Proceedings of the National Academy of Science USA **80:**80-84.

103. **Pierson, B. K., D. Valdez, M. Larsen, E. Morgan, and E. E. Mack.** 1994. Chloroflexus-Like Organisms from Marine and Hypersaline Environments - Distribution and Diversity. Photosynthesis Research **41:**35-52.

104. **Revsbech, N. P.** 1989. An Oxygen Microsensor with a Guard Cathode. Limnology and Oceanography **34:**474-478.

105. **Revsbech, N. P., and B. B. Jørgensen.** 1983. Photosynthesis of benthic microflora measured with high spatial-resolution by the oxygen microprofile method: Capabilities and limitations of the method. Limnology and Oceanography **28:**749–756.

106. **Revsbech, N. P., B. B. Jørgensen, and O. Brix.** 1981. Primary production of microalgae in sediments measured by oxygen microprofile, $H^{14}CO_3$-fixation, and oxygen-exchange methods. Limnology and Oceanography **26:**717-730.

107. **Revsbech, N. P., and D. M. Ward.** 1984. Microelectrode Studies of Interstitial Water Chemistry and Photosynthetic Activity in a Hot Spring Microbial Mat. Applied and Environmental Microbiology **48:**270-275.

108. **Sandbeck, K. A., and D. M. Ward.** 1981. Fate of Immediate Methane Precursors in Low-Sulfate, Hot-Spring Algal-Bacterial Mats. Applied and Environmental Microbiology **41:**775-782.

109. **Schmidt, K.** 1980. A comparative study on the composition of chlorosomes (chlorobium vesicles) and cytoplasimic membranes from *Chloroflexus aurantiacus* strain OK-70-fl and Chlorobium limicola f. thiosulfatophilum strain 6230. Archives of Microbiology **124:**21–31.

110. **Schmidt, K., M. Maarzahl, and F. Mayer.** 1980. Development and Pigmentation of Chlorosomes in Chloroflexus-Aurantiacus Strain Ok-70-Fl. Archives of Microbiology **127:**87-97.

111. **Shiea, J., S. C. Brassell, and D. M. Ward.** 1991. Comparative-Analysis of Extractable Lipids in Hot-Spring Microbial Mats and Their Component Photosynthetic Bacteria. Organic Geochemistry **17:**309-319.

112. **Shiozawa, J. A., F. Lottspeich, and R. Feick.** 1987. The photochemical reaction center of *Chloroflexus aurantiacus* is composed of two structurally similar polypeptides. European Journal of Biochemistry**167:** 595-600.

113. **Shiozawa, J. A., F. Lottspeich, D. Oesterhelt, and R. Feick.** 1989. The primary structure of the *Chloroflexus aurantiacus* reaction-center polypeptides. European Journal of Biochemistry **180:**75-84.

114. **Siqueira, J. F., Jr., I. N. Rocas, and A. S. Rosado.** 2005. Application of denaturing gradient gel electrophoresis (DGGE) to the analysis of endodontic infections. Journal of Endodontics **31:**775-82.

115. **Sirevåg, R.** 1995. Carbon metabolism in green bacteria, p. 871–883. *In* B. RE, M. MT, and B. CE (ed.), Anoxygenic Photosynthetic Bacteria. Kluwer Academic, Dordrecht, The Netherlands.

116. **Sorensen, K. B., D. E. Canfield, A. P. Teske, and A. Oren.** 2005. Community composition of a hypersaline endoevaporitic microbial mat. Applied and Environmental Microbiology **71:**7352-65.

117. **Stackebrandt, E., F. A. Rainey, and N. Ward-Rainey.** 1996. Anoxygenic phototrophy across the phylogenetic spectrum: current understanding and future perspectives. Archives of Microbiology **166:**211-23.

118. **Stal, L. J.** 2000. Cyanobacterial mats and stromatolites, p. 61-120. *In* B. A. Whitton and M. Potts (ed.), The Ecology of Cyanobacteria: Their Diversity in Time and Space. Kluwer Academic, Dordrecht, The Netherlands.

119. **Stolz, J. F.** 1990. Distribution of phototrophic microbes in the flat laminated microbial mat at Laguna Figueroa, Baja California, Mexico. Biosystems **23:**345-57.

120. **Stolz, J. F.** 1984. Fine structure of the stratified microbial community at Laguna Figueroa, Baja California, Mexico. II: Transmission electron microscopy as a diagnostic tool in studying microbial community in situ, p. 23–38. *In* Y. Cohen, R. W. Castenholz, and H. O. Halvorson (ed.), Microbial Mat: Stromatolites. Alan R. Liss, New York, NY.

121. **Stolz, J. F., and L. Margulis.** 1984. The stratified microbial community at Laguna Figueroa, Baja California, Mexico: a possible model for prephanerozoic laminated microbial communities preserved in cherts. Origins of Life and Evolution of Biospheres **14:**671-9.

122. **Strauß , G., and G. Fuchs.** 1993. Enzymes of a Novel Autotrophic CO2 Fixation Pathway in the Phototrophic Bacterium Chloroflexus-Aurantiacus, the 3-Hydroxypropionate Cycle. European Journal of Biochemistry **215:**633-643.

123. **Takaichi, S., T. Maoka, M. Yamada, K. Matsuura, Y. Haikawa, and S. Hanada.** 2001. Absence of carotenes and presence of a tertiary methoxy group in a carotenoid from a thermophilic filamentous photosynthetic bacterium *Roseiflexus castenholzii*. Plant Cell Physiology **42:**1355-62.

124. **Taylor, C. D., C. O. Wirsen, and F. Gaill.** 1999. Rapid microbial production of filamentous sulfur mats at hydrothermal vents. Applied and Environmental Microbiology **65:**2253-2255.

125. **Teske, A., N. B. Ramsing, K. S. Habicht, M. Fukui, J. Küver, B. B. Jørgensen, and Y. Cohen.** 1998. Sulfate-reducing bacteria andtheir activities in cyanobacterial mats of Solar Lake (Sinai, Egypt). Applied and Environmental Microbiology **64:**2943–2951.

126. **Valero-Garcés, B. L., A. Navas, J. Machin, T. Stevenson, and B. Davis.** 2000. Responses of a Saline Lake Ecosystem in a Semiarid Region to Irrigation and Climate Variability - The History of Salada Chiprana, Central Ebro Basin, Spain. AMBIO: A Journal of the Human Environment **29:**344-350.

127. **van der Meer, M. T. J., S. Schouten, M. M. Bateson, U. Nubel, A. Wieland, M. Kühl, J. W. de Leeuw, J. S. S. Damste, and D. M. Ward.** 2005. Diel variations in carbon metabolism by green nonsulfur-like bacteria in alkaline siliceous hot spring microbial mats from Yellowstone National Park. Applied and Environmental Microbiology **71:**3978-3986.

128. **van der Meer, M. T. J., S. Schouten, J. S. S. Damsté, J. W. d. Leeuw, and D. M. Ward.** 2003. Compound-specific isotopic fractionation patterns suggest different carbon metabolisms

among Chloroflexus-like bacteria in hot spring microbial mats. Applied and Environmental Microbiology **69:**6000-6006.

129. **van der Meer, M. T. J., S. Schouten, J. W. de Leeuw, and D. M. Ward.** 2000. Autotrophy of green non-sulfur bacteria in hot spring microbial mats: biological explanations for isotopically heavy organic carbon in the geological record. Environmental Microbiology **2:**428-435.

130. **van der Meer, M. T. J., S. Schouten, D. E. van Dongen, W. I. C. Rijpstra, G. Fuchs, J.S. S. Damste, J. W. de Leeuw, and D. M. Ward.** 2001. Biosynthetic controls and the C-13 contents of organic components in the photoautotrophic bacterium *Chloroflexus aurantiacus*. Journal of Biological Chemistry **276:**10971-10976.

131. **Van Gemerden, H.** 1993. Microbial Mats - a Joint Venture. Marine Geology **113:**3-25.

132. **Vasmel, H., J. Amesz, and A. J. Hoff.** 1986. Analysis by exciton theory of the optical properties of the reaction center of *Chloroflexus aurantiacus*. Biochimica et Biophysica Acta **852:**159–168.

133. **Venetskaya, S. L., and L. M. Gerasimenko.** 1988. Electron microscopic study of microorganisms in a halophilic cyanobacterial community. Microbiology **57:**377-383.

134. **Vidondo, B., B. Martínez, C. Montes, and M. C. Guerrero.** 1993. Physico-chemical characteristics of a permanent Spanish hypersaline lake: La Salada de Chiprana (NE Spain). Hydrobiologia **267:**113-125.

135. **Vila, X., R. Guyoneaud, X. P. Cristina, J. B. Figueras, and C. A. Abella.** 2002. Green sulfur bacteria from hypersaline Chiprana Lake (Monegros, Spain): habitat description and phylogenetic relationship of isolated strains. Photosynthesis Research **71:**165-172.

136. **von Wintzingerode, F., U. B. Gobel, and E. Stackebrandt.** 1997. Determination of microbial diversity in environmental samples: pitfalls of PCR-based rRNA analysis. FEMS Microbiology Reviews **21:**213-29.

137. **Ward, D. M., M. J. Ferris, S. C. Nold, and M. M. Bateson.** 1998. A natural view of microbial biodiversity within hot spring cyanobacterial mat communities. Microbiology and Molecular Biology Reviews **62:**1353-1370

138. **Wierenga, E. B. A., J. Overmann, and H. Cypionka.** 2000. Detection ofabundant sulphate- reducing bacteria in marine oxic sedimentlayers by a combined cultivation and molecular approach. Environmental Microbiology **2:**417–427.

139. **Yamada, M., H. Zhang, S. Hanada, K. V. Nagashima, K. Shimada, and K. Matsuura.** 2005. Structural and spectroscopic properties of a reaction center complex from the chlorosome-lacking filamentous anoxygenic phototrophic bacterium Roseiflexus castenholzii. Journal of Bacteriology **187:**1702-1709.

Chapter II:

Diversity and Function of *Chloroflexus*-Like Bacteria in a Hypersaline Microbial Mat: Phylogenetic Characterization and Impact on Aerobic Respiration

APPLIED AND ENVIRONMENTAL MICROBIOLOGY, June 2007, p. 3975–3983 Vol. 73, No. 12
0099-2240/07/$08.00+0 doi:10.1128/AEM.02532-06

Diversity and Function of *Chloroflexus*-Like Bacteria in a Hypersaline Microbial Mat: Phylogenetic Characterization and Impact on Aerobic Respiration▽

Ami Bachar,[1] Enoma Omoregie,[1] Rutger de Wit,[2] and Henk M. Jonkers[1,3]*

Max Planck Institute for Marine Microbiology, Celsiusstrasse 1, D-28359 Bremen, Germany[1]; CNRS and Université Montpellier II UMR 5119, Case 093, Place Eugène Bataillon, F-34095 Montpellier Cedex 05, France[2]; and Delft University of Technology, Postbox 5048, NL-2600 GA Delft, The Netherlands[3]

Received 31 October 2006/Accepted 11 April 2007

We studied the diversity of *Chloroflexus*-like bacteria (CLB) in a hypersaline phototrophic microbial mat and assayed their near-infrared (NIR) light-dependent oxygen respiration rates. PCR with primers that were reported to specifically target the 16S rRNA gene from members of the phylum *Chloroflexi* resulted in the recovery of 49 sequences and 16 phylotypes (sequences of the same phylotype share more than 96% similarity), and 10 of the sequences (four phylotypes) appeared to be related to filamentous anoxygenic phototrophic members of the family *Chloroflexaceae*. Photopigment analysis revealed the presence of bacteriochlorophyll *c* (BChl*c*), BChl*d*, and γ-carotene, pigments known to be produced by phototrophic CLB. Oxygen microsensor measurements for intact mats revealed a NIR (710 to 770 nm) light-dependent decrease in aerobic respiration, a phenomenon that we also observed in an axenic culture of *Chloroflexus aurantiacus*. The metabolic ability of phototrophic CLB to switch from anoxygenic photosynthesis under NIR illumination to aerobic respiration under non-NIR illumination was further used to estimate the contribution of these organisms to mat community respiration. Steady-state oxygen profiles under dark conditions and in the presence of visible (VIS) light (400 to 700 nm), NIR light (710 to 770 nm), and VIS light plus NIR light were compared. NIR light illumination led to a substantial increase in the oxygen concentration in the mat. The observed impact on oxygen dynamics shows that CLB play a significant role in the cycling of carbon in this hypersaline microbial mat ecosystem. This study further demonstrates that the method applied, a combination of microsensor techniques and VIS and NIR illumination, allows rapid establishment of the presence and significance of CLB in environmental samples.

Chloroflexus-like bacteria (CLB) have been reported to be conspicuously present in some microbial mats (4, 14, 16, 19, 23, 24, 29, 32, 34), while in other mats they seem to be virtually absent. CLB are multicellular filamentous anoxygenic phototrophs (13), which can move by gliding and are also characterized by the production of bacteriochlorophyll *a* (BChl*a*) and in some species by the supplemental production of BChl*c* or BChl*d*. All characterized CLB are members of the genera *Chloroflexus*, *Chloronema*, *Oscillochloris*, *Roseiflexus*, and *Heliothrix* in the family *Chloroflexaceae* in the phylum *Chloroflexi* (previously called the green nonsulfur bacteria). The phylum *Chloroflexi* accommodates additional genera, including filamentous but nonphototrophic species (*Herpetosiphon*) and even nonfilamentous nonphototrophic species (*Thermoleophilum* and *Thermomicrobium*) (13). Fluorescence microscopy with infrared detection has been used to visualize bacteriochlorophyll-containing CLB in hot spring microbial mats (27). We have used fluorescence microscopy with blue excitation to discriminate potential CLB from cyanobacteria, because the latter fluoresce in the red visible light range and the former do not fluoresce in the red visible light range. *Chloroflexus aurantiacus*, which was initially isolated and described by Pierson and Castenholz (28), is the most-studied species of the *Chloroflexaceae* and is characterized by a versatile metabolism as it can grow photohetero- and photoautotrophically, as well as chemotrophically by oxygen respiration. It produces BChlc_s, which is characterized by an in vivo absorption maximum at 740 nm instead of the 745- to 755-nm absorption maximum of BChl*c* that is produced by the phylogenetically distantly related green sulfur bacteria (22). Despite the fact that CLB bacteriochlorophyll synthesis is repressed by oxygen (25, 28), CLB are often found to be abundant in the fully oxic photic zone of microbial mats (6, 14, 15, 19, 24), where they can utilize organic photosynthetic exudates from oxygenic phototrophs, probably their most preferred substrates (2, 13). Studies of BChl*a* production in the purple sulfur bacterium (PSB) *Thiocapsa roseopersicina* have shown that an anoxic period of only a few hours (the dark period in microbial mats) during a 24-h period is sufficient for production of enough photopigment to enable phototrophic growth during the light, oxic period in mats (8, 31). The same may be true for CLB and may explain the observed abundance of CLB in the oxic zone of microbial mats; however, in situ studies of the function and metabolism of CLB are still limited (24, 29, 33, 34). The aim of the present study was to characterize the impact of CLB on the community carbon and oxygen metabolism of a hypersaline microbial mat, making use of the observation that intact mats, as well as a pure culture of *C. aurantiacus*, showed a significant decrease in aerobic respiration upon illumination with near-infrared (NIR) light. There-

* Corresponding author. Mailing address: Delft University of Technology, Postbox 5048, NL-2600 GA Delft, The Netherlands. Phone: 31 152788743. Fax: 31 152786383. E-mail: h.m.jonkers@tudelft.nl.
▽ Published ahead of print on 20 April 2007.

fore, we measured the contribution of CLB to microbial mat community oxygen respiration under different illumination regimens, including visible (VIS) light (400 to 700 nm), VIS light plus NIR light (400 to 700 plus 710 to 770 nm), and dark conditions. In this combined physiological and molecular study we obtained quantitative CLB pigment analysis data, as well as 16S rRNA gene-based evidence demonstrating the presence of CLB in the mat, and we characterized the phylogenetic diversity of the CLB.

MATERIALS AND METHODS

Sample collection. Microbial mat samples were collected in October 2004 from near-shore mats of the hypersaline lake La Salada de Chiprana located in northeastern Spain (41°14′20″N, 0°10′55″W). Intact mat samples where taken for further studies to Bremen, Germany, where they were incubated in original lake water at 21°C with illumination cycles consisting of 16 h of light (300 μmol photons m^{-2} s^{-1}) and 8 h of darkness in a glass aquarium.

Characterization of CLB in Lake Chiprana microbial mats. (i) Oxygen and hydrogen sulfide dynamics in intact mats. In order to characterize the intact microbial mat, profiles of oxygen and hydrogen sulfide concentrations were determined at 100-μm intervals in the laboratory in a flowthrough chamber with artificial illumination (83 and 300 μmol photons m^{-2} s^{-1}) using a fiber optic lamp (Schott KL 1500) which has a halogen lamp as the light source. Oxygen profiles were also determined under dark conditions and with 33 and 166 μmol photons m^{-2} s^{-1}. Clark-type amperometric oxygen (tip diameter, 10 μm) and hydrogen sulfide (tip diameter, 15 μm) microsensors were used. Details concerning the use of oxygen and hydrogen sulfide sensors and calibration procedures have been described previously (17, 35). Microsensors were mounted on a motorized micromanipulator connected to a heavy stand. Positioning and data acquisition were performed automatically with a laptop computer. Before profiling, the microsensor tip was positioned on the sediment surface of the microbial mat with the aid of a binocular microscope.

(ii) Microscopic observations. The topmost 2-mm green stratum (i.e., the photic zone of the mat) was suspended in filtered lake water, and aliquots were removed and used for fluorescence microscopy. Microscopic samples were excited with blue light, and in combination with a long-pass filter (>520 nm) filamentous bacteria that were fluorescent (cyanobacteria) or nonfluorescent in the visible part of the light spectrum could be distinguished. Nonfluorescent thin filaments without visible sulfur inclusions were considered CLB. The diversity of CLB morphotypes was determined on the basis of filament width and length. The ratio of nonfluorescent filaments to fluorescent filaments was determined visually using multiple sample preparations.

(iii) Photopigment analysis. The photic zone (0- to 2-mm surface layer) was cut off frozen microbial mat samples and freeze-dried. Pigments were extracted after sonication in high-performance liquid chromatography (HPLC)-grade acetone. The extracts from two subsequent extractions were combined, and the carboxylic groups of extracted pigments were methylated with 2 or 3 drops of diazomethane dissolved in acetone using a modification of the method recommended by Sigma-Aldrich (catalog no. Z411736; Aldrich, Milwaukee, WI) using 1-methyl-3-nitro-1-nitrosoguanidine as the precursor. The solvent was evaporated using a speed vacuum machine for a few hours until the preparation was completely dry, leaving pigments in the tube. Pigments were redissolved in a 2-ml HPLC elution solution containing 45% acetonitrile, 50% methanol, and 5% water-based 50 mM ammonium-acetate buffer (pH 7.2). The liquid was filtered through a sterile 0.2-μm-pore-size filter, and a 100-μl aliquot was injected into an HPLC for pigment identification and quantification using a binary protocol as described previously (5).

(iv) CLB phylotype diversity: DNA extraction, PCR amplification, and cloning. In order to estimate the diversity of CLB phylotypes in the mat studied, a clone library was constructed. Genomic DNA was extracted from 0.2-g mat samples as described previously (1) and purified with a Wizard DNA clean-up system (Promega). An approximately 400-bp fragment of the 16S rRNA gene was amplified from genomic DNA using two primers specific for bacteria of the phylum *Chloroflexi* (green nonsulfur bacteria) (11), GNSB-941F (5′AGCGGA GCGTGTGGTTT3′) and GNSB-1340R (5′CGCGGTTACTAGCAAC3′). Two microliters of template was added to a 50-μl reaction mixture containing 0.5 U Eppendorf *Taq*, 1× buffer, 4 mM of $MgCl_2$, 4 mM of each deoxynucleoside triphosphate, and 1 μM of each primer. The reaction was performed in a Mastercycler thermocycler (Eppendorf, Hamburg, Germany) with the following cycling conditions: 95°C for 2 min and then 30 cycles of 95°C for 30 s, 55°C for 30 s, and 72°C for 1 min, followed by a final incubation at 72°C for 10 min. The PCR product was visualized on an agarose gel, and the 16S rRNA band was excised. The excised PCR product was then purified using a QIAquick gel extraction kit (QIAGEN, Hilden, Germany). Two microliters of purified product was then ligated into the pGEM-T Easy vector (Promega, Madison, WI) and then transformed into *Escherichia coli* TOP10 cells (Invitrogen, Carlsbad, CA) according to the manufacturer's recommendations. Overnight cultures were prepared from positive transformants in a 2-ml 96-well culture plate. Plasmid DNA was extracted and purified using a Montage 96 plasmid miniprep kit (Millipore, Billerica, MA).

(v) DNA sequencing and analysis. Purified plasmids were sequenced in one direction with the M13F primer, using a BigDye Terminator v3.0 cycle sequencing kit (Applied Biosystems, Foster City, CA). Samples were run on an Applied Biosystems 3100 genetic analyzer (Foster City, CA). A phylogenetic tree was constructed with the ARB software package (http://www.arb-home.de) (21). First, the partial sequences retrieved and amplified from the mat were grouped into phylotypes based on the criterion that sequences of the same phylotype share more than 96% similarity. Phylogenetic trees were constructed with the maximum likelihood, maximum parsimony, and neighbor joining methods, using publicly available sequences that were at least 1,100 bp long. Representative sequences from each phylotype were then added to the phylogenic trees by parsimony.

Functional analysis of CLB in mats and culture. (i) Aerobic respiration of *C. aurantiacus*. In order to determine the influence of different types of light (VIS and/or NIR illumination) on the metabolism of CLB (phototrophy versus aerobic respiration), an axenic culture of the hyperthermophilic strain *C. aurantiacus* DSM 635 was used as model for CLB in the natural environment (even though C. *aurantiacus* might be quite different from CLB present in hypersaline environments, pure cultures of hypersaline CLB species are not available). *C. aurantiacus* was cultured according to DSMZ recommendations in yeast extract medium amended with 1 mM sulfide. Cultures were incubated anaerobically at 55°C under a light-dark regimen consisting of 16 h of illumination with incandescent light (approximately 25 μmol photons m^{-2} s^{-1}) and 8 h of darkness. Oxygen consumption under different light conditions was determined with sulfide-depleted cultures. Just before oxygen consumption measurement, culture aliquots were aerated and then incubated in 25-ml glass tubes in a water bath at 55°C. An oxygen microsensor, fitted in a butyl rubber stopper, was inserted into the culture (protein content, 0.58 ± 0.03 mg ml^{-1}) without introduction of air bubbles and sealed to avoid contact with ambient air during the measurement. The change in the oxygen concentration over time was recorded. Cultures killed with formaldehyde (final concentration, 2%) were used to correct for abiotic oxygen consumption. Two sets of light-dark shift experiments were performed; the set of first experiments was performed with a combined VIS and NIR light source, and the second set of experiments was performed with only a VIS light source. In the first set of experiments light was provided by a 25-W incandescent (VIS plus NIR) light bulb in combination with two 40-mA NIR light-emitting diodes (LEDs) with a peak wavelength at 740 nm and a spectral full-width at half-maximum bandwidth of a 30-nm angle (LED-740-524; Roithner LaserTechnik, Austria). The light intensity as determined with a scalar irradiance light sensor (LI-250A; LI-COR Biosciences) was 15 μmol photons m^{-2} s^{-1} near the surface of the culture tube; however, the specific intensity of the NIR light was unknown as the light meter used is not sensitive in the NIR (>700-nm) light spectrum. The light source used in the second set of experiments was two warm white high-power LEDs (LXHL-MWGC; Lumileds, United States). The light range of these LEDs is restricted to the VIS part of the spectrum (400 to 700 nm). With this light source a light intensity of 60 μmol photons m^{-2} s^{-1} was measured at the surface of the inundated culture tube.

(ii) Aerobic respiration of intact mats under different illumination conditions. In order to elucidate the effect of NIR light illumination on oxygen dynamics, intact mat pieces were incubated in a flowthrough chamber at room temperature and illuminated with LEDs with VIS radiance (400 to 700 nm: LXHL-MWGC; Lumileds) and/or with two 40-mA NIR LEDs (LED-740-524; Roithner LaserTechnik, Austria). The advantage of using separate LEDs instead of using VIS/NIR filters in combination with a full-spectrum light source is that the light intensity of the light source with one type of spectrum is not changed when the light source with the other spectral type is switched on or off. VIS LEDs were used to illuminate mats at 60 μmol photons m^{-2} s^{-1} with or without additional NIR light illumination, and oxygen profiles were recorded after steady-state conditions were reached. The microbial mat areal net oxygen production rates were calculated from the change in oxygen fluxes in the diffusion boundary layer using an oxygen diffusion coefficient of 2.1×10^{-5} (25°C, 75 ppt) (see reference 35 for details concerning the procedure used). In order to determine whether oxygen evolution occurred with NIR light illumination, the oxygen profiles in

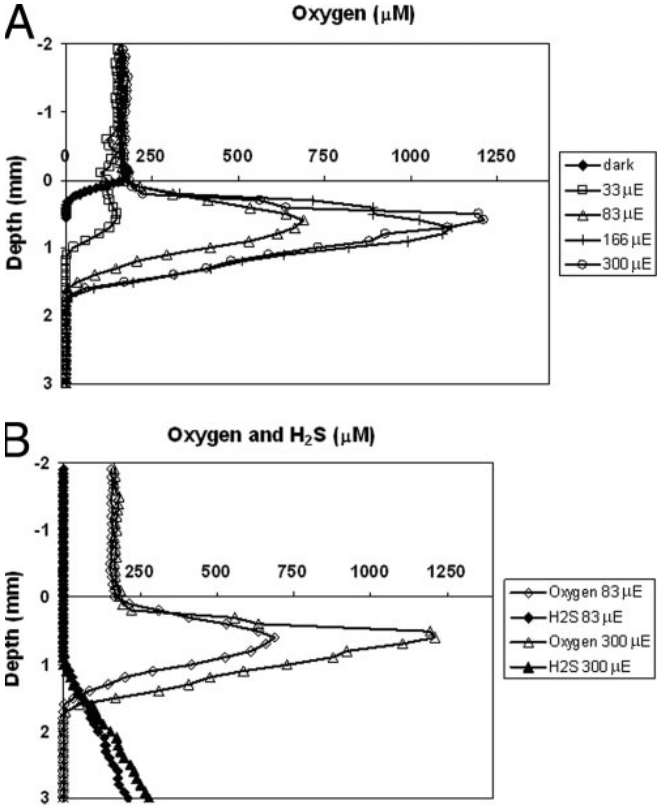

FIG. 1. Steady-state oxygen and sulfide profiles in Lake Chiprana microbial mats at different light intensities. (A) Oxygen concentration profiles with 0, 33, 83, 166, and 300 μmol photons m^{-2} s^{-1}. The oxygen concentration reaches up to six times the air saturation level at higher light intensities, indicating that CLB in the photic zone have to cope with high and fluctuating oxygen concentrations. (B) Oxygen and sulfide (H_2S) concentration profiles at light intensities of 83 and 300 μmol photons m^{-2} s^{-1}. Oxygen and sulfide cooccur in the zone between 1 and 1.5 mm deep, a zone where CLB are able to oxidize sulfide both phototrophically and chemotrophically, in the latter case using oxygen as the electron acceptor. μE, microeinsteins.

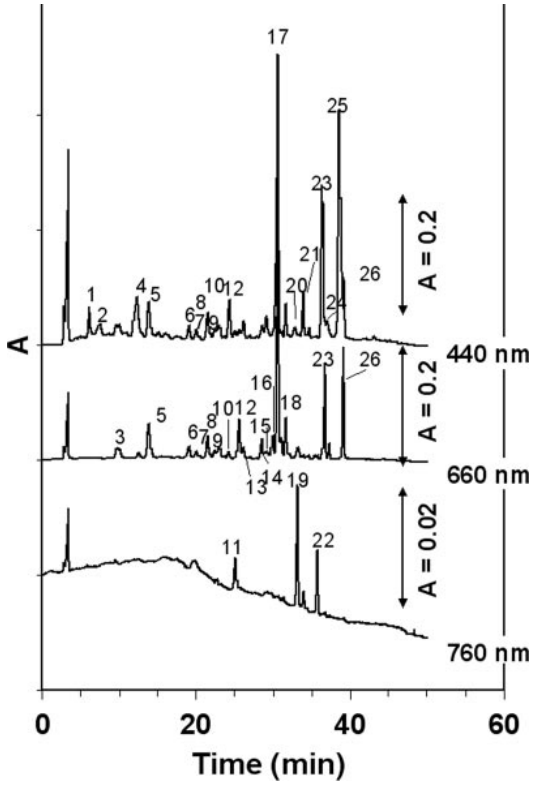

FIG. 2. HPLC chromatograms at 440, 660, and 760 nm for a sample from the top 5 mm of the Lake Chiprana microbial mat. Identified pigment molecules, indicated by numbers, are described in Table 1. The main pigments are Chl*a* (peak 17) and BChl*c* allomers (peaks 5, 6, 8, 12 to 14, and 16).

NIR light-illuminated mats were measured before and after the addition of 3-(3,4-dichlophenyl)-1-1-dimethylurea (DCMU), a specific inhibitor of the oxygen-evolving photosystem II. DCMU was added from a stock solution (1 mM dissolved in 70% ethanol) to a final concentration of 5 μM.

Nucleotide sequence accession numbers. The partial 16S rRNA gene sequences determined in this study have been submitted to the GenBank database and assigned accession numbers DQ973818 to DQ 973833.

RESULTS

Characterization of CLB in Lake Chiprana microbial mats. **(i) Microsensor characterization of the intact microbial mat.** The oxygen concentration profiles for illuminated mats show that oxygen is produced mainly in the first 1 mm and that the concentration reaches more than six times air saturation when the mats are illuminated with 300 μmol photons m^{-2} s^{-1} (Fig. 1A), while in the dark oxygen penetrated to a maximum depth of only 0.4 mm. Oxygen and hydrogen sulfide cooccurred just above the oxic-anoxic interface in the 1- to 1.5-mm layer (Fig. 1B). The mat was entirely anoxic from 1.5 mm down, while the hydrogen sulfide concentration increased below this depth. These measurements thus show that CLB present in the photic zone of the mat (0- to 2-mm surface layer) encounter high oxygen concentrations during illumination in the topmost part and also sulfide in the lower part of the photic zone. Both components are relevant for CLB metabolism, as oxygen can be used as an electron acceptor in aerobic respiration, while sulfide can be used as an electron donor during photoautotrophic growth or, alternatively, as an electron donor for energy generation in aerobic respiration.

(ii) Microscopic observations. The microbial mat comprised an association of filamentous cyanobacteria, mainly *Oscillatoria*-like (diameter, 2.5 μm), *Microcoleus*-like (diameter, up to 8 μm), and *Pseudanabaena*-like (diameter, about 3 μm) cyanobacteria, and had high densities of *Chloroflexus*-like filaments that did not exhibit red fluorescence. The last group had two different diameters (wider [>2 μm] and narrower [<1 μm]), with various lengths. The non-red-fluorescent filamentous bacteria were likely CLB, as they did not contain intracellular sulfur inclusions, typical of filamentous *Beggiatoa* strains. As CLB-specific NIR autofluorescence was not determined in this study, we cannot exclude the possibility that some of the filaments actually represented other bacteria, such as filamentous sulfate-reducing bacteria of the genus *Desulfonema* that were previously found to occur in hypersaline mats (10). The percentage of non-red-fluorescent filaments amounted to 20 to 30% of total filamentous bacteria in the photic zone.

(iii) Microbial mat photopigment analysis. HPLC analysis of the pigments of the microbial mat studied revealed the presence of BChl*a*, BChl*c*, and BChl*d*, as well as γ-carotene, pigments that are known to be produced by photosynthetic

TABLE 1. Pigment identification, retention times, and λ_{max} for the different peaks shown in the chromatograms in Fig. 2

Peak	Retention time (min)	Compound	λ_{max}
1	6.13	Unknown carotenoid	448
2	7.50	Bacteriopheaophorbide c, methyl ester	438, 505, 662
3	9.66	Phaeophorbide a, methyl ester	411, 661
4	12.29	Zeaxanthin	451, 475
5	13.90	BChl*c*	434, 663.
6	19.04	BChl*c*	430, 662
7	20.06	BChl*d*	427, 652
8	21.49	BChl*c*	431, 668
9	22.40	BChl*d*	428, 653
10	24.30	BChl*d*	428, 653
11	25.00	BChl*a*	373, 761
12	25.50	BChl*c*	434, 663
13	26.10	BChl*c*	435, 660
14	28.50	Bacteriopheaophytine *c*	412, 661
15	29.13	Bacteriopheaophytine *d*	409, 654
16	29.90	Bacteriopheaophytine *c*	411, 661
17	30.50	Chl*a*	431, 660
18	31.70	Allomer of Chl*a*	431, 659
19	33.20	Bacteriopheaophytine *a*	358, 525, 740
20	33.98	BChl*d*-like	435, 652
21	34.75	BChl*d*-like	433, 652
22	35.80	Bacteriopheaophytine *a*	359, 531, 666, 740
23	36.68	Phaeophytin *a*	409, 661
24	37.10	γ-Carotene	434, 460
25	38.70	β-Carotene	454, 480
26	39.10	Pyrophaeophytin *a*	409, 661

TABLE 2. Quantification of pigments of the Lake Chiprana microbial mat in September 2004[a]

Pigment(s)	Concn (μg cm^{-2})	
	Mean	SD
Total BChl*c*	10.7	2.6
Total BChl*d*	3.9	1.8
Chl*a*	11.2	2.8
Total phaeophytin *a* + pyrophaeophytin *a*	9.5	0.8
BChl*a*	0.15	0.06
Zeaxanthin	0.72	0.20
γ-Carotene	0.25	0.14
β-Carotene	1.14	0.26

[a] The ratio of BChl*a*, BChl*c*, and BChl*d* indicates that CLB are abundant in this mat.

members of the family *Chloroflexaceae* (12). Figure 2 shows the chromatograms at 440, 660, and 760 nm for a sample from the top layer of the mat, and the peaks are identified in Table 1. The pigment composition reflects a phototrophic community comprising cyanobacteria (chlorophyll *a* [Chl*a*], zeaxanthin, and β-carotene) and CLB (BChl*c*/*d*, γ-carotene, and minor amounts of BChl*a*). In addition, degradation products of these compounds were observed. The BChl*c*/*d* allomers eluted between 13 and 27 min (Fig. 2, peaks 5 to 10, 12, and 13). These retention times were longer than those observed for the farnesol-esterified BChl*c* homologs (BChlc_F) found in a culture of *Chlorobium tepidum*. This indicates that the BChl*c*/*d* homologs were more hydrophobic than the BChlc_F homologs and were thus esterified with another alcohol. *C. aurantiacus* contains different allomers of BChl*c* esterified with stearyl, phytyl, and geranylgeranyl alcohols. Further identification of the BChl*c*/*d* homologs requires HPLC-mass spectrometry. In addition, BChl*a* (peak 11) was found in the mats, and we also observed two late-eluting BChl*d*-like compounds. Different bacteriochlorophyll degradation products were identified as bacteriopheophorbide *c* and bacteriopheophytins *a*, *c*, and *d*. A number of peaks were quantified (Table 2). The ratio of BChl*c* to BChl*d* to BChl*a* was 72:26:1 on average.

(iv) CLB phylotype diversity. A total of 49 sequences were recovered by 16S rRNA PCR using *Chloroflexi*-specific primers designed by Gich et al. (11). This primer set targeted the 16S rRNA gene from various members of the phylum *Chloroflexi*, which includes isolated and characterized members of the anoxygenic phototrophic filamentous genera *Chloroflexus*, *Chloronema*, *Oscillochloris*, *Heliothrix*, and *Roseiflexus*. A total of eight major clusters (Fig. 3) of sequences were identified. There was significant diversity among the sequences that were recovered. Thus, we distinguished 16 different phylotypes, each comprising sequences that shared more than 96% sequence similarity. A representative sequence was selected from each phylotype that was considered in the phylogenetic analysis. Accordingly, most sequences were most closely related to the sequences from uncultured bacteria retrieved from various microbial mats, soils, sediments, and sludges. In general, the sequences recovered in this study were about 75 to 86% identical to sequences recovered in other studies. Ten of 49 sequences from this study clustered with sequences derived from members of the family *Chloroflexaceae* (clusters I to II); the remaining 39 sequences clustered with sequences from various other uncultured groups of bacteria distantly related to the family *Chloroflexaceae* (clusters III to VIII) but still within the phylum *Chloroflexi*. Some of these sequences appear to be distantly related to *Dehalococcoides* (phylum *Chloroflexi*, class *Dehalococcoides*). Seven sequences (cluster I) represented by LCC01 (two sequences), LCC77 (four sequences), and LCC57 were 90 to 99% identical to sequences recovered from a hypersaline microbial mat in Guerrero Negro, Mexico (23). Three sequences represented by LCC39 (cluster II) shared 88% identity with *C. aurantiacus*. They were the sequences most closely related to any 16S rRNA gene from a cultured organism.

Functional analysis of the CLB impact on microbial mat oxygen respiration. (i) Aerobic respiration of *C. aurantiacus*. *C. aurantiacus* pregrown under anoxic conditions in the presence of light was subjected to aerobic conditions by aerating culture aliquots just before aerobic respiration rates were measured. Examples of oxygen consumption measurements obtained during incandescent light bulb-NIR LED/dark or VIS LED/dark shifts are presented in Fig. 4. Calculated oxygen consumption rates under different illumination conditions are presented in Table 3. The oxygen consumption rate with NIR light illumination was significantly lower (ca. 50%) than that in the dark or with only VIS light illumination. No significant difference in the oxygen consumption rates between dark conditions and illumination with only VIS light was observed. The level of respiration in the dark calculated in the first experimental series was somewhat lower than that calculated in the second series (Table 3). This may have been due to the lower initial oxygen concentration in the first series. The formaldehyde-

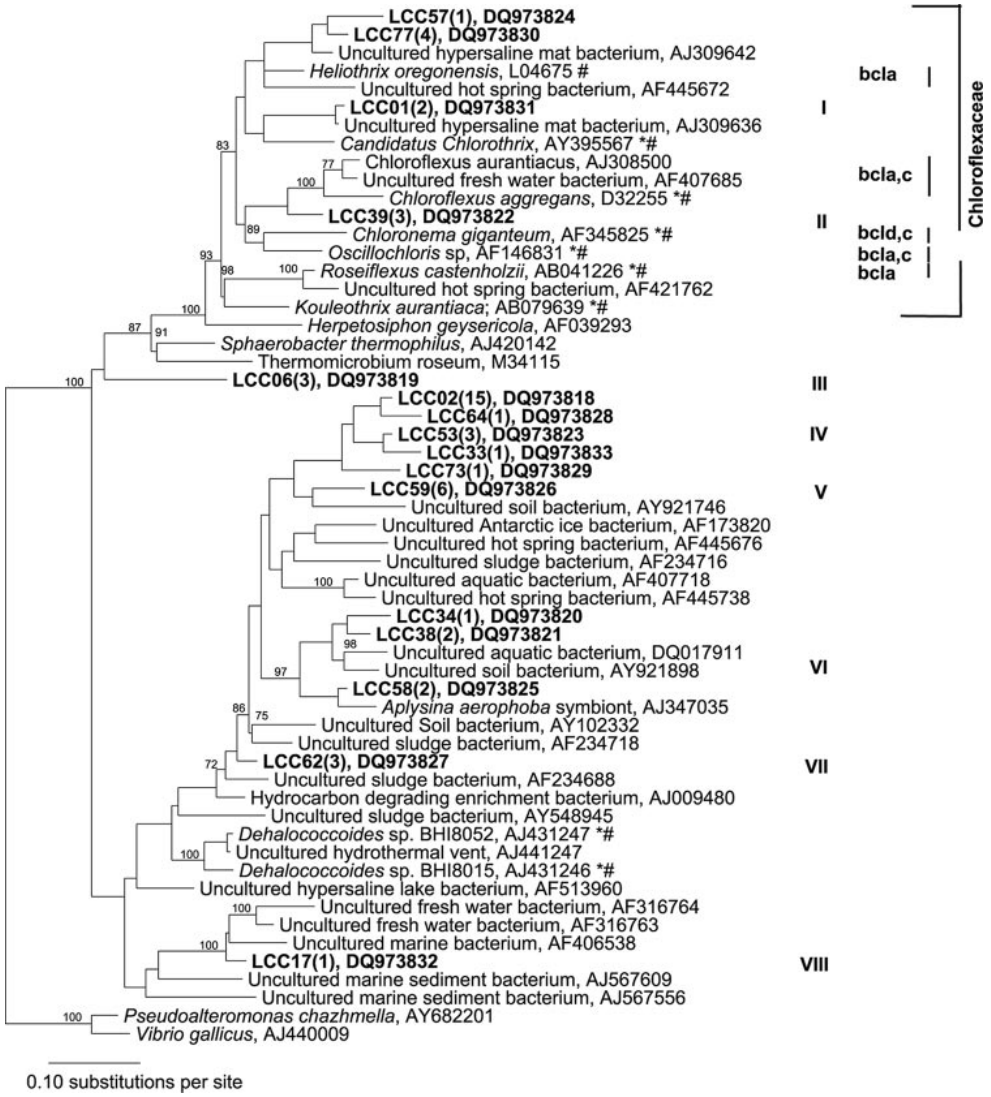

FIG. 3. 16S rRNA gene maximum parsimony tree for representative sequences obtained in this study (bold type) and sequences retrieved from the database. Sequences from this study in the tree represent groups of sequences that shared more than 96% identity; the numbers in parentheses indicate the numbers of sequences in the groups. Asterisks indicate known phototrophic species, and number signs indicate previously isolated and described species. The bootstrap values at the nodes are percentages based on 1,000 replications. Sequences from this study, as well as LO4675, AJ09636, and AJ309642, were excluded from the bootstrap analysis. Group I represents sequences recovered in this study, which formed a separate clade that included *H. oregonesis* (a chlorosome-less, BChl*a*- but not BChl*c*- or BChl*d*-producing species) and "Candidatus *Chlorothrix*" (chlorosome-containing, BChl*a*- and BChl*c*-producing species); group II represents sequences obtained in this study that formed a clade with *Chloroflexus*, *Chloronema*, and *Oscillochloris* (chlorosome-containing, BChl*a*- plus BChl*c*- or BChl*d*-producing species). Groups III to VIII represent sequences from this study which cluster with sequences distantly related to the family *Chloroflexaceae* but are still in the phylum *Chloroflexi*.

killed culture showed no measurable oxygen uptake over time. The NIR light applied to the *C. aurantiacus* culture was the maximum intensity that could be obtained with the NIR LED configuration used in this study. It may well be that this intensity was not high enough to saturate anoxygenic photosynthesis of the *C. aurantiacus* culture.

(ii) Effect of NIR light illumination on microbial mat community respiration. The effect of NIR light illumination on microbial mat community oxygen consumption was inferred from the steady-state oxygen profiles acquired under the different light conditions. Upon illumination with only NIR light, oxygen penetration significantly increased compared to that under dark conditions, from 0.40 to 0.55 mm (Fig. 5). A comparable phenomenon was observed when VIS light and NIR light were combined; the oxygen penetration depths were 0.7 and 0.9 mm when VIS light was used alone and when VIS light and NIR light were combined, respectively. With VIS light illumination alone (60 μmol photons m^{-2} s^{-1}) the oxygen concentration reached a maximum of 190 μM at a depth of 0.1 mm. When NIR light was subsequently added to the white light, the maximum oxygen concentration increased to 230 μM and oxygen penetrated to a depth of 0.175 mm. The calculated microbial mat areal net oxygen production or consumption values determined from the oxygen profiles measured under the different light conditions are presented in Table 4. Controls containing mats illuminated with only NIR light in which ox-

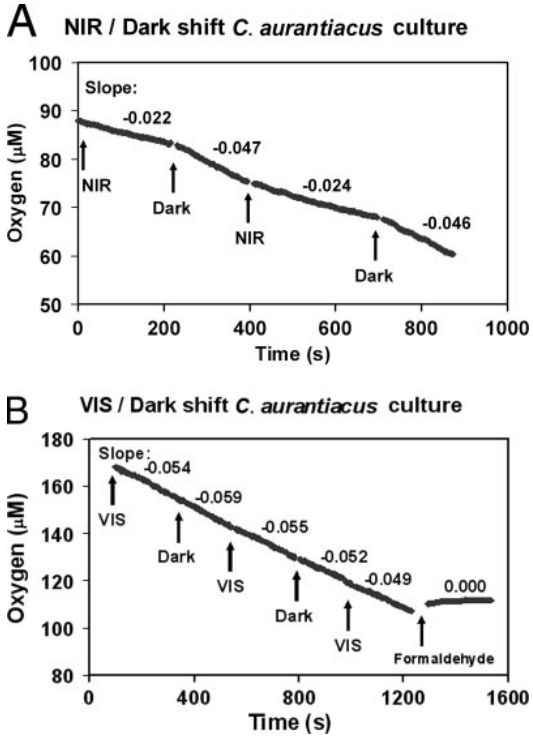

FIG. 4. Oxygen consumption in aerated axenic cultures of *C. aurantiacus* under different illumination conditions. (A) Alternating illumination with NIR light (25-W incandescent light bulb plus two 40-mA NIR LEDs [710 to 770 nm]) and darkness. (B) Alternating illumination with VIS light (two VIS LEDs [400 to 700 nm]) and darkness, as well as the formaldehyde-killed control. See Table 3 for calculated specific respiration rates.

ygen profiles were measured before and after DCMU addition showed no difference in oxygen concentration and penetration depth. These observations indicate that NIR illumination did not result in oxygenic photosynthesis in this specific hypersaline microbial mat. Otherwise, in DCMU-inhibited mats the oxygen concentration would have been decreased due to continued respiration and ceased oxygenic photosynthesis. The unchanged oxygen concentration profile after DCMU addition also shows that the addition of ethanol (part of the DCMU stock solution) to the mat did not result in increased aerobic respiration rates in the short term. The latter conclusion also

TABLE 3. *C. aurantiacus* aerobic respiration rates in aerated axenic culture aliquots ($n = 4$) under different illumination conditions

Expt series	Light conditions	Respiration rate (μmol O_2 g protein^{-1} min^{-1})[a]
1	Bulb + NIR LEDs (15)[b]	2.48 ± 0.17
	Dark	4.47 ± 0.59
2	VIS LEDs (60)[b]	5.44 ± 0.29
	Dark	5.75 ± 0.50

[a] The respiration rates under dark conditions and with VIS light illumination are not significantly different. However, the respiration rates with NIR light illumination (25-W incandescent light bulb plus two 40-mA NIR LEDs) and dark conditions are significantly different.

[b] The values in parentheses are light intensities at 400 to 700 nm expressed in μmol photons m^{-2} s^{-1}.

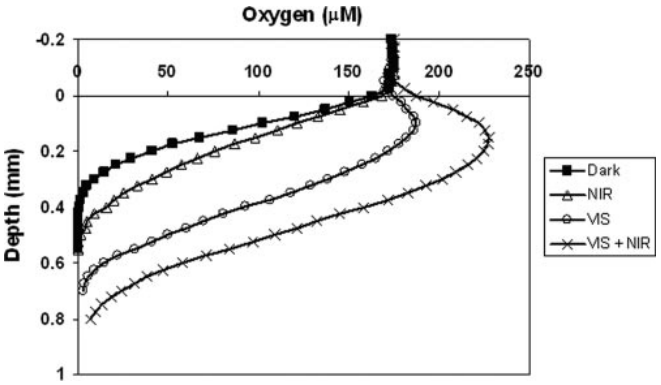

FIG. 5. Steady-state oxygen concentration profiles in the Lake Chiprana microbial mat under four different light conditions: (i) darkness, (ii) NIR light (two 40-mA NIR LEDs [710 to 770 nm]), (iii) VIS light (two VIS LEDs [400 to 700 nm]; 60 μmol photons m^{-2} s^{-1}), and (iv) two NIR LEDs plus two VIS LEDs.

supports the finding of Ludwig et al. (20) that aerobic respiration in Lake Chiprana microbial mats is not limited by organic carbon compounds.

DISCUSSION

The investigated microbial mat from hypersaline Lake Chiprana in Spain appeared to be rich in CLB in the photic zone, as demonstrated by microscopy, pigment analysis, and the diversity of CLB-related partial 16S rRNA gene sequences. The fact that CLB occur not only in hot spring microbial mats but also in hypersaline mats was also determined in previous studies (14, 23, 19, 32); however, the in situ metabolic function of CLB in carbon cycling remains to be clarified. In this study we developed a method that allows us to evaluate the proportion of the oxygen and carbon metabolism that is directly attributed to the metabolic activity of CLB in the mat. For this we used the finding that CLB can switch their metabolism from anoxygenic photosynthesis with NIR illumination to aerobic respiration in the absence of NIR illumination. We corroborated this finding for a pure culture of *C. aurantiacus*. As the electromagnetic spectrum of sunlight comprises both VIS and NIR light, we decided to use artificial illumination with specific LEDs and not filters, which were used originally (9). Filters may decrease the light intensity or otherwise affect the nontarget light field and thus may influence, e.g., the VIS light intensity and simultaneously the oxygenic photosynthesis rates, which would influence the oxygen concentration in mats and thus hamper the quantification of CLB respiration rates. In

TABLE 4. Net areal oxygen production rates calculated from oxygen concentration profiles in Lake Chiprana microbial mats under different illumination conditions[a]

Light conditions	Net areal O_2 production (nmol O_2 cm^{-2} s^{-1})
Dark	−0.13
NIR	−0.10
VIS	0.03
VIS + NIR	0.07

[a] See Fig. 4. Negative values indicate net consumption.

this study illumination with NIR light with a spectrum of 740 ± 30 nm in addition to darkness or illumination with only VIS light (with a spectrum of 400 to 700 nm) led to a substantial increase in the net areal mat oxygen production rate. As 740 nm is the specific absorption wavelength of BChlc_s, which is known to be produced by *C. aurantiacus*, and to a lesser extent of BChl*c* and BChl*d*, which are also produced by CLB species, we concluded that the observed effect on mat community oxygen dynamics was due to the metabolic activity of CLB species. Like CLB, in the presence of oxygen PSB (7) and purple nonsulfur bacteria may immediately switch their metabolism from anoxygenic photosynthesis to aerobic respiration when NIR illumination is suddenly stopped. However, these bacteria have a very low absorption cross section at 740 nm and, therefore, virtually do not use the light of the LEDs used in this study. Moreover, microscopic observations revealed only very small quantities of typical PSB morphotypes, and, in general, the specific respiration rates of *Chromatiaceae* (PSB) (7, 26) are 1 to 2 orders of magnitude lower than those that we found for *C. aurantiacus*. Green sulfur bacteria that also contain BChl*a*, BChl*c*, and BChl*d* have been found in some microbial mats. However, these bacteria are strict anaerobes that are confined to the permanent anoxic layers of the mats and cannot contribute to oxygen respiration. Recently, a cyanobacterium that produces Chl*d* and absorbs light in the NIR light spectrum was isolated (18). Whether such presumably oxygen-producing organisms comprise a substantial part of the microbial community in the mat remains to be investigated, although no Chl*d* was detected in this study. However, we concluded that if present, such organisms could not be responsible for the observed increase in oxygen concentration upon additional NIR light illumination as control experiments with DCMU, a specific inhibitor of photosystem II and thus oxygen production, did not result in a decrease in the oxygen concentration when mats illuminated with only NIR light were used.

The role that CLB play in the local carbon cycle can be inferred from their respiration rate under non-NIR light conditions. Axenic culture experiments with *C. aurantiacus* showed that the oxygen respiration decreased by about 50% upon illumination with NIR light. CLB can switch from anoxygenic phototrophy, which provides energy due to cyclic electron transport in photosystem I, to aerobic respiration to sustain energy generation under dark conditions (13). It can thus be assumed that the amount of oxygen respired under non-NIR light conditions at least equals the equivalent energy that was produced by anoxygenic photosynthesis by active CLB illuminated with NIR light. Therefore, one way to estimate the role of CLB in the local carbon cycle is to compare their non-NIR light respiration to the total community respiration. In the dark, the total community respiration, as inferred from microbial mat areal oxygen uptake, decreased from 0.13 to 0.10 nmol O_2 cm^{-2} s^{-1}, a decrease of 25%, upon illumination with NIR light. When NIR light was supplied along with VIS light, the net community areal oxygen production increased from 0.03 to 0.07 nmol O_2 cm^{-2} s^{-1}; thus, the apparent net primary production more than doubled, likely as a result of a decrease in CLB respiration due to a switch to anoxygenic phototrophy for energy generation.

The measurable change in oxygen dynamics upon illumination with NIR light (740 nm) of intact mats can thus be attributed to CLB activity. However, as this metabolic shift is directly linked to the mode of energy generation, no conclusions can be drawn as to whether a shift in the electron donor for autotrophic growth (e.g., reduced sulfur compounds) or a shift in the carbon source (organic or inorganic) for hetero- or autotrophic growth also occurs. CLB are known to be able to use various inorganic compounds as electron donors during autotrophic growth, as well as inorganic and various organic compounds as carbon sources during phototrophic or heterotrophic growth (13, 34). The fact that CLB can be found at high densities in microbial mats is likely due to this versatile metabolism. In mats light intensity and oxygen, reduced sulfur compound, and dissolved inorganic and organic carbon concentrations change rapidly during a full 24-h diel cycle, conditions to which CLB are maximally adapted. In such systems these bacteria would have a competitive advantage over more specialized but metabolically more restricted organisms.

The capacity to switch from anoxygenic photosynthesis to respiration has thus been clearly demonstrated for *C. aurantiacus* in culture experiments and has been inferred for the CLB in a microbial mat from oxygen profiles. This ability, which is apparently widespread among CLB, has important consequences for the quantification of gross photosynthesis in mats using the traditional light/dark shift method, which was introduced by Revsbech et al. in 1981 (30) and has been used in numerous studies since. This method is based on the assumption (among others) that in a microbial mat under steady-state (stable oxygen profile) conditions, the community oxygen consumption rate is unchanged initially (for at least a few seconds) when the mat is switched from light to darkness. The rate of oxygen disappearance at the start of the dark period then equals the rate of oxygen production in the light (30). This assumption, however, does not hold when *C. aurantiacus* or other CLB make up a significant part of the microbial community, as these organisms may switch within seconds from anoxygenic photosynthesis in the light to aerobic respiration in the dark. The fact that this effect can be substantial was shown in this study, where the apparent net photosynthesis more than doubled when NIR light was supplied along with VIS light. Hence, using the traditional light/dark shift method, gross photosynthesis rates are substantially overestimated in CLB-rich microbial mats. However, this effect can be compensated for, if only VIS light (400 to 700 nm) is used as a light source (CLB behave as aerobic bacteria [i.e., continuously respire]) or, alternatively, an additional NIR light source remains on continuously (CLB continue anoxygenic phototrophy and do not switch to aerobic respiration when VIS light is switched off) during measurements.

The high diversity of 16S rRNA gene phylotypes affiliated with the phylum *Chloroflexi* indicates that besides a number of sequences that group in the family *Chloroflexaceae*, nonfilamentous and even nonphototrophic *Chloroflexi* may be present in the mat examined. It is difficult to infer the type of chlorophyll that a bacterium possesses based on our 16S rRNA data given the paucity of 16S rRNA gene sequences available for cultured members of the *Chloroflexaceae*. However, the three sequences represented by LCC39 (cluster II) group with sequences from two characterized *Chloroflexus* species and are therefore likely to represent BChl*c*-producing CLB active in this system. The six sequences in cluster I that were recovered

in this study are most closely related to the 16S rRNA gene from *Heliothrix oregonensis*, a CLB that does not, like *Chloroflexus* species, produce BChl*c* or BChl*d* in addition to BChl*a*. The organisms responsible for these sequences may thus not have contributed to the observed changes in community oxygen respiration when illumination with 740-nm NIR light was manipulated. The three sequences represented by LCC39 from the mat are the sequences that are most closely related to the 16S rRNA gene from *C. aurantiacus* which originated from a hot spring microbial mat and which so far is the most intensely studied and characterized species in the family *Chloroflexaceae*. However, they share sequence identity of only 88%. The highest sequence identity obtained for the hypersaline mat studied here (cluster I) was the sequence identity with sequences that originated from a mat in Guerrero Negro, Mexico (accession no. AJ309642 and AJ309636) (23), which was also a hypersaline microbial mat but was on a different continent. The sequence similarity between these sequences was up to 99%, which indicates that at least some hypersaline *Chloroflexaceae* may have a cosmopolitan distribution.

This study focused on CLB, which are filamentous phototrophic bacteria that are members of the family *Chloroflexaceae*. Although the clone library in this study retrieved 10 of 49 sequences that grouped in the family *Chloroflexaceae*, it is not known whether all these sequences represent filamentous phototrophic bacteria, as only a few sequences from this group represent well-characterized strains. Furthermore, the clone library shows that sequences retrieved in this study that fall outside the family *Chloroflexaceae* but still cluster within the phylum *Chloroflexi* are all most closely related to sequences from uncultured organisms. The apparently high but uncharacterized diversity of *Chloroflexi*-related sequences retrieved from the specific hypersaline mat studied seems to be typical, as other studies of various hot spring mats (24, 29) and hypersaline mats (19, 23), as well as other ecosystems (3, 11), reported the same diversity. An intriguing question is what kind of species these sequences belong to and what ecological role they play in these ecosystems. Future cultivation and ecophysiological characterization studies must resolve this question.

ACKNOWLEDGMENTS

We thank Alfredo Legaz (COMENA, Caspe) and the local authorities in Chiprana for granting permission to access Lake Chiprana and take microbial mat samples. We are grateful to Dirk de Beer and Lubos Polerecky for discussions and technical help.

A. Bachar was supported by grant DFG JO-412 from the German Research Foundation. R. de Wit acknowledges support from the Deutscher Akademischer Austausch Dienst (DAAD) and the Agence National de la Recherche (program CYANOCARBO).

REFERENCES

1. **Abed, R. M. M., and F. Garcia-Pichel.** 2001. Long-term compositional changes after transplant in a microbial mat cyanobacterial community revealed using a polyphasic approach. Environ. Microbiol. **3:**53–62.
2. **Bateson, M. M., and D. M. Ward.** 1988. Photoexcretion and fate of glycolate in a hot-spring cyanobacterial mat. Appl. Environ. Microbiol. **54:**1738–1743.
3. **Bjornsson, L., P. Hugenholtz, G. W. Tyson, and L. L. Blackall.** 2002. Filamentous Chloroflexi (green non-sulfur bacteria) are abundant in wastewater treatment processes with biological nutrient removal. Microbiology **149:** 2309–2318.
4. **Boomer, S. M., D. P. Lodge, B. E. Dutton, and B. Pierson.** 2002. Molecular characterization of novel red green nonsulfur bacteria from five distinct hot spring communities in Yellowstone National Park. Appl. Environ. Microbiol. **68:**346–355.
5. **Buffan-Dubau, E., O. Pringault, and R. DeWit.** 2001. Artificial cold-adapted microbial mats cultured from Antarctic lake samples. 1. Formation and structure. Aquat. Microb. Ecol. **26:**115–125.
6. **D'Amelio, E. D., Y. Cohen, and D. J. DesMarais.** 1987. Association of a new type of gliding, filamentous, purple phototrophic bacterium inside bundles of *Microcoleus chthonoplastes* in hypersaline microbial mats. Arch. Microbiol. **147:**213–220.
7. **DeWit, R., and H. VanGemerden.** 1987. Chemolithotrophic growth of the phototrophic sulfur bacterium *Thiocapsa roseopersicina*, FEMS Microbiol. Ecol. **45:**117–126.
8. **DeWit, R., and H. VanGemerden.** 1990. Growth and metabolism of the purple sulfur bacterium *Thiocapsa roseopersicina* under combined light dark and oxic anoxic regimens. Arch. Microbiol. **154:**459–464.
9. **DeWit, R., L. Falcón, and C. Charpy-Roubaud.** 2005. Heterotrophic dinitrogen fixation (acetylene reduction) in phosphate-fertilised *Microcoleus chthonoplastes* microbial mat from the hypersaline inland lake "la Salada de Chiprana" (NE Spain). Hydrobiology **534:**245–253.
10. **Fukui, M., A. Teske, B. Assmus, G. Muyzer, and F. Widdel.** 1999. Physiology, phylogenetic relationships, and ecology of filamentous sulfate-reducing bacteria (genus *Desulfonema*). Arch. Microbiol. **172:**193–203.
11. **Gich, F., J. Garcia-Gil, and J. Overmann.** 2001. Previously unknown and phylogenetically diverse members of the green nonsulfur bacteria are indigenous to freshwater lakes. Arch. Microbiol. **177:**1–10.
12. **Gich, F., R. L. Airs, M. Danielsen, B. J. Keely, C. A. Abella, J. Garcia-Gil, M. Miller, and C. M. Borrego.** 2003. Characterization of the chlorosome antenna of the filamentous anoxygenic phototrophic bacterium *Chloronema* sp. strain UdG9001. Arch. Microbiol. **180:**417–426.
13. **Hanada, S., and B. K. Pierson.** November 2002, posting date. The family Chloroflexaceae. *In* M. Dworkin et al. (ed.), The prokaryotes: an evolving electronic resource for the microbiological community, 3rd ed., release 3.11. Springer-Verlag, New York, NY. http://link.springer-ny.com/link/service/books/10125. Accessed 28 August 2006.
14. **Jonkers, H. M., R. Ludwig, R. DeWit, O. Pringault, G. Muyzer, H. Niemann, N. Finke, and D. DeBeer.** 2003. Structural and functional analysis of a microbial mat ecosystem from a unique permanent hypersaline inland lake: 'La Salada de Chiprana' (NE Spain). FEMS Microbiol. Ecol. **44:**175–189.
15. **Jørgensen, B. B., and D. C. Nelson.** 1988. Bacterial zonation, photosynthesis, and spectral light-distribution in hot-spring microbial mats of Iceland. Microb. Ecol. **16:**133–147.
16. **Klappenbach, J. A., and B. K. Pierson.** 2004. Phylogenetic and physiological characterization of a filamentous anoxygenic photoautotrophic bacterium 'Candidatus Chlorothrix halophila' gen. nov., sp. nov. recovered from hypersaline microbial mats. Arch. Microbiol. **181:**17–25.
17. **Kühl, M., C. Steuckart, G. Eickert, and P. Jeroschewski.** 1998. A H_2S microsensor for profiling biofilms and sediments: application in an acidic lake sediment. Aquat. Microb. Ecol. **15:**201–209.
18. **Kühl, M., M. Chen, P. J. Ralph, U. Schreiber, and A. W. D. Larkum.** 2005. A niche for cyanobacteria containing chlorophyll d. Nature **433:**820.
19. **Ley, R. E., J. K. Harris, J. Wilcox, J. R. Spear, S. R. Miller, B. M. Bebout, J. A. Maresca, D. A. Bryant, M. L. Sogin, and N. R. Pace.** 2006. Unexpected diversity and complexity of the Guerrero Negro hypersaline microbial mat. Appl. Environ. Microbiol. **72:**3685–3695.
20. **Ludwig, R., O. Pringault, R. DeWit, D. DeBeer, and H. M. Jonkers.** 2006. Limitation of oxygenic photosynthesis and oxygen consumption by phosphate and organic nitrogen in a hypersaline microbial mat: a microsensor study. FEMS Microbiol. Ecol. **57:**9–17.
21. **Ludwig, W., O. Strunk, R. Westram, L. Richter, H. Meier, Yadhukumar, A. Buchner, T. Lai, S. Steppi, G. Jobb, W. Forster, I. Brettske, S. Gerber, A. W. Ginhart, O. Gross, S. Grumann, S. Hermann, R. Jost, A. Konig, T. Liss, R. Lussmann, M. May, B. Nonhoff, B. Reichel, R. Strehlow, A. Stamatakis, N. Stuckmann, A. Vilbig, M. Lenke, T. Ludwig, A. Bode, and K. H. Schleifer.** 2004. ARB: a software environment for sequence data. Nucleic Acids Res. **32:**1363–1371.
22. **Madigan, M. T., J. M. Martinko, and J. Parker.** 2000. Brock—biology of microorganisms, 9th ed. Prentice-Hall, Inc., Englewood Cliffs, NJ.
23. **Nübel, U., M. M. Bateson, M. T. Madigan, M. Kühl, and D. M. Ward.** 2001. Diversity and distribution in hypersaline microbial mats of bacteria related to *Chloroflexus* spp. Appl. Environ. Microbiol. **67:**4365–4371.
24. **Nübel, U., M. M. Bateson, V. VanDieken, A. Wieland, M. Kühl, and D. M. Ward.** 2002. Microscopic examination of distribution and phenotypic properties of phylogenetically diverse *Chloroflexaceae*-related bacteria in hot spring microbial mats. Appl. Environ. Microbiol. **68:**4593–4603.
25. **Oelze, J.** 1992. Light and oxygen regulation of the synthesis of bacteriochlorophylls *a* and *c* in *Chloroflexus aurantiacus*. J. Bacteriol. **174:**5021–5026.
26. **Overmann, J., and N. Pfennig.** 1992. Continuous growth and respiration of Chromatiaceae species at low oxygen concentrations. Arch. Microbiol. **158:** 59–67.
27. **Pierson, B. K., and H. M. Howard.** 1972. Detection of bacteriochlorophyll containing microorganisms by infrared fluorescence photomicrography. J. Gen. Microbiol. **73:**359–363.
28. **Pierson, B. K., and R. W. Castenholz.** 1974. Studies of pigments and growth in *Chloroflexus aurantiacus*, a phototrophic filamentous bacterium. Arch. Microbiol. **100:**283–305.

29. **Pierson, B. K., D. Valdez, M. Larsen, E. Morgan, and E. E. Mack.** 1994. *Chloroflexus*-like organisms from marine and hypersaline environments—distribution and diversity. Photosynth. Res. **41:**35–52.
30. **Revsbech, N. P., B. B. Jørgensen, and O. Brix.** 1981. Primary production of microalgae in sediments measured by oxygen microprofile, H-CO-14(3)-fixation, and oxygen-exchange methods. Limnol. Oceanogr. **26:**717–730.
31. **Schaub, B. E. M., and H. VanGemerden.** 1994. Simultaneous phototrophic and chemotropic growth in the purple sulfur bacterium *Thiocapsa roseopersicina* M1. FEMS Microbiol. Ecol. **13:**185–195.
32. **Sorensen, K. B., D. E. Canfield, A. P. Teske, and A. Oren.** 2005. Community composition of a hypersaline endoevaporitic microbial mat. Appl. Environ. Microbiol. **71:**7352–7365.
33. **van der Meer, M. T. J., S. Schouten, J. S. S. Damste, J. W. DeLeeuw, and D. M. Ward.** 2003. Compound-specific isotopic fractionation patterns suggest different carbon metabolisms among *Chloroflexus*-like bacteria in hot-spring microbial mats. Appl. Environ. Microbiol. **69:**6000–6006.
34. **van der Meer, M. T. J., S. Schouten, M. M. Bateson, U. Nübel, A. Wieland, M. Kühl, J. W. De Leeuw, J. S. S. Damste, and D. M. Ward.** 2005. Diel variations in carbon metabolism by green nonsulfur-like bacteria in alkaline siliceous hot spring microbial mats from Yellowstone National Park. Appl. Environ. Microbiol. **71:**3978–3986.
35. **Wieland, A., and M. Kühl.** 2000. Short-term temperature effects on oxygen and sulfide cycling in a hypersaline cyanobacterial mat (Solar Lake, Egypt). Mar. Ecol. Prog. Ser. **196:**87–102.

Chapter III:

Contribution of *Chloroflexus* respiration to oxygen cycling in a hypersaline microbial mat from Lake Chiprana, Spain

Environmental Microbiology (2007) **9**(8), 2007–2024 doi:10.1111/j.1462-2920.2007.01317.x

Contribution of *Chloroflexus* respiration to oxygen cycling in a hypersaline microbial mat from Lake Chiprana, Spain

Lubos Polerecky,[1]* Ami Bachar,[1] Raphaela Schoon,[1] Mor Grinstein,[2] Bo Barker Jørgensen,[1] Dirk de Beer[1] and Henk M. Jonkers[1,3]

[1]*Max-Planck-Institute for Marine Microbiology, Celsiusstrasse 1, DE-28359 Bremen, Germany.*

[2]*The Institute of Earth Sciences, The Hebrew University of Jerusalem, Israel.*

[3]*Delft University of Technology, Postbox 5048, NL-2600 GA Delft, the Netherlands.*

Summary

In dense stratified systems such as microbial mats, photosynthesis and respiration are coupled due to a tight spatial overlap between oxygen-producing and -consuming microorganisms. We combined microsensors and a membrane inlet mass spectrometer with two independent light sources emitting in the visible (VIS) and near infrared (NIR) regions to study this coupling in more detail. Using this novel approach, we separately quantified the activity of the major players in the oxygen cycle in a hypersaline microbial mat: gross photosynthesis of cyanobacteria, NIR light-dependent respiration of *Chloroflexus*-like bacteria (CLB) and respiration of aerobic heterotrophs. Illumination by VIS light induced oxygen production in the top ~1 mm of the mat. In this zone CLB were found responsible for all respiration, while the contribution of the aerobic heterotrophs was negligible. Additional illumination of the mat with saturating NIR light completely switched off CLB respiration, resulting in zero respiration in the photosynthetically active zone. We demonstrate that microsensor-based quantification of gross and net photosyntheses in dense stratified systems should carefully consider the NIR light-dependent behaviour of CLB and other anoxygenic phototrophic groups.

Received 12 December, 2006; accepted 11 March, 2007. *For correspondence. E-mail lpolerec@mpi-bremen.de; Tel. (+49) 421 2028 834; Fax (+49) 421 2028 690.

Introduction

Microbial mats are condensed, complete ecosystems where full biogeochemical cycles fuelled by light take place. Microbial populations are organized in vertical layers aligned according to the gradients of environmental parameters such as light, O_2, H_2S, pH, dissolved organic matter. Microbial mats are found usually in extreme habitats, where mostly prokaryotes and only a few eukaryotic species (e.g. brine shrimps, some algae, like diatoms) are able to thrive. One such extreme environment is the hypersaline lake *La Salada de Chiprana* in north-east Spain, with average salinity of 78 g l^{-1} dominated by magnesium sulfate. The Chiprana mats have been extensively studied as to their microbial composition, photosynthetic and calcification activity, carbon cycling and microenvironments encountered during light and dark conditions (Vidondo *et al*., 1993; Valero-Garces *et al*., 2000; Vila *et al*., 2002; Camacho and de Wit, 2003; Jonkers *et al*., 2003; de Wit *et al*., 2005; Jonkers *et al*., 2005; Ludwig *et al*., 2005). An interesting aspect of these mats is the high abundance of anoxygenic *Chloroflexus*-like bacteria (CLB) found in the fully oxic top layer (1–2 mm) of the mat along with oxygen-producing cyanobacteria (Jonkers *et al*., 2003).

Chloroflexus-like bacteria are filamentous anoxygenic phototrophs (Pierson and Castenholz, 1995). They are members of the family Chloroflexaceae which is composed of five genera: *Chloroflexus*, *Chloronema*, *Oscillochloris*, *Heliothrix* and *Roseiflexus* (Castenholz, 2001). *Chloroflexus aurantiacus*, the first-described (Pierson and Castenholz, 1974) and most-studied species of the Chloroflexaceae, originated from a thermal spring microbial mat and is physiologically highly versatile. *Chloroflexus* species grow photoheterotrophically (using light as energy source and various organic compounds as carbon source) and chemoheterotrophically (organic carbon serves both as energy and as carbon source) using organic cyanobacterial exudates (van der Meer *et al*., 2003; Hanada and Pierson, 2006), as well as photoautotrophically (using light as energy source, sulfide and/or hydrogen as electron donor, and CO_2 as carbon source) (Madigan and Brock, 1975; Holo and Sirevaeg, 1986; van der Meer *et al*., 2000). Prevailing *in situ* conditions

apparently largely determine which metabolic mode is preferred. *Chloroflexus* in illuminated sulfidic hot spring mats was found to grow photoautotrophically, but switches to photoheterotrophy when cyanobacteria co-occur, apparently due to organic carbon cross-feeding (van der Meer *et al*., 2003). It was suggested that the mode of metabolism of *Chloroflexus* and *Roseiflexus* species is apparently dependent on the time of the day; during the morning, under low-light and sulfidic conditions, a potential for photoautotrophic metabolism was observed, while chemotrophic and photoheterotropic organic carbon incorporation was preferred in the dark at night and under high-light conditions, respectively (van der Meer *et al*., 2005). From these studies it can be concluded that CLB prefer light as energy source and only switch to aerobic respiration in the dark. Moreover, they prefer organics as carbon source but, if present, additionally oxidize sulfide and other reduced compounds such as hydrogen for CO_2 fixation. Due to this metabolic versatility, *Chloroflexus* can be important in various benthic ecosystems, e.g. in cyanobacterial mats, where particularly high densities of CLB are found.

Oxygenic phototrophs like cyanobacteria utilize light in the visible (VIS) region using light-harvesting pigments Chlorophyll *a* and phycobilins (Chl *a*: around 430 + 675 nm; phycoerythrin: 550 nm; phycocyanin: 625 nm) (Madigan *et al*., 2000). In contrast, bacteria of the family Chloroflexaceae produce the photopigment Bacteriochlorophyll *a*, with or without additional Bacteriochlorophyll *c* or *d* (Hanada and Pierson, 2006), and harvest light energy in the near infrared (NIR; BChl *a*: 805 + 830–890 nm; BChl *c*: 745–755 nm; BChl c_s: 740 nm; BChl *d*: 705–740 nm) (Madigan *et al*., 2000). Cyanobacteria and CLB thus make use of complementary spectral regions of light that penetrates the top few millimetres of the mat.

Although CLB are often encountered as abundant community members in diverse systems, such as marine and hypersaline microbial mats (Pierson *et al*., 1994; Nübel *et al*., 2001; Jonkers *et al*., 2003; Villanueva *et al*., 2004), freshwater sediments (Gich *et al*., 2001; Nübel *et al*., 2002) or wastewater treatment plants (Bjornsson *et al*., 2002), their *in situ* activity has not been investigated in much detail. Furthermore, our knowledge of their metabolic traits is based on a very limited number of isolates (Pierson and Castenholz, 1974; 1995). Recently, Bachar and colleagues (2007) exploited the ability of CLB to switch between phototrophy in the NIR light and aerobic respiration in the dark to qualitatively assess the contribution of CLB to community respiration. In that study it was shown that, in comparison with the respiration in the dark, *C. aurantiacus* in pure culture dramatically decreased oxygen respiration under NIR illumination (715–745 nm) while its respiration under VIS illumination (400–700 nm) remained unchanged. Likewise, the community respiration of an intact microbial mat from Lake Chiprana decreased significantly upon addition of NIR light to VIS illumination, which was attributed to the high abundance of CLB in the mat.

The aim of this work was to quantify the contribution of CLB to the total O_2 budget (gross production versus respiration) in an intact microbial mat under controlled laboratory conditions. As a model, we used the microbial mat from the hypersaline Lake Chiprana, inhabited by high abundances of *Chloroflexus*-like filamentous bacteria, three types of cyanobacteria (unicellular *Halothece*-like cells, filamentous *Oscillatoria*-like and *Pseudoanabaena*-like cells) and diatoms (*Nitzschia* and *Navicula* spp.) in the top 2 mm (Jonkers *et al*., 2003). High spatial resolution profile of CLB respiration in the mat was quantified in the same manner as the gross photosynthesis, i.e. by applying the microsensor-based light–dark shift method (Revsbech *et al*., 1981; Revsbech and Jørgensen, 1983), but using the NIR (715–745 nm) light–dark (or dark–light) transition instead of the VIS light–dark transition. Alternatively, we used a NIR differential microprofile approach, which is essentially based on the measurement of steady-state O_2 profiles inside the mat at both VIS and NIR illumination (c^{++}) and at only VIS (i.e. no NIR) illumination (c^{+-}), and fitting the difference c^{++}–c^{+-} with the diffusion model by Berg and colleagues (1998). Both of these approaches were facilitated by the unique absorption properties of the CLB's light-harvesting pigments (BChl *c*, absorbing around 740 nm) and by the fact that NIR illumination induces a decrease in CLB respiration (Bachar *et al*., 2007). Gross photosynthesis rate by oxygenic phototrophs was determined by the traditional VIS (400–700 nm) light–dark shift method, whereas the respiration rate of the aerobic autotrophs and heterotrophs was calculated by subtracting the net photosynthesis rate derived from c^{++} from the gross photosynthesis rate. We also conducted membrane inlet mass spectrometry (MIMS) measurements using $^{18}O_2$ stable isotope as a tracer to independently validate that the NIR light affects only CLB respiration. This was done with another sample of the same mat inside a gas-tight chamber, whereby $^{18}O_2$ was monitored in the overlying water during a sequence of illumination periods, each characterized by a specific combination of VIS and NIR illumination. Finally, we used diffusivity, light, O_2 and H_2S microsensors to characterize the physicochemical microenvironments in the mat layers inhabited by CLB.

Results

Light measurements

Scalar irradiance in the mat exhibited pronounced wavelength-dependent attenuation with depth (Fig. 1A).

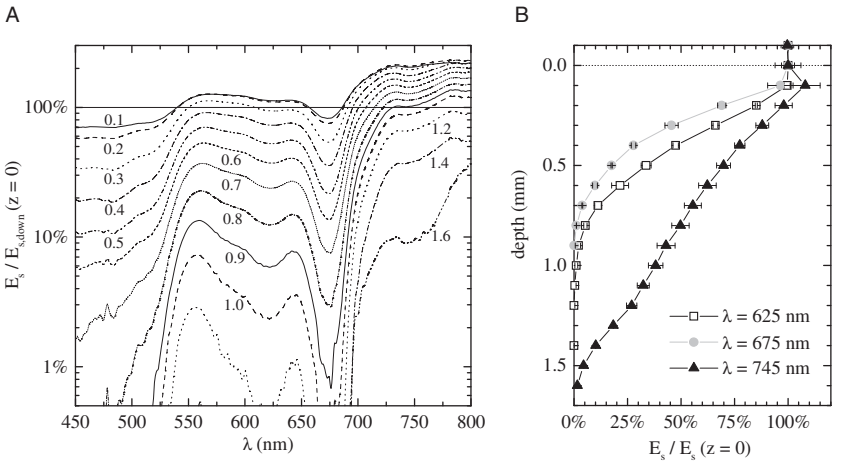

Fig. 1. A. Scalar irradiance spectra at various depths in the mat (shown by numbers in mm), normalized to the downwelling scalar irradiance measured at the mat surface [$E_{s,down}$ ($z = 0$)].
B. Depth profiles of the scalar irradiances at specific wavelengths, each normalized to the scalar irradiance at the mat surface at the respective wavelength [E_s ($z = 0$)]. Averages and standard deviations from three profiles are shown.

The enhanced absorption features in the VIS region correspond to the absorption peaks of Chl *a* (~675 nm), phycocyanin (~625 nm) and carotenoids + Chl *a* (below 525 nm), and represent the spectral signature of diatoms (Chl *a*) and cyanobacteria (Chl *a* and phycocyanin) present in the mat. The spectral signature of CLB, which absorb around 745 nm due to the photopigment BChl *c* (Madigan *et al*., 2000), was detectable but less pronounced. Scalar irradiance between 550 and 650 nm was locally enhanced in the top 0.3 mm when compared with the downwelling scalar irradiance at the mat surface. This effect, caused by multiple light scattering (Jørgensen and Marais, 1988), was much more pronounced in the NIR region, where the scalar irradiance was greater than the surficial downwelling scalar irradiance down to ~0.9 mm depth. VIS scalar irradiance at wavelengths of Chl *a* and phycocyanin absorption decreased with depth much more steeply than the NIR irradiance in the BChl *c* absorption region. For example, scalar irradiances at 675 nm and 625 nm reached 50% of their surface values at ~0.3 mm and 0.4 mm, respectively, and decreased below 1% at depths ≥ 1 mm, whereas the scalar irradiance at 745 nm reached 50% of its surface value at ~0.8 mm and decreased to ~2% at 1.6 mm (Fig. 1B).

Parallel O_2 and H_2S concentrations measurements

Oxygen and sulfide profiles were typical for this type of mats in that O_2 concentrations exhibited a pronounced peak during VIS illumination and decreased steeply to zero in the VIS dark, while H_2S increased steeply with depth under both conditions (Fig. 2). In the VIS dark, oxygen penetration increased from ~0.3 mm to ~0.5 mm after the addition of saturating NIR illumination, whereas it

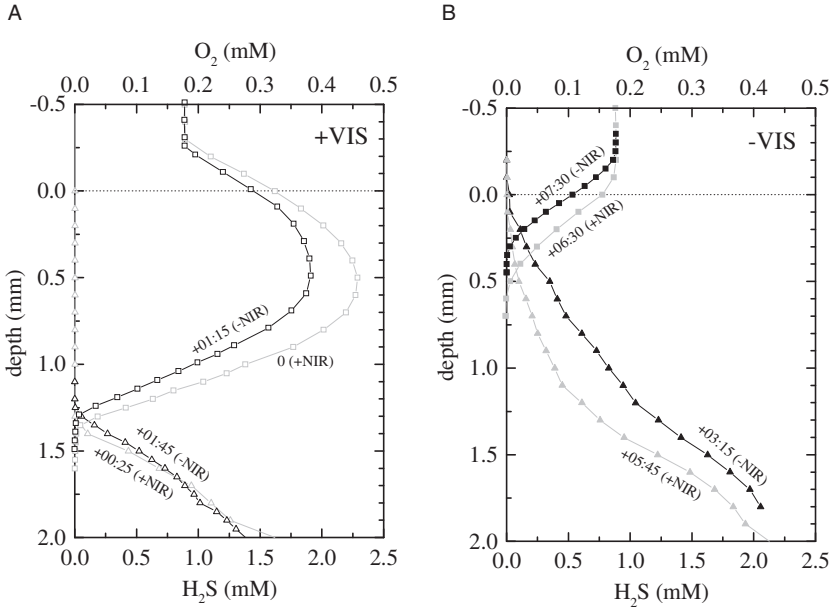

Fig. 2. Steady-state O_2 (squares) and H_2S (triangles) profiles measured in the same spot of the mat under four combinations of the VIS/NIR illumination. VIS light was on and off in (A) and (B), respectively. Annotations specify the times at which the profiles were taken relative to the initial profile (O_2 profile recorded at both VIS and NIR lights on) and the status of the NIR light. Downwelling scalar irradiances of the VIS and NIR lights at the mat surface were 80 μE m^{-2} s^{-1} and 42 μE m^{-2} s^{-1}, respectively.

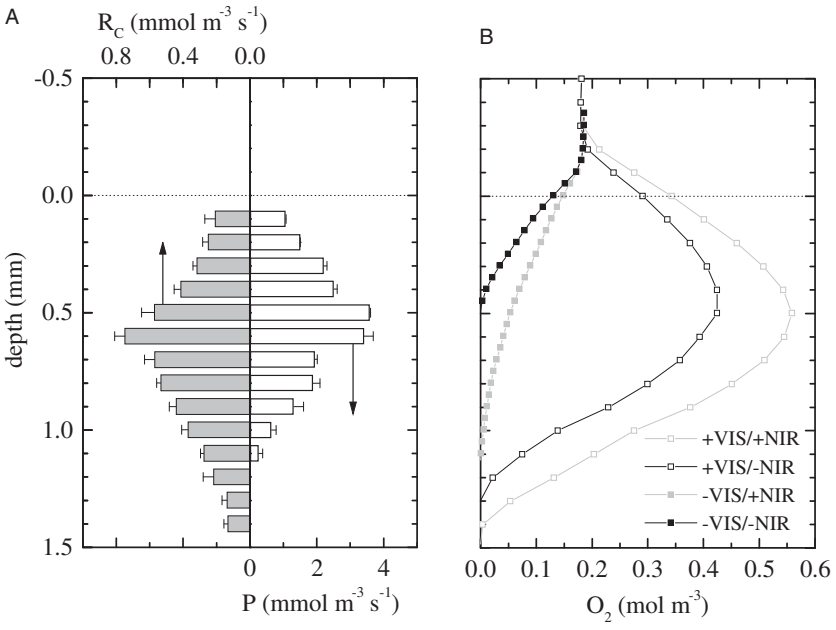

Fig. 3. A. Depth profiles of gross photosynthesis (P) and CLB respiration (R_C) in the mat, measured in triplicates at each depth. Note the different scales for P and R_C. B. Steady-state O_2 concentration profiles at four combinations of VIS/NIR illumination (see Table 2 for abbreviations). Measurements in (A) and (B) were conducted in sequence in the same spot of the mat. Downwelling scalar irradiances of the VIS and NIR lights at the mat surface were 80 μE m^{-2} s^{-1} and 42 μE m^{-2} s^{-1}, respectively.

increased further to 1.3–1.4 mm but remained practically independent of NIR illumination in the VIS light. The depth and thickness of the zone where O_2 and H_2S overlapped was dramatically influenced by the VIS light, whereas the effect of the NIR illumination on the overlapping zone thickness was only minor (Fig. 2).

Most striking in the O_2 and H_2S profiles is the relatively fast and significant change in the O_2 and H_2S concentrations in the mat upon change in NIR light (Fig. 2). In VIS light, removal of NIR illumination lead to a decrease in the peak O_2 concentration in the mat from ~0.47 mM to ~0.38 mM within ~75 min (Fig. 2A). When the measured O_2 profiles were integrated over the depth of O_2 penetration, the resulting O_2 pool per area of the mat decreased after the NIR light was removed by a factor of ~1.4 (at VIS light) and ~2.4 (at VIS dark) in comparison with the pool measured with the NIR light on. Although the effect of the NIR light on the H_2S profile in the VIS light was only minor (Fig. 2A), addition of the NIR light in the VIS dark resulted in a significant and rapid decrease in H_2S concentrations in the anoxic part of the mat (Fig. 2B).

Parallel O_2 concentrations and rate measurements

Under the specific downwelling scalar irradiances (I_{VIS} = 80 μE m^{-2} s^{-1}, I_{NIR} = 42 μE m^{-2} s^{-1}), the entire O_2 cycle took place in the top ~1.5 mm of the mat and was significantly influenced by the NIR light, both in the VIS light and dark (Fig. 3). Typical volumetric gross photosynthesis rates, P, measured by the VIS light–dark shift method, were in the range of 1.0–3.5 mmol m^{-3} s^{-1}, reaching maxima at depths 0.5–0.7 mm (Fig. 3A). The thickness of the VIS photic zone, defined as the zone where P was measurable, was 1.1 mm.

The NIR light–dark transition induced immediately (< 0.25 s) a change in the rate of oxygen evolution measured by the microsensor inside the mat (data not shown), indicating that CLB respiration is immediately affected by the change in the NIR light availability. Volumetric rates of CLB respiration, R_C, derived from the NIR light–dark shift measurement conducted at saturating NIR intensity, were approximately five times lower than the gross photosynthesis rates measured in the same spot (0.2–0.7 mmol m^{-3} s^{-1}; Fig. 3A). In the VIS photic zone, R_C and P were spatially correlated (R = 0.72, P = 0.01). The lower boundary of the NIR photic zone, i.e. where the NIR-induced change in CLB respiration was measurable, coincided with the oxygen penetration depth of ~1.5 mm (Fig. 3).

Integrating the volumetric rates over the depth of the VIS photic zone (0–1.1 mm), the areal rate of gross photosynthesis was P_a = 2.04 ± 0.12 μmol m^{-2} s^{-1}, whereas the areal rate of CLB respiration in that zone was $R_{C,a}$ = 0.48 ± 0.08 μmol m^{-2} s^{-1}. Integrating over the entire NIR photic zone (0–1.5 mm), the total CLB respiration influencing the O_2 budget in the mat in the VIS light was $R_{C,a}$ = 0.52 ± 0.06 μmol m^{-2} s^{-1}. Thus, only ~10% of the total CLB respiration activity was encountered between the VIS and NIR photic zone boundaries (1.1–1.5 mm). These values slightly varied when measured in different spots across the mat (Table 1).

Averaging measurements made in four different positions across the mat surface, the diffusion coefficient in the mat normalized to the coefficient in the overlying water (D_m /D_w) varied between 0.52 and 0.54 in the top 1.5 mm

Table 1. Summary of the O_2 microsensor measurements.

	Spot 1	Spot 2	Spot 3
VIS/NIR downwelling irradiance	80/42	80/42	80/42
$z_{photic,VIS}/z_{photic,NIR}$ (mm)	1.1/1.3	1.0/1.1	–/1.2
$J^{++}(0)$	1.40 ± 0.02	1.67 ± 0.06	0.87 ± 0.03
$J^{++}(z_{photic,VIS})$	0.61 ± 0.03	1.13 ± 0.02	0.56 ± 0.06
NP_a^{++} $(0 - z_{photic,VIS})$	2.01 ± 0.05	2.80 ± 0.08	1.43 ± 0.09
P_a $(0 - z_{photic,VIS})$	2.04 ± 0.12	2.68 ± 0.12	–
R_a^{++} $(0 - z_{photic,VIS})$	0.03 ± 0.17	–0.12 ± 0.20	–
$\Delta R_{C,a}$ $(0 - z_{photic,VIS})$			
NIR light–dark shift method	0.48 ± 0.08	0.14 ± 0.03	0.29 ± 0.05
NIR dark–light shift method	–	–	0.25 ± 0.05
NIR differential profile method	0.47 ± 0.05	0.13 ± 0.02	0.26 ± 0.02
$\Delta R_{C,a}$ $(0 - z_{photic,NIR})$			
NIR light–dark shift method	0.52 ± 0.06	0.14 ± 0.03	0.29 ± 0.05
NIR differential profile method	0.51 ± 0.03	0.13 ± 0.02	0.26 ± 0.02

Areal rates and diffusive fluxes are given in μmol m^{-2} s^{-1}, downwelling irradiance is in μE m^{-2} s^{-1} (μmol photons m^{-2} s^{-1}). Mean values and standard errors are based on triplicate measurements. See Table 2 for symbol definitions.

and 0.56–0.59 at depths from 2 to 3 mm. Using the local D_m value and the NIR differential profile approach, the areal rate of CLB respiration in the NIR photic zone (0–1.5 mm) of $R_{C,a} = 0.51 \pm 0.03$ μmol m^{-2} s^{-1} was found, as calculated from the difference between the steady-state O_2 profiles measured at +VIS/+NIR and +VIS/–NIR illuminations shown in Fig. 3B (see Eq. 9b in *Experimental procedures*). This value agreed very well with the areal rate obtained by depth-integrating the values from the NIR light–dark shift measurement ($R_{C,a} = 0.52 \pm 0.06$ μmol m^{-2} s^{-1}, see above). This agreement was achieved irrespective of the choice of the integration range (e.g. both in the NIR and in the VIS photic zones) and was reproduced in three independently measured spots (Table 1), thus confirming that the NIR light–dark shift and the NIR differential profile measurements give similar results.

The areal rate of gross photosynthesis in the VIS photic zone ($P_a = 2.04 \pm 0.12$ μmol m^{-2} s^{-1}) was practically equal to the areal rate of net photosynthesis calculated from the steady-state O_2 profile measured during VIS and saturating NIR illumination ($NP_a^{++} = 2.01 \pm 0.05$ μmol m^{-2} s^{-1}). This was confirmed in another spot of the mat (Table 1) as well as in measurements conducted at 34°C (data not shown). It implies that the total respiration in the VIS photic zone of the mat was not significantly different from zero when the mat was illuminated by VIS light and saturating NIR light. This also means that respiration in this zone was completely controlled by CLB, and that it could be completely 'switched off' by a sufficiently bright NIR light (around 740 nm).

Gross photosynthesis rates were nearly identical when measured with or without the saturating NIR light (Fig. 4), indicating no effect of NIR illumination on oxygenic photosynthesis in this mat. The average values of CLB respiration derived from the NIR light–dark shift measurement were somewhat higher than those obtained by the NIR dark–light shift measurement; however, the difference was not significant (Fig. 4). This agreement and the additional agreement with the NIR differential profile measurement (Table 1) confirm that all three approaches constitute equally valid methods for the determination of CLB respiration.

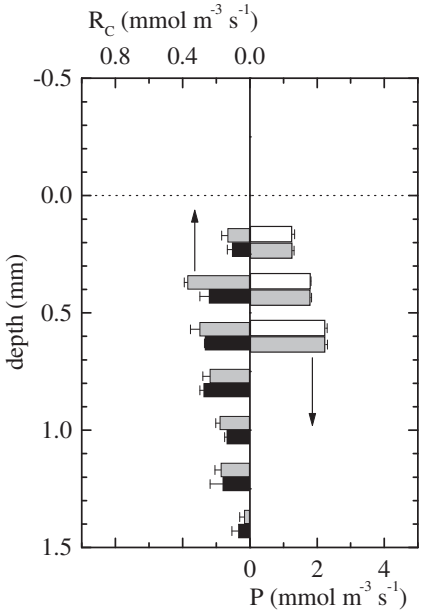

Fig. 4. Gross photosynthesis rates (P) at selected depths in the mat measured by the VIS light–dark shift method with NIR switched off (open bars) and on (grey bars). *Chloroflexus*-like bacteria respiration rates (R_C) at selected depths measured by the NIR light–dark shift (grey bars) and NIR dark–light shift (black bars) methods. All measurements were performed in the same spot and in triplicates at each depth. Downwelling scalar irradiances of the VIS and NIR lights at the mat surface were 80 μE m^{-2} s^{-1} and 42 μE m^{-2} s^{-1}, respectively.

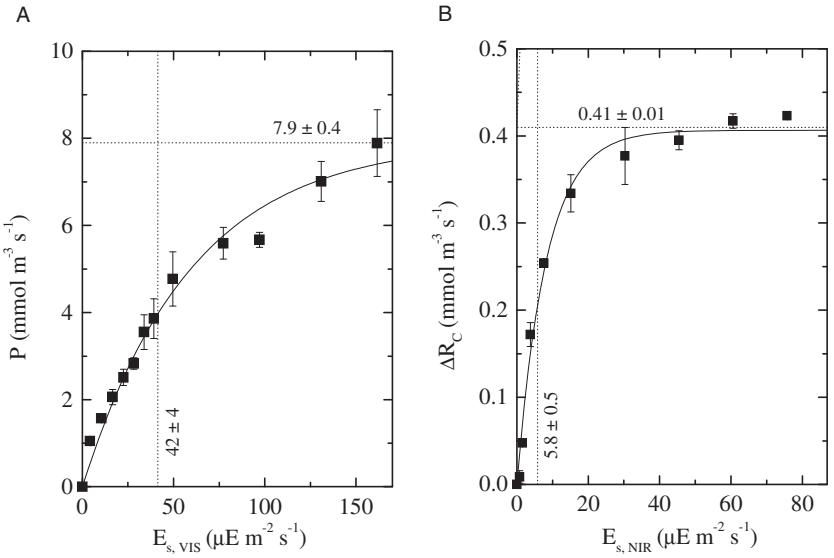

Fig. 5. Volumetric rates of gross photosynthesis (A) and the decrease of CLB respiration (B) as a function of the local scalar irradiance (E_s) of the VIS and NIR lights in the mat, respectively. All measurements were conducted at depth 0.6 mm in the same spot as those shown in Fig. 3 and in triplicates for each light intensity. Vertical line indicates the intensity at which the respective rate reaches half of the saturation value (horizontal line). The corresponding mean ± STD values determined from the fitting procedure are also shown.

P–I$_{VIS}$ *and* R–I$_{NIR}$ *curves*

Both the cyanobacterial photosynthetic activity (P) and the decrease of CLB respiration (ΔR_C) measured at a specific depth ($z = 0.6$ mm) varied exponentially with the local scalar irradiance of the respective light (Fig. 5). At low values, the rates P and ΔR_C increased approximately linearly with the scalar irradiances, whereas they started to saturate at higher scalar irradiances. Using the measured scalar irradiances at depth 0.6 mm integrated over the VIS and NIR regions (Fig. 1A), the scalar irradiances at half-saturation of P and ΔR_C were $E_{s,VIS} \sim 42$ μE m^{-2} s^{-1} and $E_{s,NIR} \sim 5.8$ μE m^{-2} s^{-1}, respectively (Fig. 5). Saturation of the gross photosynthesis at depth 0.6 mm was not reached because the maximum local scalar irradiance reached only ~160 μE m^{-2} s^{-1} in this experiment. This was due to the strong attenuation of the VIS light in the mat (Fig. 1A) and the limited downwelling scalar irradiance of the VIS light source used (maximum ~500 μE m^{-2} s^{-1}). On the other hand, saturation of ΔR_C was reached comfortably, mainly because the NIR light in the mat was attenuated much less and was even enhanced at the mat surface (Fig. 1A), and because the saturation occurred at a much lower scalar irradiance (~42 μE m^{-2} s^{-1}).

As the local NIR scalar irradiance in the VIS photic zone of the mat was greater than 70% of the downwelling NIR scalar irradiance at the mat surface (Fig. 1A), the local NIR scalar irradiance corresponding to a downwelling NIR scalar irradiance of 42 μE m^{-2} s^{-1} at the surface was saturating in the *entire* VIS photic zone (0–1.1 mm). This confirms that the values determined by the NIR light–dark shift and NIR differential profile measurements shown above (Figs 3A and 4) indeed represent the *total* CLB respiration (see *Experimental procedures*). On the other hand, as the NIR light attenuation was more pronounced below 1.1 mm, the local NIR scalar irradiances were not completely saturating at these depths and thus the measured rates of CLB respiration may be underestimated.

MIMS measurements

The MIMS measurements showed that the $^{18}O_2$ removal from the overlying water was dramatically influenced by the NIR light, which extended up to ~950 nm. When the tracer, after being injected into the stirred overlying water, was monitored in the dark following a period of full light (+VIS/+NIR), the rate of its removal increased with time (Fig. 6A and B, periods –VIS/–NIR$_{1,2}$). Inversely, the rate of $^{18}O_2$ removal decreased with time when the mat was illuminated by both VIS and NIR lights (Fig. 6A and B, periods +VIS/+NIR$_{1,2}$). However, when the mat was illuminated only with the VIS light, the tracer removal remained fast or was even slightly faster than that observed at the end of the periods of complete darkness (compare periods +VIS/–NIR, open squares, and –VIS/–NIR$_{1,2}$, filled squares, in Fig. 6A and B). Microsensor measurements conducted in the same mat sample immediately before the MIMS measurements indicated the same qualitative effects of the NIR light on the O_2 profiles as described above, i.e. a dramatic decrease of O_2 concentrations in the mat upon removal of the NIR light (Fig. 6C). As the MIMS chamber was closed for gas exchange, O_2 concentrations in the overlying water also changed over time.

Discussion

Recently, Bachar and colleagues (2007) proposed to use multiple light sources with different spectral characteristics to independently probe the activity of distinct pho-

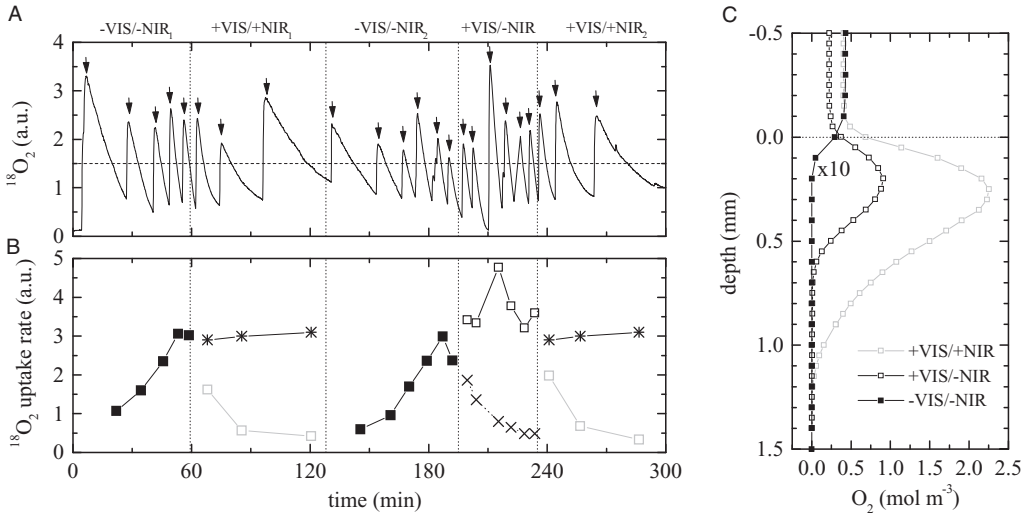

Fig. 6. A. MIMS signal of $^{18}O_2$ in the overlying water covering the mat as a function of time, measured in a gas-tight chamber during a progression of changes in light illuminating the mat. Arrows indicate times at which aliquots of $^{18}O_2$-saturated water were injected into the overlying water. Vertical dotted lines indicate the duration of the light condition specified above the graph (see Table 2 for abbreviations). Subscripts 1 and 2 refer to the repeated application of the same light condition. a.u. = arbitrary units.
B. $^{18}O_2$ uptake rates by the mat (squares) calculated as a rate of change in the $^{18}O_2$ signal shown in (A) at a specific $^{18}O_2$ signal (indicated by a dashed horizontal line in A). Crosses during +VIS/–NIR illumination are numerically simulated values based on the rates measured during the +VIS/+NIR period, assuming that the decrease in the $^{18}O_2$ uptake rate during the +VIS/+NIR illumination was caused by the isotope dilution effect (see *Discussion*) and that the NIR illumination enhanced photosynthesis in the mat. Stars during +VIS/+NIR illumination are simulated values based on the rates measured during the +VIS/–NIR period, using the same assumptions.
C. Vertical profiles of O_2 concentrations in the mat under various light conditions, measured after ~30 min of the corresponding illumination. Note that the concentrations measured in the dark were multiplied by a factor of 10 for clarity. Also note the change of O_2 in the overlying water.

totrophic groups in mixed microbial communities. Here we further explored the original idea, both formally and experimentally, and designed a method that enabled us to independently quantify the roles of oxygenic phototrophs (cyanobacteria), anoxygenic phototrophs (CLB) and non-photosynthetic aerobic heterotrophs and autotrophs in the O_2 cycle in an intact microbial mat. Experiments involved microsensor profiling and light–dark shift measurements and employed two light sources with mutually exclusive spectral characteristics (VIS and NIR) that could be switched on and off independently. Measurements were performed under well-defined laboratory conditions but the equipment can also be used in the field. The budget assessment was performed for specific groups of microorganisms living in a microbial mat, but the methodology can be applied to a variety of mixed communities provided that the metabolism of the community members can be selectively modified by different light sources.

O_2 budget in the mat

Our microsensor measurements indicated that, following the cyanobacteria, CLB were the second most important players in the photosynthetically active zone (top ~1.1 mm) of the studied Chiprana mat with respect to O_2 budget in the light. Under the VIS/NIR light conditions provided in our experiment, CLB respired an estimated 24% of the total oxygen produced by cyanobacteria in this zone ($R_{C,a} = 0.48$ μmol m^{-2} s^{-1} versus $P_a = 2.04$ μmol m^{-2} s^{-1}; Table 1, spot 1). Furthermore, which is more striking, CLB were found to be responsible for *all* respiration in the photosynthetically active zone under only VIS illumination, and, under both VIS and saturating NIR illumination, community respiration in this zone was zero (Table 1). This major result suggests that the aerobic heterotrophs living in this layer are much less active and thus play a much less important role in the O_2 cycle in the mat than previously thought (Paerl *et al.*, 1993; VanGemerden, 1993; Jonkers and Abed, 2003). Whether or not this scenario is valid only for this specific mat or it is a more general phenomenon is a question deserving more attention. It appears that, at least in the Chiprana mat, aerobic heterotrophs are outcompeted by CLB. However, considering the abundance of aerobic heterotrophic bacteria in Chiprana mats (most-probable-number counts revealed that they outnumbered colourless sulfur bacteria, anoxygenic phototrophs (purple sulfur bacteria) and sulfate-reducing bacteria both in the photic (0–3 mm) and aphotic (3–6 mm) depths zones; (Jonkers *et al.*, 2003), the physiological or ecological reason for this observation is unclear.

Effects of NIR light on O_2 and H_2S dynamics in the mat and CLB metabolism

The direct effect of the NIR light on CLB metabolism, and thus on the microenvironments and O_2 budget in the mat, was demonstrated in several ways. In VIS light, additional NIR illumination resulted in a significant increase of O_2 within the oxic zone and a slightly deeper O_2 penetration (Figs 2A and 3B). This demonstrated the change of CLB from oxygen-consuming chemotrophy (–NIR) to anoxygenic phototrophy (+NIR), both in the presence of oxygen. The same metabolic shift was visible from the O_2 profile measured in the dark, where NIR illumination resulted in a significant increase of the O_2 penetration depth (Fig. 2B). A shift to anoxygenic photosynthesis in the absence of oxygen was demonstrated by a relatively rapid (~2.5 h) decrease of H_2S concentrations in the anoxic part of the mat induced by the NIR light (Fig. 2B). However, as no parallel pH profiles were available, the H_2S profile time evolution could not be used for direct quantification of the anoxygenic photosynthesis. In the VIS light, the H_2S profile was mainly controlled by aerobic sulfide-oxidizing bacteria instead of anoxygenic phototrophic processes (Fig. 2A), possibly because the NIR light intensity had dropped too low below the oxygen penetration depth (Fig. 1B; cf. Jørgensen and Marais, 1988).

Recent findings by Kühl and colleagues (2005) demonstrated that NIR light can also be harvested by certain oxygenic phototrophic cyanobacteria, resulting in O_2 production. Therefore, our results of the NIR light induced O_2 dynamics in the mat are ambiguous in that they do not directly discriminate whether the NIR light switches off the CLB respiration or induces O_2 production in cyanobacteria similar to those discovered by Kühl and colleagues (2005). Control experiments with the specific oxygenic photosynthesis inhibitor DCMU conducted with these mats previously (Bachar *et al*., 2007) resolved this ambiguity and confirmed our assumption that the NIR illumination results in a loss of community respiration rather than an enhancement in O_2 production.

The MIMS technique provides another way of resolving this ambiguity. Quantification of the community respiration from the MIMS data alone is, however, somewhat complicated by the fact that the observed rate of $^{18}O_2$ decrease in the overlying water is influenced not only by the community respiration but also, due to its effect on the momentary O_2 distribution in the mat, by photosynthesis. We refer to this as the isotope dilution effect, as photosynthesis, via production of $^{16}O_2$ from water, dilutes the relative concentration of $^{18}O_2$ in the total pool of oxygen ($^{16}O_2 + {}^{18}O_2$) and thus effectively lowers the rate at which $^{18}O_2$ is respired. To quantitatively account for this effect, the MIMS measurements in dense systems such as mats must therefore be accompanied by temporally resolved O_2 profiles. In the present study, O_2 profiling in the mat could not be synchronized with the $^{18}O_2$ tracer monitoring by the MIMS apparatus, and only a non-calibrated signal proportional to $^{18}O_2$ concentration is available. Thus, the results allow only a qualitative interpretation, which we based on numerical simulation (see *Experimental procedures*).

First, the numerical model parameters were adjusted so that the simulated O_2 profiles in the mat were close to those measured inside the MIMS chamber (Fig. 6C). Subsequently, simulations were conducted assuming that NIR illumination during the +VIS/+NIR period (see Fig. 6A and B) resulted either in (partial) inhibition of mat's respiration or in enhanced oxygenic photosynthesis in the mat's photic zone in comparison with the situation under +VIS/–NIR illumination. We found that, within the duration of the +VIS/+NIR period, the rate of $^{18}O_2$ uptake would be only by a factor of 1.1–1.2 lower than the rate at +VIS/–NIR illumination, if the latter effect of NIR light was considered (predicted rates depicted by crosses and stars in Fig. 6B). In fact, the dramatic decrease of the $^{18}O_2$ uptake rate observed under +VIS/+NIR illumination, in comparison with the rates measured both under +VIS/–NIR and at the end of the dark (–VIS/–NIR) period, could not be explained unless complete stop of respiration in the mat's photic zone by NIR light was assumed in the model. This is the same conclusion as reached from the microsensor measurements. The slightly increased $^{18}O_2$ uptake during +VIS/–NIR in comparison with the dark uptake could be a result of the stimulating effects of photosynthetic exudates excreted by the oxygenic phototrophs on CLB respiration, as also suggested by the model.

It should be noted that the NIR light during the MIMS experiment extended up to ~950 nm and thus this measurement did not specifically target only CLB but also other anoxygenic phototrophs capable of aerobic respiration in the NIR dark [e.g. purple (non-)sulfur bacteria and species from the family Chloroflexaceae which only produce BChl *a*]. It was not the aim of the MIMS experiment to selectively quantify the respiration of a specific group of anoxygenic phototrophs in the mat community. Instead, the purpose was to independently verify that the addition of NIR induced indeed a decrease in community respiration and not O_2 production, which was unambiguously, although only qualitatively, demonstrated in this measurement.

Effect of NIR light on CLB respiration

The rates of CLB respiration were not significantly different when determined by the NIR light–dark shift or the NIR dark–light shift method (Fig. 4). Furthermore, we showed that CLB respiration completely stops at sufficiently high NIR light intensities. These findings indicate

that the type of CLB metabolism (O_2 respiration or phototrophy for energy generation) is determined only by the availability of the NIR light, that phototrophy is clearly preferred over chemotrophy (also shown in a previous study with pure cultures of *C. aurantiacus*; Bachar *et al*., 2007), and that CLB respiration can be completely switched off by NIR light.

The observation that photosynthesis can inhibit aerobic respiration in CLB may be explained by the chemiosmotic theory of Mitchell (1957; 1961; 1966). Central in this theory is a membrane potential generated primarily by electron transport processes. The oxidation-reduction processes in the electron transport chain are tightly coupled to proton translocation across the membrane, leading to a charge and pH difference. The electron transport in CLB can be driven either by a respiratory process, where the electrons are finally donated to oxygen, or by light. The resulting membrane potential, the Proton Motive Force (PMF), is used for all membrane associated energy consuming processes, like ATP generation and *trans*-membrane transport of substrates and products via specific exchanging carriers. Due to back-coupling, a high PMF inhibits further electron transport, as it is tightly coupled to proton translocation, which cannot occur against a too strong PMF. In phototrophic prokaryotes like CLB, the photosynthetic apparatus and the respiratory apparatus are in the same membrane (Zannoni and Fuller, 1988), thus both are coupled through the PMF, and additionally coupled by menaquinone which functions in both electron transport routes (Hale *et al*., 1983). When CLB are energized by saturating light, and the PMF is high, the redox couples in the ETC become oxidized, including the terminal electron donor, and respiration stops. Indeed, the light-induced inhibition of the respiration can be alleviated by PMF-dissipating uncouplers (Richaud *et al*., 1986). The inhibitory effect of light on respiration is well documented for purple non-sulfur bacteria (Melandri and Zannoni, 1978; McCarty and Ferguson, 1982), in which also nitrate respiration is inhibited by light (Sabaty *et al*., 1993), in *Halobacterium halobium* (Oesterhelt and Krippahl, 1973), cyanobacteria (Imafuku and Katoh, 1976; Scherer and Boeger, 1982; Dominy and Williams, 1987; Meunier *et al*., 1995), and for *C. aurantiacus* (Pierson and Castenholz, 1974; 1995). It should be noted that this tight coupling of photosynthesis and respiration may not necessarily occur in eukaryotic phototrophs, where the respiration and photosynthesis are located in different cell organelles (mitochondria and chloroplasts) (Imafuku and Katoh, 1976). Here the coupling between respiration and photosynthesis occurs through transport of photosynthates from the chloroplasts to the mitochondria. Respiration and photosynthesis in prokaryotes, both oxygenic and anoxygenic, are coupled by a feedback mechanism through the PMF, and thus they are competitive processes. In phototrophic eukaryotes photosynthesis and respiration are chemically coupled through organic carbon compounds. This, conversely, can drive elevated respiration in the light.

Methodological implications

The fact that, in mixed communities of oxygenic and anoxygenic phototrophs, light not only induces oxygen production but also inhibits oxygen respiration is important not only when applying the light–dark shift method but also when performing standard microsensor measurements at varying light conditions. Selecting a light source with the appropriate spectral characteristics is of primary importance. Equations 1–5 (see *Experimental procedures*) imply that the apparent gross photosynthesis rates determined with the light–dark shift method can significantly overestimate the true *gross* photosynthesis rates of the microbial community if a light source is used whose emission spectrum extends beyond the VIS region (such as natural sunlight, or Schott lamps without an IR filter, which are typically used in laboratory experiments). This is because the darkening of such a source will result not only in an immediate stop of oxygen production ($P = 0$), but also in an immediate increase of respiration (by ΔR_C) of active anoxygenic phototrophs. Since the effects of these two phenomena on the observed O_2 dynamics are additive ($\partial c/\partial t = -P - \Delta R_C$), applying the 'wrong' light source may lead to overestimation of the true *P*. For example, in our measurements conducted at specific VIS and NIR intensities, the apparent gross oxygenic photosynthesis would amount to ~2.5 μmol m^{-2} s^{-1} instead of ~2.0 μmol m^{-2} s^{-1} (i.e. a 25% overestimate) if both VIS and NIR lights were darkened in the light–dark shift measurement (Table 1).

In addition to the gross photosynthesis, *P*, the use of a light source emitting both in the VIS and NIR regions may also lead to an overestimation of the *net* photosynthesis rate, *NP*. Again, the NIR light may (partially or fully, depending on the intensity) inhibit respiration of anoxygenic phototrophs (term $R_C - \Delta R_C \rightarrow 0$ in Eq. 2), resulting in higher oxygen concentrations and thus gradients calculated from the measured profiles. This is clearly demonstrated in Fig. 2 and in Table 1 (spot 1), where the additional illumination by the NIR light caused an increase in *NP* in the photic zone from 1.53 to 2.01 μmol m^{-2} s^{-1} (by ~30%).

The situation is reverse if, on the other hand, the microbial community contains organisms that harvest NIR light to produce oxygen (such as those containing Chl *d* discovered recently; Kühl *et al*., 2005). In such case, not including the NIR light in the microprofile and light–dark shift measurements would lead to underestimated rates of net and gross photosyntheses, respectively. Clearly, if

these two groups, distinct in function but overlapping in absorption properties, are present at the same time, independent quantification of their respective activities with our method is not possible. This complication, however, did not occur in our measurements, as the inhibitor studies with DCMU and the pigment analysis provided no evidence of Chl *d*, i.e. of oxygenic phototrophs that could utilize the light in the NIR region used to characterize CLB respiration (Bachar *et al*., 2007).

Interestingly, even if both gross and net photosyntheses are overestimated due to the use of the VIS + NIR light source in the light–dark shift and steady-state concentration measurements, the community respiration, which is calculated as $P - NP$, is *not* affected. This is because both P and NP are overestimated by the same amount, namely by $R_C - \Delta R_C$ (see *Experimental procedures*), provided that both P and NP were measured with the same light source. It must be realized, however, that thus estimated rates of NP, P and R represent the photosynthetic and respiration activity of the community at *specific* light conditions (i.e. also determined by the spectral quality of the light source).

We argued that the observed inhibition of CLB respiration by NIR light is a consequence of the feedback mechanism between the photosynthetic and respiratory apparatus that are coupled to the PMF in the cell membrane. As this coupling is characteristic for all phototrophic prokaryotic cells, most notably for cyanobacteria (Imafuku and Katoh, 1976; Scherer and Boeger, 1982; Dominy and Williams, 1987; Meunier *et al*., 1995), based on the parallel with anoxygenic phototrophs it is to be expected that the oxygenic photosynthesis induced by VIS light is accompanied by simultaneous inhibition of respiration in these microorganisms. As already discussed above for the NIR light, this may have profound consequences for the assessment of O_2 and carbon budgets in microbial communities, especially if methods based only on the measurements of *total* O_2 concentrations are employed. For example, the light–dark shift measurement may result in overestimated gross photosynthesis rates if the respiration of the oxygenic phototrophs increases within the short (2–3 s) period of the darkness following the light period. Whether or not this complication occurred in this or, for that matter, in any previous microsensor-based study of O_2 budgets is a concern that requires special attention. In this regard, stable O_2 isotope measurements similar to those described in this study, which inherently discriminate between oxygen production and consumption, may be crucial in providing the necessary answers. However, when applied in dense and/or stratified systems, where transport may be a limiting factor leading to highly spatio-temporally variable isotope dilution effects, such measurements must be combined with microsensor measurements to facilitate correct data interpretation. To address this issue would go beyond the scope of this article and requires further research.

Ecological implications

We showed that, additionally to the VIS light, the O_2 budget in the Chiprana mat is significantly influenced by the light in a specific NIR region (715–745 nm) due to a high abundance of CLB. We also showed that the extent to which this influence is significant clearly depends on the spectral quality of the light to which the mixed microbial community is exposed. The light–dark shift and steady-state microprofile measurements with independent VIS and NIR light sources allow not only to separately quantify the activity of the oxygenic and anoxygenic phototrophs, facultative autotrophs and heterotrophs, but also, through the measurement of P–I_{VIS} and R–I_{NIR} curves and light attenuation in the mat, to reconstruct the O_2 budget under natural conditions.

As an example, we modelled the depth distribution of the gross photosynthesis (P) and total respiration ($R_{tot} = R + R_C - \Delta R_C$; Eq. 2 in *Experimental procedures*) rates in the mat illuminated by sunlight characterized by downwelling scalar irradiances ranging between 0 and 1000 μE m^{-2} s^{-1}. First, we estimated the depth distribution of the potential activity of cyanobacteria and CLB by combining (i) the depth profiles of the measured photosynthesis (P) and CLB respiration (R_C) rates determined at the specific VIS and NIR downwelling irradiances (I_{VIS} = 80 μE m^{-2} s^{-1}, I_{NIR} = 42 μE m^{-2} s^{-1}; Fig. 3A), (ii) the depth distribution of the scalar irradiances integrated over the VIS (400–700 nm) and NIR (715–745 nm) regions (Fig. 1A), and (iii) the measured response of P and ΔR_C to the local scalar irradiance (Fig. 5). Then we calculated the depth distribution of the sunlight scalar irradiance in the mat using the measured spectral attenuation properties of the mat (Fig. 1A). Finally, we assumed that the light saturation characteristics of P and ΔR_C (i.e. the P–I_{VIS} and R–I_{NIR} curves) over the entire photic zone were the same as those measured at the specific depth of z = 0.6 mm (Fig. 5), and combined the scalar irradiance profiles with the estimated potential activity distribution to estimate the depth profiles of the actual P and R_{tot}.

The results at three specific sunlight downwelling scalar irradiances are shown in Fig. 7A–C. At low light intensity (e.g. $E_{s,down}$ = 10 μE m^{-2} s^{-1}), CLB respiration dominates the O_2 budget in the mat, mainly because the NIR light intensity is too low to have a significant effect on the CLB respiration (i.e. CLB respire at approximately a full rate) and the cyanobacterial photosynthesis is also low due to the insufficient VIS light intensity (Fig. 7A). On the other hand, at high light intensity (e.g. $E_{s,down}$ = 500 μE m^{-2} s^{-1}), sunlight in the NIR region is sufficiently strong and pen-

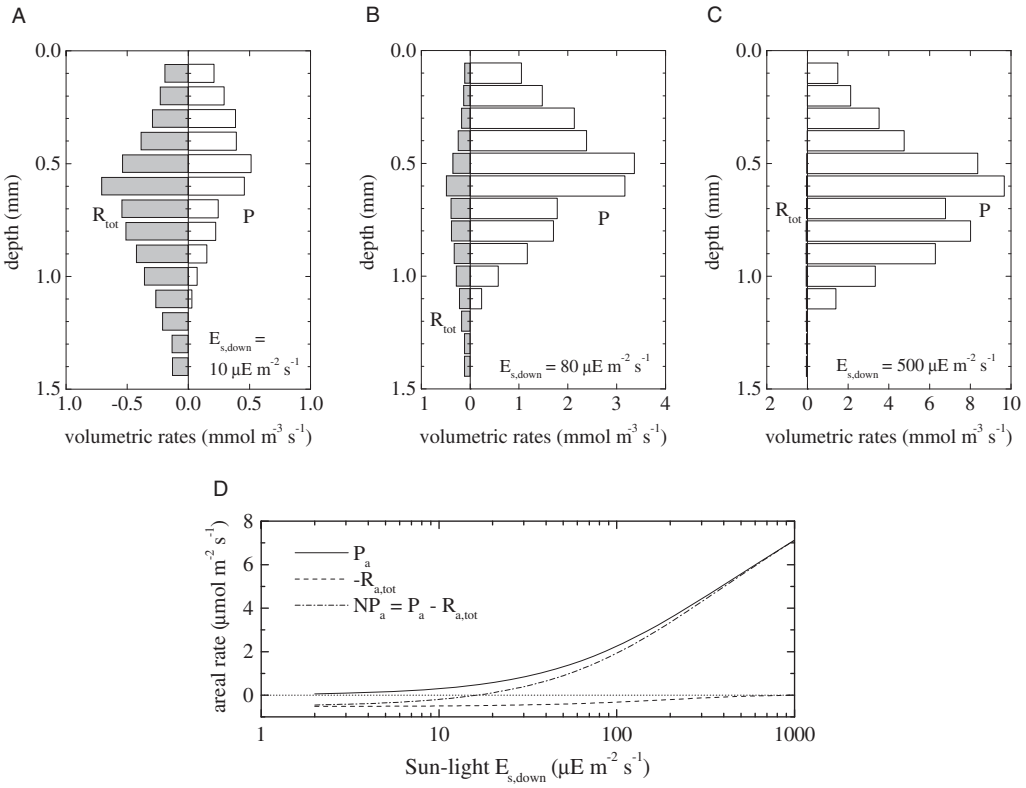

Fig. 7. A–C. Modelled depth distributions of the volumetric rates of photosynthesis (P) and total respiration ($R_{tot} = R + R_C - \Delta R_C$) in the mat at specific downwelling scalar irradiances of the sunlight (shown in legend). Note the different scales of the x-axis.
D. Modelled areal rates of gross photosynthesis (P_a), total respiration ($R_{a,tot}$) and net photosynthesis (NP_a) of the mat at a range of downwelling scalar irradiances of the illuminating sunlight.

etrates sufficiently deep into the mat to completely stop CLB respiration (Fig. 7C). Because, as we showed, the mat respiration in the VIS photic zone is entirely dominated by CLB, O_2 at high light intensities is thus only produced in the photic zone and transported by diffusion to the overlying water and to the deeper mat layers to be used, e.g. by sulfide oxidizers. At intermediate light intensity (e.g. $E_{s,down} = 80$ µE m^{-2} s^{-1}), O_2 is produced at high rates by cyanobacteria but a part of it is consumed by CLB, also at relatively high rates (Fig. 7B). This is because the energy from the sunlight that can be utilized by CLB (i.e. sunlight spectrum integrated over 715–745 nm) is much lower than the amount of light energy that can be utilized by cyanobacteria (i.e. spectrum integrated over 400–700 nm). The areal rates, obtained by depth-integrating the volumetric rates over the respective photic zones, show this transition from the respiration-dominated O_2 budget at low light to the production- and transport-dominated O_2 budget at high light more clearly (Fig. 7D). They also show the expected trend in the relative importance of the different functional groups (cyanobacteria versus CLB) in the O_2 budget at variable intensities of natural light. It should be noted that the calculated NP_a continues to increase at high light intensities. This is because no restrictions on the maximum gross photosynthesis rates were applied in the model. In reality, regulation of gross photosynthesis at high light intensities will result in levelling off of P, which will result in parallel levelling off of NP_a at high intensities (cf. Epping and Jørgensen, 1996).

Summary

In conclusion, our measurements indicate that CLB play a very important role in the top ~1.5 mm of the Chiprana mat. Their respiration and anoxygenic photosynthesis, which are controlled by the availability of NIR light, O_2, organic as well as inorganic substrates such as H_2S, constitute a significant sink for O_2 and H_2S in the mat. This study demonstrates that future research on oxygen dynamics (oxygenic photosynthesis and respiration) in microbial mats should consider NIR-dependent behaviour of CLB and possible other anoxygenic phototrophic groups. The method combining oxygen microsensor measurements with specific VIS/NIR light treatments provides a quick and direct way to establish the importance of these groups in mats and other systems with mixed microbial communities. We showed that respiration in the photic

Table 2. Abbreviations and notations used throughout the article.

Chloroflexus-like bacteria	CLB
VIS light on/off; NIR light on/off	+/–VIS; +/–NIR
Steady-state O_2 concentration profile at ±VIS/±NIR illumination[a]	$c^{\pm\pm}$
VIS light–dark transition	+VIS → –VIS
NIR light–dark transition	+NIR → –NIR
NIR dark–light transition	–NIR → +NIR
Volumetric/areal gross photosynthesis rate induced by VIS light	P/P_a
Volumetric/areal respiration rate of CLB in NIR dark	$R_C/R_{C,a}$
Decrease in CLB respiration rate induced by NIR light, volumetric/areal	$\Delta R_C/\Delta R_{C,a}$
Volumetric/areal light-independent respiration rate	R/R_a
Volumetric/areal net photosynthesis rate	NP/NP_a
Diffusion coefficient	D
Depth in the mat	z
Diffusive flux at depth z[a]	$J^{\pm\pm}(z) = -D\,\partial c^{\pm\pm}/\partial z$
NIR differential profile[a]	$\Delta c = c^{++} - c^{+-}$
NIR differential flux at depth z	$\Delta J(z) = -D\partial\Delta c/\partial z$
Thickness of the VIS photic zone (i.e. where $P > 0$)	$z_{photic,VIS}$
Thickness of the NIR photic zone (i.e. where $\Delta R_C > 0$)	$z_{photic,NIR}$

a. First and second superscripts refer to the status of the VIS and NIR light, respectively.

zone of the mat was entirely dominated by CLB and the contribution of the facultative or strict aerobic autotrophs and heterotrophs was insignificant. Whether this is a unique characteristics of the Chiprana mat due to its high abundance of CLB, or it is a more general phenomenon remains to be seen. The new technique outlined in this study provides a quick way to find out.

Experimental procedures

Basic theory

The microsensor-based light–dark shift method, introduced more than two decades ago by Revsbech and colleagues (Revsbech *et al.*, 1981; Revsbech and Jørgensen, 1983), has been widely used to quantify primary production in diverse microbial systems, such as microbial mats, sediments and corals (Revsbech and Jørgensen, 1986). Its mathematical basis, as described by Revsbech and colleagues (1981), was formulated to quantify a single parameter (gross photosynthesis) using the probing light in a single spectral region (VIS). However, the basic idea can be straightforwardly extended towards probing lights in multiple, but mutually exclusive, spectral regions (e.g. VIS and NIR) to independently characterize multiple parameters. To explain the basic steps of the measurement procedure employed in this article and for the purpose of methodological completeness, we outline the mathematical basics below.

A functional description of a microbial mat or any stratified system with respect to the O_2 budget and its dynamics can be formulated by dividing the system into horizontal layers, each comprised of species (biological and/or chemical) characterized by specific rates of oxygen production and consumption. In a microbial mat like the Chiprana mat, the relevant species include (i) oxygenic phototrophs (e.g. cyanobacteria), which harvest VIS light and produce O_2 with a gross photosynthesis rate P, (ii) anoxygenic phototrophs (e.g. CLB), which, in the presence of oxygen and absence of NIR light, consume oxygen with a respiration rate R_C, (iii) and the remaining facultative or strict aerobic autotrophic and heterotrophic bacteria whose respiration rate R is affected neither by the VIS nor by the NIR light due to the lack of photopigments. In this model, we assume that the respiration of oxygenic phototrophs is not affected by light and is thus included in the rate R. This is equivalent to the assumption made in the original work of Revsbech and Jørgensen (1983) and consistently adopted in all subsequent applications of this method (see section *Methodological implications* in *Discussion*). Assuming that the system is homogeneous in the horizontal dimension and O_2 is transported by diffusion, the volume-specific rates P, R_C and R (in mol m^{-3} s^{-1}) are explicit functions of depth z inside the mat and the vertical distribution of O_2 concentration, c, is mathematically described by a time-dependent, one-dimensional diffusion–reaction equation.

The form of the equation describing c as a function of z and time (t) depends on the status of the illuminating light. Specifically, in a steady state characterized by a constant illumination with VIS light but no NIR light (+VIS/–NIR), oxygen concentration in the mat, denoted by c^{+-} (see Table 2 for notation), fulfils equation

$$+\text{VIS}/-\text{NIR}:\ \partial c^{+-}/\partial t = D\partial^2 c^{+-}/\partial z^2 + P - R - R_C = 0. \quad (1)$$

Upon illumination with the NIR light, CLB switch to anoxygenic photosynthesis and simultaneously completely stop or at least decrease respiration, using the NIR light for generation of cellular energy (Bachar *et al.*, 2007). This switch of activity can be quantified as a NIR light-induced decrease of CLB respiration, denoted as ΔR_C. Steady-state oxygen distribution under both VIS and NIR illuminations (+VIS/+NIR), c^{++}, can thus be described as

$$+\text{VIS}/+\text{NIR}:\ \partial c^{++}/\partial t = D\partial^2 c^{++}/\partial z^2 + P - R - (R_C - \Delta R_C) = 0. \quad (2)$$

After the VIS illumination is switched off while keeping the NIR light status unchanged, the oxygen production stops ($P = 0$) while CLB respiration remains unchanged, as it is not affected by VIS light (Bachar *et al.*, 2007). Consequently, oxygen concentration starts to decrease as a result of the unbalanced respiration and diffusive transport. Depending on the status of the NIR light, the initial rate of the concentration change after the +VIS to –VIS transition (+VIS → –VIS) is given by

$$-\text{NIR: } \partial c^{+-}/\partial t_{\text{init}}(+\text{VIS} \rightarrow -\text{VIS}) = D\partial^2 c^{+-}/\partial z^2 - R - R_c. \quad (3a)$$

$$+\text{NIR: } \partial c^{++}/\partial t_{\text{init}}(+\text{VIS} \rightarrow -\text{VIS}) = D\partial^2 c^{++}/\partial z^2 - R - (R_C - \Delta R_C). \quad (3b)$$

By subtracting Eq. 1 from 3a or, alternatively, Eq. 2 from 3b, one can immediately see that the volumetric rate of gross photosynthesis, *P*, can be quantified by darkening the VIS light after a prolonged VIS illumination and measuring the initial rate of O_2 concentration decrease during this period, as originally proposed by Revsbech and colleagues (Revsbech *et al.*, 1981; Revsbech and Jørgensen, 1983):

$$+\text{NIR or } -\text{NIR: } P = -\partial c/\partial t_{\text{init}}(+\text{VIS} \rightarrow -\text{VIS}). \quad (4)$$

It should be noted that this principle should be valid irrespective of the status of the NIR light, as long as it remains unchanged, as follows from Eqs 1–3.

Exploiting the fact that the loss of CLB respiration, ΔR_C, is induced by the NIR light, CLB respiration can be quantified in the same manner as the gross photosynthesis but using the NIR light–dark transition. This can be practically realized independently of the VIS illumination by using a separate NIR light source. In particular, ΔR_C can be determined by darkening the NIR light after a prolonged NIR illumination and measuring the initial rate of O_2 concentration decrease during this period resulting from the unbalanced O_2 production, consumption and diffusion:

$$+\text{VIS: } \Delta R_C = -\partial c/\partial t_{\text{init}}(+\text{NIR} \rightarrow -\text{NIR}). \quad (5a)$$

ΔR_C can alternatively be determined using the opposite NIR light transition, namely by switching the NIR light on after a prolonged NIR darkness and measuring the initial rate of O_2 concentration increase:

$$+\text{VIS: } \Delta R_C = \partial c/\partial t_{\text{init}}(-\text{NIR} \rightarrow +\text{NIR}). \quad (5b)$$

We will refer to these procedures as the 'NIR light–dark shift' (Eq. 5a) and 'NIR dark–light shift' (Eq. 5b) methods.

An alternative approach to ΔR_C quantification is based on the calculation of the second derivative of the steady-state differential profile, defined as $\Delta c = c^{++} - c^{+-}$ (Table 2), which can easily be derived by subtracting Eq. 1 from 2. First, the steady-state O_2 profiles measured under +VIS/+NIR (c^{++}) and +VIS/–NIR (c^{+-}) illuminations are subtracted from each other. Subsequently, thus obtained differential profile, $\Delta c = c^{++} - c^{+-}$, is fitted with the diffusion-based model, as described by Berg and colleagues (1998). The spatial distribution of ΔR_C is then calculated as the second derivative of the fit:

$$+\text{VIS: } \Delta R_C = D\partial^2 \Delta c_{\text{fit}}/\partial z^2. \quad (6)$$

We will refer to this procedure as the 'NIR differential profile approach'. It should be noted that these steps are preferred over an alternative approach, where the second derivatives of the steady-state profiles c^{++} and c^{+-} would be calculated first (by fitting each profile separately) and subtracted from each other only afterwards. This is because the precision of the ΔR_C estimation is generally higher when using the former procedure, as the second derivative determined from the profile fit (calculated twice in the latter approach) is rather sensitive to experimental uncertainties.

It should be noted that the loss of CLB respiration, ΔR_C, measured by the above procedures (Eqs 5 and 6) will equal the total CLB respiration only if the NIR light intensity completely inhibits CLB respiration. Such saturating light ($I_{\text{NIR,sat}}$) can be determined by conducting the NIR light–dark shift and/or dark–light shift measurements with a range of NIR light intensities, similar to the P–I_{VIS} curve characterizing the response of gross and/or net photosynthesis to the VIS light intensity (Wieland and Kühl, 2006).

The last step in the O_2 budget assessment involves the quantification of the respiration rate of the aerobic autotrophs and heterotrophs, *R*. In many microsensor studies, this is commonly done by fitting the measured steady-state O_2 profile and calculating the second derivative of the fit (Berg *et al.*, 1998), which is equal to the negative of the net photosynthesis, *NP* (Gieseke and de Beer, 2004). A preferable approach is to fit the profile measured while both VIS and NIR lights are on (c^{++}), with the NIR light intensity equal to or above $I_{\text{NIR,sat}}$ so as to ensure that the term $R_C - \Delta R_C$ in Eq. 2 equals zero. In such case, *NP* equals *P*–*R* and the light-independent respiration rate is determined by subtracting the modelled net photosynthesis from the experimentally determined gross photosynthesis:

$$+\text{VIS/+NIR, } I_{\text{NIR}} \geq I_{\text{NIR,sat}}: R = P - NP^{++}, NP^{++} = -D\partial^2 c_{\text{fit}}^{++}/\partial z^2. \quad (7)$$

In addition to volume-specific rates, microbial activity in stratified systems is alternatively characterized by areal rates, which are defined as the integral of the volumetric rates over a specific depth interval from z_1 to z_2. As the microsensor technique allows the determination of the volumetric rates only in discrete locations (P_i in z_i), the areal rate of gross photosynthesis, P_a, is typically approximated by the sum of P_i multiplied by the step size $\Delta z_i = z_{i+1} - z_i$ between the discrete locations. Similarly, the areal rates of the CLB respiration decrease are calculated as a sum of the volumetric rates $\Delta R_{C,i}$ measured by the NIR light–dark and/or dark–light shift methods multiplied by the step size:

$$\Delta R_{C,a} = \sum_i \Delta R_{C,i} \Delta z_i. \quad (9a)$$

From the mathematical form of the diffusion equation it follows that the areal rate of net oxygen production/consumption in a region extending from z_1 to z_2 is equal to the difference of diffusive fluxes at the region's boundaries (Berg *et al.*, 1998). Thus, the decrease in the areal rate of CLB respiration is alternatively calculated from the differential fluxes as

$$\Delta R_{C,a} = \Delta J_C(z_1) - \Delta J_C(z_2), \quad (9b)$$

where the differential fluxes are calculated from the gradient of the differential profile Δc determined from the steady-state profiles measured at +VIS/+NIR and +VIS/–NIR illuminations (Table 2). Similarly, the areal rate of the respiration *R* is determined by subtracting the areal net photosynthesis from the areal gross photosynthesis, the former calculated from the O_2 fluxes measured in the VIS and saturating NIR lights (Table 2):

$$R_a = P_a - [J^{++}(z_1) - J^{++}(z_2)]. \quad (10)$$

Sampling

Microbial mat was sampled from the hypersaline Lake Chiprana, Spain (41°14′20 N, 0°10′55 W; salinity 80 g l^{-1},

temperature 20°C) in September 2005. Intact mat pieces were stored in an aquarium filled with aerated *in situ* water and exposed to a 16 h light/8 h dark illumination regime. The emission spectrum of the lamps covered both VIS and NIR regions and the downwelling scalar irradiances in the VIS (400–700 nm) and NIR (715–745 nm) regions were ~300 and ~10 μmol photons m^{-2} s^{-1} (μE m^{-2} s^{-1}), respectively.

Experimental set-up for O_2 and H_2S microprofile measurements

A mat core was taken with a cut-off syringe (inner diameter 3.5 cm) and covered with *in situ* water. A gentle stream of air over the water surface induced laminar water flow over the mat surface, resulting in a stable and well defined diffusive boundary layer and sufficient exchange of O_2 between the overlying water and the atmosphere to maintain air saturation.

Oxygen concentrations were determined using a Clark-type oxygen microelectrode with a guard cathode (tip diameter 20 μm, response time ≤ 0.5 s; Revsbech and Jørgensen, 1986; Kühl *et al*., 2005), while H_2S was measured using a microelectrode with an internal reference cathode (tip diameter 40 μm; Kühl *et al*., 1998). Microelectrodes were connected to a custom-made pA-meter and the output was read by a 16-bit analogue input of the data acquisition device (DAQ-Pad 6015, National Instruments) connected to a computer. Microelectrodes were calibrated as described previously (Wieland *et al*., 2003).

Both microelectrodes were attached to a motorized linear positioning stage (VT-80, Micos) equipped with a motor controller (3564K 024 BC, Faulhaber), allowing positioning of the microsensor tip inside the microbial mat with ±1 μm vertical precision. Precise horizontal positioning of the sensor tips to the same spot (±5 μm) and alignment with the mat surface was aided by a dissection microscope (Stemi SV6, Zeiss).

Illumination in the visible range of the spectrum (400–700 nm) was provided by two warm-white high-power light emitting diodes (LXHL-MWGC, Lumileds) equipped with a 25° collimating optics (LXHL-NX05-25, Lumileds). The NIR light in the 715–745 nm region was generated by an array of NIR LEDs (ELD-740-524, Roithner Lasertechnik) equipped with a band-pass filter (730AF30, Omega Optical). Downwelling irradiances in the range of 0–560 μE m^{-2} s^{-1} (VIS) and 0–53 μE m^{-2} s^{-1} (NIR) were achieved by adjusting the current through the respective LEDs (white: 0–350 mA, NIR: 0–50 mA). The current was provided by two custom-made power supplies that could rapidly (< 1 ms) and independently be switched on or off via the digital outputs of the DAQ device.

Data acquisition and microsensor positioning were performed by a computer using software for automated microprofile measurements (μ-Profiler, Garching Innovation GmbH, developed by Polerecky). During the measurements, water salinity and temperature were kept constant at 80 g l^{-1} and 20°C, respectively.

Light measurements

Scalar irradiance (in μE m^{-2} s^{-1}) in the VIS spectral region (400–700 nm) was measured using a spherical quantum sensor (US-SQS/L, Walz) connected to a light meter (LI-250A, LI-COR Biosciences). The scalar irradiance of the NIR light (715–745 nm), to which the spherical quantum sensor is insensitive, was determined using the spectrum of the combined VIS and NIR light source, which was measured by a spectrometer (USB2000, OceanOptics). First, the signal from the spectrometer (in counts s^{-1}) was integrated separately in the VIS and in the NIR regions. The ratio between the integrals over the NIR and VIS regions was then multiplied by the light meter reading, giving the NIR scalar irradiance in μE m^{-2} s^{-1}.

Scalar irradiance spectra in the mat were measured using a fibre-optic scalar irradiance microprobe (Lassen *et al*., 1992) with a light-scattering sphere of 130 μm in diameter. The microprobe was connected to a spectrometer (USB2000, OceanOptics) and attached to the motorized linear positioner. The mat sample was illuminated from the top by light from the VIS and NIR LEDs (the 715–745 nm band-pass filter was not used in this case). Automatic recording of the spectra at depths 0–1.5 mm with vertical steps of 100 μm was performed from the top at ~45° from the vertical direction using software developed by Polerecky. The scalar irradiance spectra were normalized to the downwelling scalar irradiance at the mat surface, measured by positioning the microprobe over a water-immersed black light-trap located at the same position relative to the light field as the mat surface (Wieland *et al*., 2003).

Parallel O_2 and H_2S concentrations measurements

The influence of the light quality on the O_2 and H_2S concentrations in the mat was determined by measuring the O_2 and H_2S profiles in the same spot of the mat in sequence under all four combinations of VIS and NIR illumination. After each change in illumination, sufficient time was allowed for the profiles to reach steady state, which was confirmed by measuring at least two replicate profiles immediately after each other. During the measurements, downwelling scalar irradiances in the VIS and NIR regions were 80 and 42 μE m^{-2} s^{-1}, respectively.

Parallel O_2 concentrations and rate measurements

Rates of O_2 production and consumption were determined by conducting steady-state O_2 microprofile and light–dark shift measurements. These measurements were performed on the same mat sample and using the same downwelling scalar irradiances as the parallel O_2 and H_2S measurements (I_{VIS} = 80 μE m^{-2} s^{-1}, I_{NIR} = 42 μE m^{-2} s^{-1}). The NIR downwelling scalar irradiance was sufficient to inhibit completely the CLB respiration in the entire oxic zone of the mat (see *Results*). First, the mat was illuminated by both VIS and NIR lights. Vertical oxygen profiles were recorded until a steady state (c^{++}, Table 2) was reached. Afterwards, the depth profile of gross photosynthesis (P) was measured using the VIS light–dark shift method (NIR kept on). In accordance with the protocol described by Revsbech and Jørgensen (1983), the dark periods during which the slope of the oxygen decrease was determined lasted 3 s to ensure a spatial resolution of ~100 μm. The subsequent light periods during which

oxygen profiles approached steady state lasted 3–5 min. At each depth, three replicate measurements were performed. After these measurements, VIS light was kept on and the NIR light–dark shift measurements were conducted to quantify the depth profile of the CLB respiration (R_C). The durations of the dark and light periods and the number of replicate measurements at each depth were the same as during the VIS light–dark shift measurements. Then, the NIR light was switched off while the VIS remained on and oxygen profiles were recorded until a steady state (c^{+-}), was reached. Subsequently, both lights were switched off and steady-state dark profiles (c^{--}) were recorded. Finally, the saturating NIR light was switched back on while the VIS light was switched off, and the steady-state profiles c^{-+} were measured. The measurements were conducted in the same spot to enable direct comparison of all related quantities. They were also repeated in two additional spots to assess horizontal heterogeneity.

To verify that the gross photosynthetic activity P does not depend on the status of the NIR light (Eq. 4), additional VIS light–dark shift measurements were conducted with both NIR light continuously on and off at three depths in the mat. To confirm that the CLB respiration rates are equivalent irrespective of the NIR light transition (Eq. 5), two profiles of ΔR_C were measured in the same spot, one using the NIR light–dark shift and the other applying the NIR dark–light shift method. Both measurements were performed at equivalent depths, employed the same light intensities and timing protocol as stated above and were repeated three times at each depth.

Measurements of P–I$_{VIS}$ *and* R–I$_{NIR}$ *curves*

The dependence of the gross photosynthesis (P) and the decrease of CLB respiration (ΔR_C) on the scalar irradiance of the respective illuminating light, i.e. the P–I_{VIS} and R–I_{NIR} curves, were determined using the respective light–dark shift methods (see above). The light–dark shift measurements were conducted only at one depth in the mat ($z = 0.6$ mm), which coincided with the maximum values of P and ΔR_C measured in the previous experiment, and were performed in triplicates at each light intensity. Both VIS and NIR intensities were changed from lower to higher values. Obtained P and ΔR_C values were plotted against the *local* scalar irradiance integrated over the VIS (400–700 nm) and NIR (715–745 nm) spectral regions, as determined from the parallel light microprobe measurements conducted at the same downwelling scalar irradiance. These plots were fitted by the exponential model $r = r_{sat}[1 - \exp(-I/I_0)]$ (Webb *et al.*, 1974), where r is either P or ΔR_C, from which the scalar irradiance at which the rate reaches half of the saturated value was determined.

Diffusion coefficient measurements

Oxygen fluxes at the mat/water interface were determined from the O_2 gradient measured in the diffusive boundary layer (Berg *et al.*, 1998), using the O_2 diffusion coefficient in water corrected for temperature and salinity ($D_w = 1.827 \times 10^{-9}$ m^2 s^{-1}; Li and Gregory, 1974). Fluxes inside the mat were calculated from the microprofiles by Fick's law of diffusion using the local diffusion coefficient in the mat, D_m, which was measured with a diffusivity sensor (Revsbech *et al.*, 1998) purchased from Unisense. Prior to and after the diffusivity measurements, the sensor was calibrated using water and water-saturated glass beads of 40–60 μm size (Unisense; Revsbech *et al.*, 1998). As the diffusivity microsensor is based on the measurement of an equilibrium H_2 concentration around its tip (diameter 160 μm), the microbial mat sample was treated in a 4% formaldehyde solution over night prior to diffusivity measurements to suppress all microbial activity which could potentially influence the microsensor signal. The microsensor was positioned manually using a micromanipulator, and measurements in the top 0–3 mm were made with a step size of 0.5 mm in four positions across the mat.

MIMS measurements

$^{16}O_2$ and $^{18}O_2$ isotope measurements were conducted with another sample of the same mat using a membrane inlet mass spectrometer (MIMS) based on the Balzers QMG 421 quadrupole mass spectrometer (Tchernov *et al.*, 1997), whereby $^{18}O_2$ was used as a tracer to monitor oxygen respiration. The mat was placed at the bottom of a transparent cylindrical gas-tight chamber (inner diameter 2 cm). Through an opening in the lid, the MIMS inlet or an O_2 microsensor could be inserted, sealing the opening against gas exchange. The mat was illuminated using a lamp (KL 1500, Schott) emitting in both VIS and NIR (the NIR region extended up to ~950 nm). To achieve illumination by VIS light only, a short-pass filter ($\lambda_{cut\text{-}off} = 650$ nm) was used to cut off the NIR light. The downwelling VIS scalar irradiance achieved with and without the filter was ~650 and ~1000 μE m^{-2} s^{-1}, respectively. Both VIS and NIR illuminations were thereby saturating (see *Results*). Before the $^{16}O_2$ and $^{18}O_2$ isotope measurements, O_2 microprofiles were measured in the dark (–VIS/–NIR) and in the light (+VIS/+NIR and +VIS/–NIR) as described above. Then the microsensor was replaced by the MIMS inlet and both O_2 isotopes were continuously monitored during the following series of light conditions: –VIS/–NIR, +VIS/+NIR, –VIS/–NIR, +VIS/–NIR, +VIS/+NIR. During each illumination interval, which lasted 50–60 min, small aliquots (100–200 μl) of $^{18}O_2$ saturated water were injected into the overlying water (volume of 9.7 ml) in 5–20 min intervals (depending on the respiration activity) to avoid tracer depletion. During the measurements, the overlying water in the chamber was constantly stirred using a small stirrer driven by an electromotor to achieve a stable signal, and the temperature and salinity were kept constant at 34°C and 85 g l^{-1}, respectively.

$^{16}O_2$ and $^{18}O_2$ dynamics in the overlying water depend on the dynamics of both oxygen isotopes inside the mat, which are controlled by light and diffusion. Oxygenic photosynthesis results in production of $^{16}O_2$ but not of $^{18}O_2$, because the overlying water was predominantly light ($H_2{}^{16}O$). On the other hand, mat's respiratory activity results in uptake of both isotopes. To interpret the MIMS data, we compared it with the expected $^{18}O_2$ dynamics in the overlying water derived from the numerical simulations of the $^{16}O_2$ and $^{18}O_2$ dynamics inside the mat at variable photosynthesis and respiration

rates. As $^{18}O_2$ was used as a tracer, i.e. its concentration was negligible compared with $^{16}O_2$ concentration ($^{18}O_2 << {}^{16}O_2$, $O_{2,tot} \approx {}^{16}O_2$), we considered in the model that the $^{16}O_2$ dynamics in the mat was not affected by $^{18}O_2$. In contrast, the effect of $^{16}O_2$ on $^{18}O_2$, to which we refer as the isotope dilution effect, was accounted for by considering that the rate at which $^{18}O_2$ was locally taken up in the mat was given by the local respiration rate multiplied by the local isotope concentration ratio $^{18}O_2/^{16}O_2$ (isotope fractionation was neglected).

Acknowledgements

This work would not have been possible without the excellent technical support and assistance from Gaby Eickert, Ines Schroeder, Karin Hohmann, Cecilia Wigand, Ingrid Dohrmann, Harald Osmers, Paul Faerber, Georg Harz, Alfred Kutsche and Thomas Holler (all from MPI Bremen), which we greatly appreciate. We are also thankful to Boaz Luz, Jonathan Erez and Eugeni Barkan (Hebrew University of Jerusalem) for their hospitality and help with the MIMS measurements, and Aron Kaplan (HUJ), Bjoern Rost, Klaus-Uwe Richter (both Afred-Wegener-Institute, Bremerhaven), Peter Stief (University of Aarhus) and Lars Borregaard Pedersen (Unisense) for fruitful discussions. This work was financially supported by the Max-Planck Society, GIF Grant G-720-145. 8/2001 and grant DFG JO-412 from the German Research Foundation.

References

Bachar, A., Omoregie, E., de Wit, R., and Jonkers, H.M. (2007) Diversity and function of *Chloroflexus*-like bacteria in a hypersaline microbial mat: phylogenetic characterization and impact on aerobic respiration. *Applied and Environmental Microbiology*, in press.

Berg, P., Risgaard-Petersen, N., and Rysgaard, S. (1998) Interpretation of measured concentration profiles in sediment pore water. *Limnol Oceanogr* **43:** 1500–1510.

Bjornsson, L., Hugenholtz, P., Tyson, G.W., and Blackall, L.L. (2002) Filamentous Chloroflexi (green non-sulfur bacteria) are abundant in wastewater treatment processes with biological nutrient removal. *Microbiol-SGM* **148:** 2309–2318.

Camacho, A., and de Wit, R. (2003) Effect of nitrogen and phosphorus additions on a benthic microbial mat from a hypersaline lake. *Aquat Microb Ecol* **32:** 261–273.

Castenholz, R.W. (2001) Class I: 'Chloroflexi'. In *Bergey's Manual of Systematic Bacteriology*. Boone, D.R., Castenholz, R.W., and Garrity, G.M. (eds). New York, USA: Springer-Verlag, p. 427.

Dominy, P.J., and Williams, W.P. (1987) The role of respiratory electron flow in the control of excitation energy distribution in blue-green algae. *Biochim Biophys Acta* **892:** 264–274.

Epping, E.H.G., and Jørgensen, B.B. (1996) Light-enhanced oxygen respiration in benthic phototrophic communities. *Mar Ecol Prog Ser* **139:** 193–203.

Gich, F., Garcia-Gil, J., and Overmann, J. (2001) Previously unknown and phylogenetically diverse members of the green nonsulfur bacteria are indigenous to freshwater lakes. *Arch Microbiol* **177:** 1–10.

Gieseke, A., and de Beer, D. (2004) Use of microelectrodes to measure in situ microbial activities in biofilms, sediments, and microbial mats. In *Molecular Microbial Ecology Manual*. Akkermans, A.D.L., and van Elsas, D. (eds). 2nd edition. Dordrecht, the Netherlands: Kluwer, pp. 1581–1612.

Hale, B., Blankenship, R.E., and Fuller, R.C. (1983) Menaquinone is the sole quinone in the facultative aerobic green photosynthetic bacterium *Chloroflexus aurantiacus*. *Biochim Biophys Acta* **723:** 376–382.

Hanada, S., and Pierson, B.K. (2006) The family Chloroflexaceae. In *The Prokaryotes – An Evolving Electronic Resource for the Microbiological Community* 3rd edition, release 3.11. New York, USA: Springer-Verlag. doi: 10.1007/0-387-30747-8_33.

Holo, H., and Sirevaeg, R. (1986) Autotrophic growth and CO2 fixation of *Chloroflexus aurantiacus*. *Arch Microbiol* **145:** 173–180.

Imafuku, H., and Katoh, T. (1976) Intracellular ATP levels and light induced inhibition of respiration in a blue-green alga *Anabena variabilis*. *Plant Cell Physiol* **17:** 515–524.

Jonkers, H.M., and Abed, R.M.M. (2003) Identification of aerobic heterotrophic bacteria from the photic zone of a hypersaline microbial mat. *Aquat Microb Ecol* **30:** 127–133.

Jonkers, H.M., Ludwig, R., De Wit, R., Pringault, O., Muyzer, G., Niemann, H., *et al.* (2003) Structural and functional analysis of a microbial mat ecosystem from a unique permanent hypersaline inland lake: 'La Salada de Chiprana' (NE Spain). *FEMS Microbiol Ecol* **44:** 175–189.

Jonkers, H.M., Koh, I.O., Behrend, P., Muyzer, G., and de Beer, D. (2005) Aerobic organic carbon mineralization by sulfate-reducing bacteria in the oxygen-saturated photic zone of a hypersaline microbial mat. *Microb Ecol* **49:** 291–300.

Jørgensen, B.B., and Marais, D.J.D. (1988) Optical-properties of benthic photosynthetic communities – fiber-optic studies of cyanobacterial mats. *Limnol Oceanogr* **33:** 99–113.

Kühl, M., Steuckart, C., Eickert, G., and Jeroschewski, P. (1998) A H2S microsensor for profiling biofilms and sediments: application in an acidic lake sediment. *Aquat Microb Ecol* **15:** 201–209.

Kühl, M., Chen, M., Ralph, P.J., Schreiber, U., and Larkum, A.W.D. (2005) A niche for cyanobacteria containing chlorophyll *d*. *Nature* **433:** 820–820.

Lassen, C., Ploug, H., and Jørgensen, B.B. (1992) A fiberoptic scalar irradiance microsensor – application for spectral light measurements in sediments. *FEMS Microbiol Ecol* **86:** 247–254.

Li, Y.-H., and Gregory, S. (1974) Diffusion of ions in sea water and deep-sea sediments. *Geochim Cosmochim Acta* **38:** 703–714.

Ludwig, R., Al-Horani, F.A., de Beer, D., and Jonkers, H.M. (2005) Photosynthesis-controlled calcification in a hypersaline microbial mat. *Limnol Oceanogr* **50:** 1836–1843.

McCarty, J.E.G., and Ferguson, S.J. (1982) Respiratory control and the basis of light induced inhibition of respiration in chromatophores *Rhodopseudomonas capsulata*. *Biochem Biophys Res Commun* **107:** 1406–1411.

Madigan, M.T., and Brock, T. (1975) Photosynthetic sulfide oxidation by *Chloroflexus aurantiacus*, a filamentous, photosynthetic gliding bacterium. *J Bacteriol* **122:** 782–784.

Madigan, M.T., Martinko, J.M., and Parker, J. (2000) *Biology of Microorganisms*. NJ, USA: Prentice Hall International.

van der Meer, M.T.J., Schouten, S., de Leeuw, J.W., and Ward, D.M. (2000) Autotrophy of green non-sulphur bacteria in hot spring microbial mats: biological explanations for isotopically heavy organic carbon in the geological record. *Environ Microbiol* **2:** 428–435.

van der Meer, M.T.J., Schouten, S., Damste, J.S.S., de Leeuw, J.W., and Ward, D.M. (2003) Compound-specific isotopic fractionation patterns suggest different carbon metabolisms among *Chloroflexus*-like bacteria in hot-spring microbial mats. *Appl Environ Microbiol* **69:** 6000–6006.

van der Meer, M.T.J., Schouten, S., Bateson, M.M., Nübel, U., Wieland, A., Kühl, M., *et al.* (2005) Diel variations in carbon metabolism by green nonsulfur-like bacteria in alkaline siliceous hot spring microbial mats from Yellowstone National Park. *Appl Environ Microbiol* **71:** 3978–3986.

Melandri, A.B., and Zannoni, D. (1978) Photosynthetic and respiratory electron flow in the dual functional membrane of facultative photosynthetic bacteria. *J Bioenergetics Biomembranes* **10:** 109–138.

Meunier, P.C., Burnap, R.L., and Sherman, L.A. (1995) Interaction of the photosynthetic and respiratory electron transport chains producing slow O-2 signals under flashing light in *Synechocystis* sp. PCC 6803. *Photosynth Res* **45:** 31–40.

Mitchell, P. (1957) General theory of membrane transport from studies of bacteria. *Nature* **180:** 134–136.

Mitchell, P. (1961) Coupling of phosphorylation to electron and hydrogen transfer by a chemi-osmotic type of mechanism. *Nature* **191:** 144–148.

Mitchell, P. (1966) Chemiosmotic coupling in oxidative and photosynthetic phosphorylation. *Biol Rev Camb Philos Soc* **41:** 445&.

Nübel, U., Bateson, M.M., Madigan, M.T., Kühl, M., and Ward, D.M. (2001) Diversity and distribution in hypersaline microbial mats of bacteria related to *Chloroflexus* spp. *Appl Environ Microbiol* **67:** 4365–4371.

Nübel, U., Bateson, M.M., Vandieken, V., Wieland, A., Kühl, M., and Ward, D.M. (2002) Microscopic examination of distribution and phenotypic properties of phylogenetically diverse Chloroflexaceae-related bacteria in hot spring microbial mats. *Appl Environ Microbiol* **68:** 4593–4603.

Oesterhelt, D., and Krippahl, G. (1973) Light inhibition of respiration in *Halobacterium halobium*. *FEBS Lett* **36:** 72–76.

Paerl, H.W., Bebout, B.M., Joye, S.B., and Marais, D.J.D. (1993) Microscale characterization of dissolved organic-matter production and uptake in marine microbial mat communities. *Limnol Oceanogr* **38:** 1150–1161.

Pierson, B.K., and Castenholz, R.W. (1974) A phototrophic gliding filamentous bacterium of hot springs, *Chloroflexus aurantiacus*, gen. and sp. nov. *Arch Microbiol* **100:** 5–24.

Pierson, B.K., and Castenholz, R.W. (1995) Taxonomy and physiology of filamentous anoxygenic phototrophs. In *Anoxygenic Photosynthetic Bacteria*. Blankenship, R.E., Madigan, M.T., and Bauer, C.E. (eds). Dordrecht, the Netherlands: Kluwer Academic Publishers, pp. 31–47.

Pierson, B.K., Valdez, D., Larsen, M., Morgan, E., and Mack, E.E. (1994) *Chloroflexus*-like organisms from marine and hypersaline environments – distribution and diversity. *Photosynth Res* **41:** 35–52.

Revsbech, N.P., and Jørgensen, B.B. (1983) Photosynthesis of benthic microflora measured with high spatial-resolution by the oxygen microprofile method – capabilities and limitations of the method. *Limnol Oceanogr* **28:** 749–756.

Revsbech, N.P., and Jørgensen, B.B. (1986) Microelectrodes – their use in microbial ecology. *Adv Microb Ecol* **9:** 293–352.

Revsbech, N.P., Jørgensen, B.B., and Brix, O. (1981) Primary production of microalgae in sediments measured by oxygen microprofile, H-Co-14(3)-fixation, and oxygen-exchange methods. *Limnol Oceanogr* **26:** 717–730.

Revsbech, N.P., Nielsen, L.P., and Ramsing, N.B. (1998) A novel microsensor for determination of apparent diffusivity in sediments. *Limnol Oceanogr* **43:** 986–992.

Richaud, P., Marrs, B.L., and Vermeglio, A. (1986) Two modes of interaction between photosynthetic and respiratory electron chains in whole cells of *Rhodopseudomonas capsulata*. *Biochim Biophys Acta* **850:** 256–263.

Sabaty, M., Gans, P., and Vermeglio, A. (1993) Inhibition of nitrate reduction by light and oxygen in *Rhodobacter sphaeroides* f. sp. denitrificans. *Arch Microbiol* **159:** 153–159.

Scherer, S., and Boeger, P. (1982) Respiration of blue-green algae in the light. *Arch Microbiol* **132:** 329–332.

Tchernov, D., Hassidim, M., Luz, B., Sukenik, A., Reinhold, L., and Kaplan, A. (1997) Sustained net CO2 evolution during photosynthesis by marine microorganisms. *Curr Biol* **7:** 723–728.

Valero-Garces, B.L., Navas, A., Machin, J., Stevenson, T., and Davis, B. (2000) Responses of a saline lake ecosystem in a semiarid region to irrigation and climate variability – the history of Salada Chiprana, central Ebro basin, Spain. *Ambio* **29:** 344–350.

VanGemerden, H. (1993) Microbial mats – a joint venture. *Mar Geol* **113:** 3–25.

Vidondo, B., Martinez, B., Montes, C., and Guerrero, M.C. (1993) Physicochemical characteristics of a permanent Spanish Hypersaline Lake – La-Salada-De-Chiprana (Ne Spain). *Hydrobiologia* **267:** 113–125.

Vila, X., Guyoneaud, R., Cristina, X.P., Figueras, J.B., and Abella, C.A. (2002) Green sulfur bacteria from hypersaline Chiprana Lake (Monegros, Spain): habitat description and phylogenetic relationship of isolated strains. *Photosynth Res* **71:** 165–172.

Villanueva, L., Navarrete, A., Urmeneta, J., White, D.C., and Guerrero, R. (2004) Combined phospholipid biomarker-16S rRNA gene denaturing gradient gel electrophoresis analysis of bacterial diversity and physiological status in an intertidal microbial mat. *Appl Environ Microbiol* **70:** 6920–6926.

Webb, W.L., Newton, M., and Starr, D. (1974) Carbon dioxide exchange of Alnus rubra: a mathematical model. *Oecologia* **17:** 281–291.

Wieland, A., and Kühl, M. (2006) Regulation of photosynthesis and oxygen consumption in a hypersaline cyanobacterial mat (Camargue, France) by irradiance, temperature and salinity. *FEMS Microbiol Ecol* **55:** 195–210.

Wieland, A., Kühl, M., McGowan, L., Fourcans, A., Duran, R., Caumette, P., *et al.* (2003) Microbial mats on the Orkney Islands revisited: microenvironment and microbial community composition. *Microb Ecol* **46:** 371–390.

de Wit, R., Falcon, L.I., and Charpy-Roubaud, C. (2005) Heterotrophic dinitrogen fixation (acetylene reduction) in phosphate-fertilised Microcoleus chthonoplastes microbial mat from the hypersaline inland lake 'la Salada de Chiprana' (NE Spain). *Hydrobiologia* **534:** 245–253.

Zannoni, D., and Fuller, R.C. (1988) Functional and spectral characterization of the respiratory chain of *Chloroflexus aurantiacus* grown in dark oxygen saturated conditions. *Arch Microbiol* **150:** 368–373.

Chapter IV:

Two-dimensional mapping of photopigment distribution and activity of *Chloroflexus*-like bacteria in a hypersalinemicrobialmat

RESEARCH ARTICLE

Two-dimensional mapping of photopigment distribution and activity of *Chloroflexus*-like bacteria in a hypersaline microbial mat

Ami Bachar[1], Lubos Polerecky[1], Jan P. Fischer[1], Kyriakos Vamvakopoulos[1], Dirk de Beer[1] & Henk M. Jonkers[1,2]

[1]Max-Planck-Institute for Marine Microbiology, Bremen, Germany; and [2]Delft University of Technology, Delft, The Netherlands

Correspondence: Henk M. Jonkers, Delft University of Technology, PO Box 5048, 2600 GA Delft, The Netherlands. Tel.: +31 0 15 278 2313; fax: +31 0 15 278 6383; e-mail: h.m.jonkers@tudelft.nl

Received 21 December 2007; revised 15 April 2008; accepted 6 May 2008.

DOI:10.1111/j.1574-6941.2008.00534.x

Editor: Riks Laanbroek

Keywords
Chloroflexaceae; photopigments; hyperspectral imaging; microbial mat.

Abstract

Pigment analysis in an intact hypersaline microbial mat by hyperspectral imaging revealed very patchy and spatially uncorrelated distributions of photopigments Chl *a* and BChl *a*/*c*, which are characteristic photopigments for oxygenic (diatoms and cyanobacteria) and anoxygenic phototrophs (*Chloroflexaceae*). This finding is in contrast to the expectation that these biomarker pigments should be spatially correlated, as oxygenic phototrophs are thought to supply the *Chloroflexaceae* members with organic substrates for growth. We suggest that the heterogeneous occurrence is possibly due to sulfide, whose production by sulfate-reducing bacteria may be spatially heterogeneous in the partially oxic photic zone of the mat. We furthermore mapped the near-infra-red-light controlled respiration of *Chloroflexaceae* under light and dark conditions and found that *Chloroflexaceae* are responsible for a major part of oxygen consumption at the lower part of the oxic zone in the mat. The presence of *Chloroflexaceae* was further confirmed by FISH probe and 16S rRNA gene clone library analysis. We assume that species related to the genera *Oscillochloris* and '*Candidatus* Chlorothrix', in contrast to those related to *Chloroflexus* and *Roseiflexus*, depend less on excreted photosynthates but more on the presence of free sulfide, which may explain their presence in deeper parts of the mat.

Introduction

Filamentous anoxygenic phototrophic bacteria related to the family *Chloroflexaceae* are conspicuous bacteria that have been found to be quantitatively important community members in both hot spring and hypersaline microbial mats (Castenholz, 1988; Pierson *et al*., 1994; Nübel *et al*., 2001, 2002; van der Meer *et al*., 2003, 2005). The family accommodates so far six scientifically described genera, of which the species of two genera (*Heliothrix* and *Roseiflexus*) only produce bacteriochlorophyll *a* (BChl *a*), while species of the other four genera (*Chloroflexus*, *Chloronema*, *Oscillochloris* and 'Candidatus *Chlorothrix*') produce BChl *c* and other possible bacteriochlorophylls in addition to BChl *a* (Klappenbach & Pierson, 2004). All the *Chloroflexaceae* members characterized so far are generally described as anoxygenic phototrophs. Enzymatic studies have shown that *Chloroflexus aurantiacus* apparently uses the 3-hydroxypropionate pathway for inorganic carbon fixation during autotrophic growth (Strauss & Fuchs, 1993). The finding that homologous genes encoding for different steps in that pathway also occur in *Roseiflexus*-like organisms suggests that representatives of this genus might also be capable of autotrophic bicarbonate fixation (Klatt *et al*., 2007). In addition to phototrophy, at least some of the cultured and physiologically characterized species of the *Chloroflexaceae* family appear to be able to additionally perform aerobic respiration (Pierson & Castenholz, 1974). In two recently published studies, it was shown by near-infra-red (NIR) light manipulations that BChl *c*-containing *Chloroflexaceae* were likely responsible for a significant part (up to 100% in certain cases) of the microbial mat's community aerobic respiration (Bachar *et al*., 2007; Polerecky *et al*., 2007). These and other reported studies on the *in situ* physiology of *Chloroflexaceae* members (Bateson & Ward, 1988; van der Meer *et al*., 2003, 2005) contributed to the notion that these organisms may play an important role in carbon and sulfur cycling in at least some microbial mats.

Although the metabolic switch from anoxygenic photosynthesis under NIR light illumination to aerobic respiration under NIR light-deprived conditions for *C. aurantiacus* was proved in pure culture (Bachar *et al.*, 2007), the direct link between the presence of an organism and a certain physiological property in intact natural systems is often obscured by the presence of other community members. Moreover, the spatial heterogeneity both in the vertical and in the horizontal direction of such ecosystems often hampers our ability to establish a firm relationship between the presence of specific community members (community structure) and their function.

Currently, a practical difficulty in establishing the two-dimensional (2-D, i.e., both horizontal and vertical) distribution of different *Chloroflexaceae* species in microbial mats is that specific fluorescent gene probes for FISH studies are available only for two (*Chloroflexus* and *Roseiflexus*) of the six known *Chloroflexaceae* genera (Nübel *et al.*, 2002). However, bacteriochlorophyll *c* (BChl *c*), which is produced presumably by oxygen-respiring members of *Chloroflexaceae* (Bachar *et al.*, 2007; Polerecky *et al.*, 2007), could be used as another possible, although less specific, biomarker. Bacteriochlorophylls and other photopigments are routinely quantified by HPLC. However, this method requires extraction of pigments from mat sections, which limits the vertical spatial resolution to 0.25–0.5 mm, and smears possible horizontal patchiness.

In this work, we applied hyperspectral imaging to visualize the 2-D distribution of BChl *a* and *c* and other photopigments in the mat. This was done to test the working hypothesis that *Chloroflexaceae* members are spatially correlated with oxygenic phototrophs (e.g. *Cyanobacteria*), which are thought to supply the former with organic substrates for growth (D'Amelio *et al.*, 1987; Bateson & Ward, 1988; Castenholz, 1988; Hanada & Pierson, 2006; Nübel *et al.*, 2002). Furthermore, we exploited the observation that NIR light can inhibit *Chloroflexaceae* respiration and adopted the recently developed NIR light manipulation method (Polerecky *et al.*, 2007) to map *Chloroflexaceae* respiration activity in 2-D, with the aim to compare it with the distribution of the photosynthetic activity and to establish a link with the 2-D BChl *c* distribution in the mat. Additionally, we used HPLC to provide supplementary data on vertical pigment distribution, and applied available FISH probes and additional 16S rRNA gene techniques to investigate the presence, distribution and diversity of *Chloroflexaceae* members in the investigated mat. Several characterized species of the *Chloroflexaceae* family are known to be able to use sulfide as source of electrons for energy generation in the process of cyclic electron transport as well as for CO_2 fixation. Therefore, we measured sulfide concentration profiles and sulfate reduction rates in distinct depth zones to additionally establish the potential availability of sulfide as an electron donor for anoxygenic photosynthetic activity. Finally, we used microsensors to measure light and oxygen penetration in undisturbed mat samples to estimate their availability for photosynthesis and aerobic respiration, respectively.

Materials and methods

Microbial mats

A microbial mat was maintained in a continuous flow-through mesocosm consisting of an open plastic basin (1.2 m × 1.2 m × 0.5 m) with a continuous in- and outflow of hypersaline water. The mesocosm system was inoculated with mat samples taken from the hypersaline Lake Chiprana, Spain (41°14′20″N, 0°10′54″W), and grown over 3 years in water with a salt composition similar to the natural lake water (seawater plus 80 g L^{-1} $MgSO_4 \cdot 7H_2O$). The mats were illuminated with a light intensity of 500 μmol photons m^{-2} s^{-1} and a light regime of 16 h light and 8 h dark.

Microsensor measurements

A microbial mat piece was taken from the mesocosm system and incubated in the laboratory in a continuous flow-through chamber at room temperature. After *c.* 5 h of mat stabilization, high spatial resolution depth profiles of oxygen (O_2), sulfide (H_2S), pH and light were measured continuously after light conditions were changed (switch from light, 500 μmol photons m^{-2} s^{-1}, to dark and vice versa) until a steady state was reached. O_2 was measured using a Clark-type oxygen microsensor with a guard cathode (Revsbech, 1989), which had a tip diameter < 10 μm and a response time < 1 s. H_2S and pH were measured with microsensors made and calibrated as described by Kühl *et al.* (1998). Light spectra inside the mat in the region from 400 to 900 nm were measured in 500-μm intervals using a fiber-optic scalar irradiance microprobe (Kühl & Jørgensen, 1992, 1994) connected to a spectrometer (USB2000, Ocean Optics). The recorded light intensity at each wavelength was normalized to the intensity measured at the mat surface.

Oxygen imaging and rate calculation

O_2-sensitive planar optodes were used to map the distributions of oxygen concentration, net oxygenic photosynthesis and NIR light-dependent respiration in intact microbial mat samples. A piece of the mat was taken from the mesocosm system, vertically cut and placed in an aquarium against a glass wall equipped with a planar oxygen optode. The optode was constructed by depositing a thin (*c.* 20 μm) layer of an oxygen-sensitive cocktail (see Precht *et al.*, 2004, for cocktail composition) onto a fused fiber-optic bundle

element (Fiber Optic Faceplate, 50 mm × 50 mm × 10 mm; SCHOTT North America Inc.), which was subsequently glued into an opening in the aquarium's side wall. The mat was illuminated from above by two warm-white high-power light-emitting diodes (LEDs; LXHL-MWGC Lumileds) emitting in the visible region (VIS, 400–700 nm; intensity 200 μmol photons m^{-2} s^{-1}). The saturating NIR light (NIR, 715–745 nm, $\lambda_{max} = 740$ nm; intensity *c.* 60 μmol photons m^{-2} s^{-1}) was generated by an array of NIR LEDs (ELD-740-524, Roithner Lasertechnik) equipped with a band-pass filter (730AF30, Omega Optical). The wavelength region was selected so as to match specifically the *in vivo* absorption maximum of BChl *c*. The mat was illuminated from the side through the optode window to ensure maximal exposure of the BChl *c*-containing organisms to NIR light. The VIS and NIR LEDs could be switched on and off independently of each other. Each of the four possible illumination combinations (VIS+NIR, VIS-only, NIR-only and dark) lasted for 3 h, during which oxygen images were recorded at 5-min intervals using an oxygen imaging system (see Holst & Grunwald, 2001 for details). Temperature was maintained constant at 20 °C and the overlying water was aerated during the measurement.

NIR light-dependent respiration of BChl *c*-containing bacteria was calculated from the steady state oxygen images by expanding the 1-D method described by Polerecky *et al.* (2007) to 2-D. Specifically, O_2 images measured at the end of the VIS+NIR and VIS-only periods were subtracted from each other to obtain the differential oxygen image during VIS illumination, denoted as $\delta O_2(+\mathrm{VIS})$. The same was done for the images measured at the end of the NIR-only and dark periods to obtain differential oxygen image in the absence of VIS illumination, denoted as $\Delta O_2(-\mathrm{VIS})$. Subsequently, 2-D maps of the respiration activity of the BChl *c*-containing bacteria (supposedly *Chloroflexaceae*) in the VIS light $[R_C(+\mathrm{VIS})]$ and in the dark $[R_C(-\mathrm{VIS})]$ were calculated from the second derivative of the respective differential oxygen images and oxygen diffusion coefficient *D*, as suggested by Polerecky *et al.* (2007). For simplicity, the second derivatives were calculated only in the vertical (*z*) direction, i.e., $R_C(\pm\mathrm{VIS}) \approx -D\partial^2\Delta O_2(\pm\mathrm{VIS})/\partial^2 z$. This was done numerically by applying the Savitzky–Golay filter on the vertical profiles extracted from each differential oxygen image. 2-D maps of net photosynthesis in the VIS light and dark were calculated similarly but using the respective oxygen images, i.e. $\mathrm{NP}(\pm\mathrm{VIS}) \approx -D\partial^2 O_2(\pm\mathrm{VIS}, -\mathrm{NIR})/\partial^2 z$.

Photopigment analysis by HPLC and hyperspectral imaging

For HPLC pigment analysis, frozen microbial mat cores (0.9 cm diameter) were horizontally sliced in 250-μm thick sections using a rotary HM 505E cryomicrotome (Micron) from the surface down to 10 mm depth. Pigments were extracted in 5-mL 100% acetone for 24 h at −35 °C in the dark. Extracts were subsequently centrifuged for 10 min at 16 000 ***g*** and supernatant aliquots were analyzed by HPLC as described before (Jonkers *et al.*, 2003). Standards for chlorophyll *a* (Chl *a*) and Zeaxanthin were obtained from DHI Water and Environment, Denmark. Cultures of *Thiocapsa roseopersicina* (BChl *a*), *C. aurantiacus* (BChl *c*) and *Chlorobium tepidum* (BChl *c*) were used as a source for the respective bacteriochlorophyll standards. Because no quantitative bacteriochlorophyll standards were available, these pigments were quantified only in arbitrary units (A.U.).

2-D mapping of photopigment distribution in the mat was carried out using a newly developed hyperspectral imaging system (L. Polerecky *et al.*, unpublished data). Briefly, the system comprises a laboratory hyperspectral camera (Resonon Inc., Bozeman) attached to a motorized stage (VT-80, Micos), which is mounted onto a heavy stand. The hyperspectral camera allowed simultaneous acquisition of light spectra from a line of 480 pixels in the wavelength region 460–913 nm (resolution *c.* 2 nm). A 1-mm thick vertical mat section was placed between two microscope slides and kept moist with hypersaline water. The slides were gently pressed to achieve maximal optical contact with the mat, and to ensure that the imaged face of the mat was flat. The sample was then placed *c.* 5 cm in front of the objective lens and illuminated from above. The hyperspectral images were acquired by moving the camera (at 80 μm s^{-1}) over the sample while recording the spectral information from the line of pixels at 3.75 fps. The resulting hyperspectral images had a spatial resolution of *c.* 30 μm × 30 μm.

Both the absorption and the autofluorescence properties of the pigments in the mat were used for hyperspectral pigment imaging. For the absorption measurements, the sample was placed on a white standard substrate (Spectralon), which allowed simultaneous acquisition of the reference and reflected spectra in one scan, and illuminated by either a combination of warm-white and NIR LEDs or a halogen lamp emitting in the VIS+IR region (Table 1). Spectral reflectance $R(\lambda)$ in each pixel of the mat was obtained by dividing the spectrum of the light reflected from the sample with that reflected from the white standard. The emission spectra were measured under illumination by a narrow band LED equipped with a 5° collimating optics (LXHL-NX05-5; Lumileds) and a short-pass optical filter, and the emitted autofluorescence was imaged through a complementary long-pass optical filter (see Table 1 for the light source+filter combinations used). During these measurements, the sample was placed on a black substrate to minimize reflections of the excitation light.

The hyperspectral images obtained were analyzed using the available *in vivo* absorption and fluorescence

Table 1. Combinations of light sources together with excitation and emission filters used for hyperspectral imaging of pigments in the mat

Hyperspectral imaging mode	Light source	Excitation/emission filter	Target group
Absorption	LXHL-MWGC* (450–720 nm)	–	Diatoms
	+ELD-740–524† (710–770 nm)	–	Cyanobacteria
	or halogen lamp (450–900 nm)	–	BChl *a*- and *c*- producing bacteria
Emission	LXHL-LR5C*	455DF70/510ALP‡	Diatoms
	(λ_{max} = 455 nm, blue)	(λ_c = 510 nm)	BChl *a*- and *c*- producing bacteria
Emission	LXHL-LL3C*	DC-Red/R-61§	Cyanobacteria
	(λ_{max} = 590 nm, amber)	(λ_c = 610 nm)	

*Lumileds.
†Roithner Lasertechnik.
‡Omega Optical.
§Linos Photonics.

Table 2. Absorption and emission characteristics of pigments found in the studied mat; only spectral features associated with target microorganisms of this study are listed

Pigment	Absorption maximum (λ_{max}) (nm)	Excitation/emission maximum (λ_{max}) (nm)	Target group
Chl a	673	455/677	Diatoms
Chl a	673	–	*Cyanobacteria*
Phyco-cyanin*	622	590/652	*Cyanobacteria*
BChl *a*†	807+845	455/867	*Chloroflexaceae*/ Purple sulfur bacteria
BChl *c*‡	733	455/756	Green sulfur bacteria/ some *Chloroflexaceae*

*Hofstraat *et al*. (1994).
†Kühl & Fenchel (2000).
‡Saga & Tamiaki (2004).

characteristics of the targeted pigments (Table 2). Specifically, the fourth derivative of the reflectance in the wavelength corresponding to the absorption maximum (λ_{max}; Table 2) of a given pigment was taken as a relative measure of the local pigment concentration, i.e. [pigment] $\approx d^4R(\lambda_{max})/d\lambda^4$ (Butler & Hopkins, 1970; Fleissner *et al*., 1996). The emission spectra were fitted by a linear combination of Lorenzian and/or Gaussian peak functions centered at specific wavelengths corresponding to *in vivo* emission maxima of the targeted pigments (Table 2), similarto that performed by Combe *et al*. (2005) and Barille *et al*. (2007) for reflectivity spectra. The magnitude of the peaks was then taken as a relative measure for the local concentration of the corresponding pigment. In both absorption and emission measurement modes, the calculated concentrations of the targeted pigment were color-coded and displayed as R, G and B channels in composite RGB images. To allow quantitative comparison with the 1-D HPLC-determined pigment distributions, the 2-D maps were also horizontally averaged over 0.5-mm intervals and plotted as vertical profiles.

Distribution of *Chloroflexaceae* in intact mat samples by FISH analysis

The spatial distribution of two specific groups within the *Chloroflexaceae* family was studied by FISH using previously developed specific probes (Nübel *et al*., 2002). The FISH probing was limited to members phylogenetically related to two genera, *Chloroflexus* and *Roseiflexus*, as specific probes for the other four genera within the *Chloroflexaceae* family (*Chloronema*, *Heliothrix*, *Oscillochloris* and 'Candidatus *Chlorothrix*') were not available at the time of this study. As the members of the genera *Chloroflexus* and *Roseiflexus* characterized so far produce BChl *a*+*c*, and BChl *a* but not BChl *c*, respectively, we assumed in this study that the applied FISH probes targeted corresponding pigment-producing phylotypes of these two genera. For the FISH procedure, mat pieces were firstly fixed in filter-sterilized 4.5% formaldehyde in seawater for 12 h at room temperature. Subsequently, formaldehyde was rinsed out twice with a saline phosphate buffer (1.37 M NaCl, 85 mM $Na_2HPO_4 \cdot 2H_2O$, 27 mM KCl, 15 mM KH_2PO_4). In order to maintain the spatial organization, the mat was then embedded in a methacrylate resin, which enabled precise vertical sectioning of thin samples (30 μm) using a rotary HM 505E cryomicrotome (Microm). These sections were hybridized with probes CFX1238 (CGCATTGTCGTGGC CATT) attached to fluorophore Alexa 647 and RFX1238 (CGCATTGTCGGCGCCATT) attached to fluorophore Alexa 488, targeting *Chloroflexus*- and *Roseiflexus*-related phylotypes, respectively (Nübel *et al*., 2002). Sections of thus plasticized mat samples were mixed with a 5-μL probe and 45-μL hybridization buffer (40% formamide) in a 125-μL reaction vial, incubated for 6 h at 45 °C and washed in prewarmed washing buffer for 10 min at 47 °C. Hybridized mat sections were subsequently covered with antifading immersion oil (Citifluor Ltd, UK) and evaluated using a

fluorescence microscope (Axio Imager M1, Zeiss, equipped with Plan Apochromat objectives).

Chloroflexaceae diversity in the mat

As the FISH probe analysis carried out in this study targeted phylotypes of only two out of six known *Chloroflexaceae* genera, a 16S rRNA gene clone library was additionally constructed in order to obtain an estimate of the diversity of *Chloroflexaceae* genera present in the mat. Specific PCR primers (CCR-344-F and CCR-1338-R) developed by Nübel *et al.* (2001), targeting the 16S rRNA gene of all presently known *Chloroflexaceae* members, were applied. Genomic DNA was extracted from a 1-cm thick intact mat sample by phenol–chloroform extraction and purified with the Wizard® DNA clean-up system (Promega, Madison, WI). Approximately 1000-bp fragments of the present 16S rRNA genes were amplified from genomic DNA using the specific primers. PCR conditions were applied as described in Nübel *et al.* (2001). The PCR product was subsequently visualized on an agarose gel, and the 16S rRNA gene band was excised. The excised PCR product was then purified using the QIAquick Gel Extraction Kit (Qiagen, Hilden, Germany). Two microliters of purified product was ligated into the pGEM T-Easy vector (Promega) and transformed into *Escherichia coli* TOP10 cells (Invitrogen, Carlsbad, CA) according to the manufacturer's recommendations. Overnight cultures were prepared from positive transformants in a 2-mL 96-well culturing plate. Plasmid DNA was extracted and purified using the Montage Plasmid Miniprep 96 kit (Millipore, Billerica). Purified plasmids were sequenced in one direction with the M13F primer using the BigDye Terminator v3.0 Cycle Sequencing kit (Applied Biosystems, Foster City, CA). Samples were run on an Applied Biosystems 3100 Genetic Analyzer. Sequences of > 800 bp were matched with the nucleotide–nucleotide BLAST (BLASTN) tool (www.ncbi.nlm.nih.gov/blast/Blast.cgi) and closest matches with sequences from both environmental clones and isolated bacteria present in the database were determined.

Sulfate reduction rates

For the determination of sulfate reduction rates in distinct deep layers of the mat, 1.5-cm diameter microbial mat cores overlain with 2 mL water were injected each with 3 MBq $^{35}SO_4^{2-}$ divided over five injections of 5 μL each to ensure an equal distribution of tracer. Triplicate cores were incubated for 5 h either under light (500 μmol photons m^{-2} s^{-1}) or dark conditions at room temperature. Cores were fixed in liquid nitrogen after incubation. Duplicate control cores were fixed in liquid nitrogen immediately after tracer injection. Cores were then horizontally cut into 4-mm thick slices to a depth of 24 mm and fixed in 20% zinc acetate solution. Reduced-labeled sulfate was extracted following the single-step chromium reduction method according to the procedure described in Kallmeyer *et al.* (2004) and quantified with a liquid scintillation counter (2500 TR, Packard) using Lumasafe Plus (Lumac BV, Holland) scintillation cocktail. Microbial mat pore water sulfate was quantified by ion chromatography to enable calculation of specific sulfate reduction rates (Kallmeyer *et al.*, 2004).

Results

General description of the microbial mat

The mesocosm-incubated microbial mat investigated consisted of distinctly colored layers (Figs 1, 6a and 7a). Microscopic analysis revealed that the top *c.* 2-mm thick yellow–brown layer was mainly composed of various morphotypes of diatoms and thin filamentous bacteria. Below this layer, a 3–4-mm-thick green layer was dominated by filamentous cyanobacteria. Underneath this layer was a 2–3-mm-thick purple layer dominated by filamentous bacteria and purple sulfur-like bacteria (1–5-μm diameter spherical bacteria with apparent sulfur inclusions).

Vertical profiles of oxygen, light intensity, sulfide and sulfate reduction rates

Oxygen, measured both with microsensors and planar optodes, penetrated down to *c.* 2 and 6–9 mm in the dark

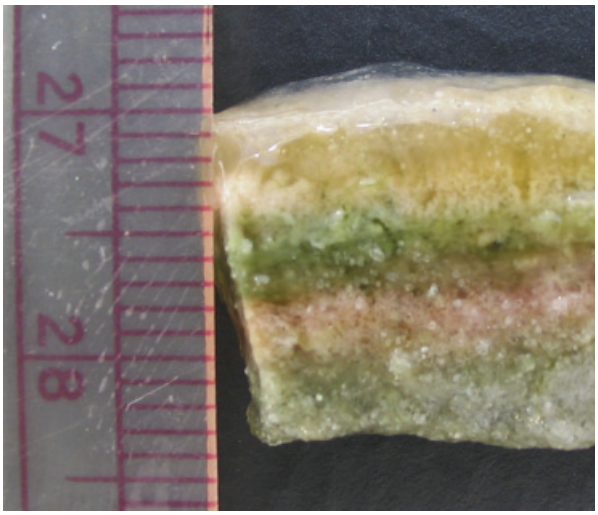

Fig. 1. Photograph of a vertically cut subsample of a mesocosm-incubated microbial mat used in this study for oxygen, sulfide and light microsensor measurements, HPLC photopigment determination, *Chloroflexus* and *Roseiflexus* FISH analysis and sulfate reduction measurements. For oxygen and hyperspectral imaging, other subsamples of the same mat were used (see Figs 3, 4, 6 and 7). Scale with 0.5-cm intervals is depicted on the paper beside the mat.

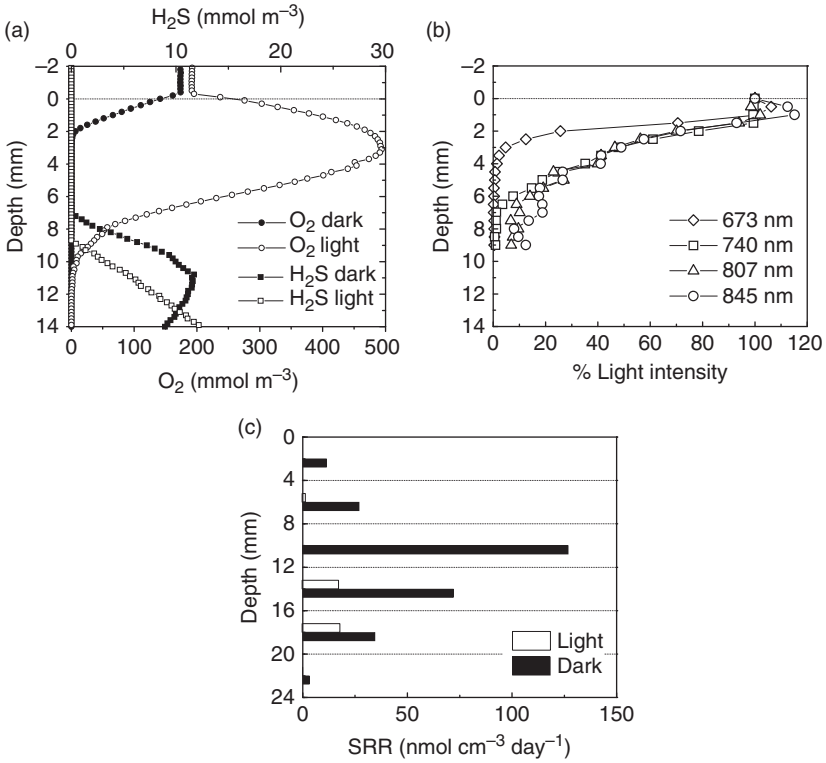

Fig. 2. (a) Oxygen and total free sulfide ($H_2S+HS^-+S^{2-}$) concentration profiles in the mat measured in the dark and under visible illumination (500 μmol photons m^{-2} s^{-1}). (b) Vertical profiles of scalar irradiance in the mat at selected wavelengths corresponding to absorption maxima of targeted pigments (see Table 2). Values are expressed as percentage of the irradiance at the mat surface. (c) Vertical profiles of sulfate reduction rates in dark and light (500 μmol photons m^{-2} s^{-1}) incubated mat samples.

and light incubated mats, respectively (Figs 2a and 3). Light microsensor measurements (Fig. 2b) revealed that NIR light, which can be used by the BChl *a*- and *c*-producing bacteria, penetrated in significant amounts to depths >7 mm. On the other hand, the intensity of the VIS light at 673 nm, which corresponds to the i*n vivo* absorption maximum of Chl *a*, decreased below 1% of the surface value already at depths of 4–4.5 mm. Free sulfide was detected only in deeper parts of the mat, both under dark (>7 mm) and under light (>8 mm) conditions (Fig. 2a). ^{35}Sulfate-radiotracer measurements revealed that in dark incubated mats, sulfate reduction occurred throughout the entire mat (thickness, *c.* 2 cm), reaching a maximum at depths 8–12 mm. In illuminated mats, significant rates of sulfate reduction were detectable in deeper anoxic parts (>12 mm) of the mat, although low rates were also observed in the 4–8 mm zone (Fig. 2c). It thus appears that in this mat sulfate reduction was not restricted to anoxic zones only but also occurred in the oxic zone of the mat (Fig. 2c).

Spatial distribution of photopigments

As for this study, the hyperspectral imaging technique was optimized for the detection of BChl *a* and *c* in addition to other major photosynthetic pigments (Chl *a* and phycobilins); the results of this technique (Figs 6 and 7) are compared with those obtained with traditional HPLC photopigment detection (Fig. 5). The presence of Chl *a* (produced by algae and cyanobacteria), BChl *a* (produced by purple and green sulfur bacteria and *Chloroflexaceae*) and BChl *c* (produced by some green sulfur bacteria and some *Chloroflexaceae*) in the mat was detected by both HPLC and hyperspectral methods. The typical cyanobacterial pigments phycocyanin (a phycobilin) and zeaxanthin (a carotenoid) detected by hyperspectral imaging and HPLC analysis, respectively, were used as specific proxies for the distribution of cyanobacteria.

HPLC analysis revealed abundant Chl *a* content in the top 8 mm of the mat, reaching local maxima at depth zones of 2–3 and 6–7 mm (Fig. 5). These maxima coincided well with the bands in which zeaxanthin was observed. BChl *a* was almost not detected by HPLC in the top 5.5 mm of the mat (with the exception of depth *c.* 3.5 mm), but was found only at depths of 5.5–7 mm. In contrast, BChl *c* was detected only in a narrow zone at depths of 3–4 mm, coinciding with low amounts of BChl *a*, the local minimum of zeaxanthin and depreciated Chl *a* concentrations.

Hyperspectral imaging was sensitive to detect target photopigments in both absorption and emission modes. In the absorption mode, the presence of a pigment was detected as a pronounced valley in the reflectance spectrum centered at a specific wavelength λ_{max} corresponding to the pigment's *in vivo* absorption maximum (Fig. 6e, Table 2). In

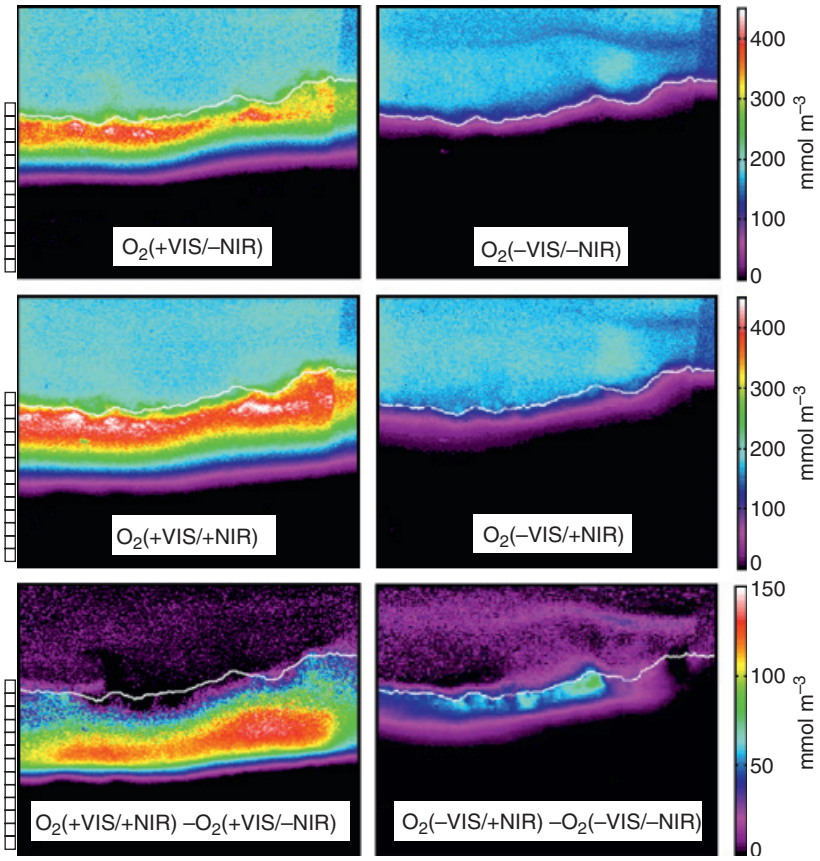

Fig. 3. Oxygen imaging across a vertical section of the microbial mat (shown in Fig. 7a) using planar optodes. Top and middle panels show steady-state oxygen distributions at four combinations of illumination by visible (VIS) and saturated NIR lights, respectively. + and − indicate the presence and absence of the light, respectively. Differential oxygen images, calculated as the difference between the oxygen distributions obtained with (middle panel) and without (top panel) NIR illumination, are shown in the bottom panel. Approximate mat surface is depicted by a white horizontal line; scale bar in mm is shown on the left, and color scaling on the right.

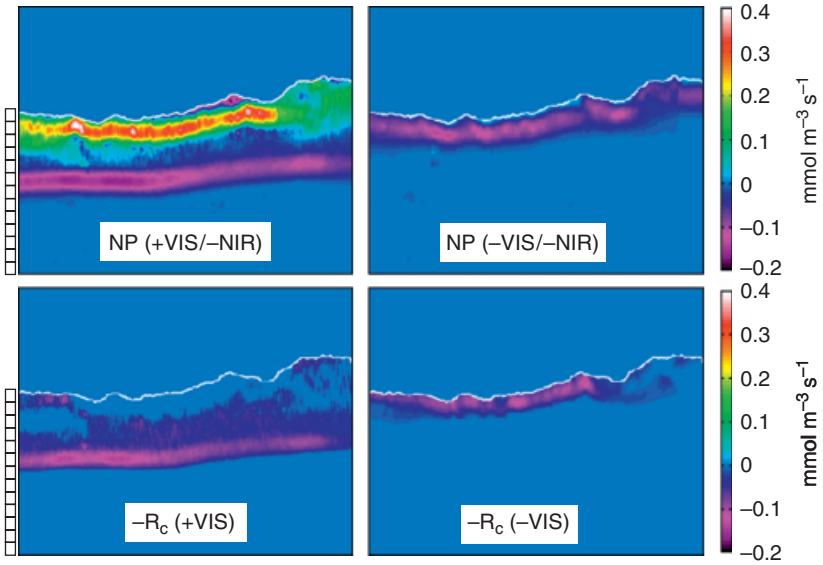

Fig. 4. Distributions of rates of net photosynthesis (NP; top) and respiration by BChl *c*-producing *Chloroflexaceae* (R_C; bottom) in the presence (left) and absence (right) of illumination by visible light (NIR illumination was absent in both cases). NP and R_C images were calculated from the oxygen images in the top row and from the differential oxygen images in the bottom row of Fig. 3, respectively. Positive and negative NP values represent net production and consumption, respectively. Note that R_C is displayed as a negative value to enable direct visual comparison with the NP rates. Approximate mat surface is depicted by the white horizontal line; scale bar in mm is shown on the left and color scaling on the right.

the emission mode, pigment was detected by its strong autofluorescence. Detection of Chl *a* (in algae and cyanobacteria) and BChls *a* and *c* was possible using blue excitation ($\lambda_{max} = 455$ nm) and emission at 677, 867 and 756 nm, respectively, while phycocyanin (in cyanobacteria) could be detected using amber excitation ($\lambda_{max} = 590$ nm) and emission at 652 nm (Fig. 6f, Table 2). Although more emission peaks were observed using these two excitation wavelengths, only those mentioned above were analyzed in more detail to remain focused on the targeted groups of microorganisms.

Pigment distributions in the studied mat derived from hyperspectral imaging exhibited a very patchy character,

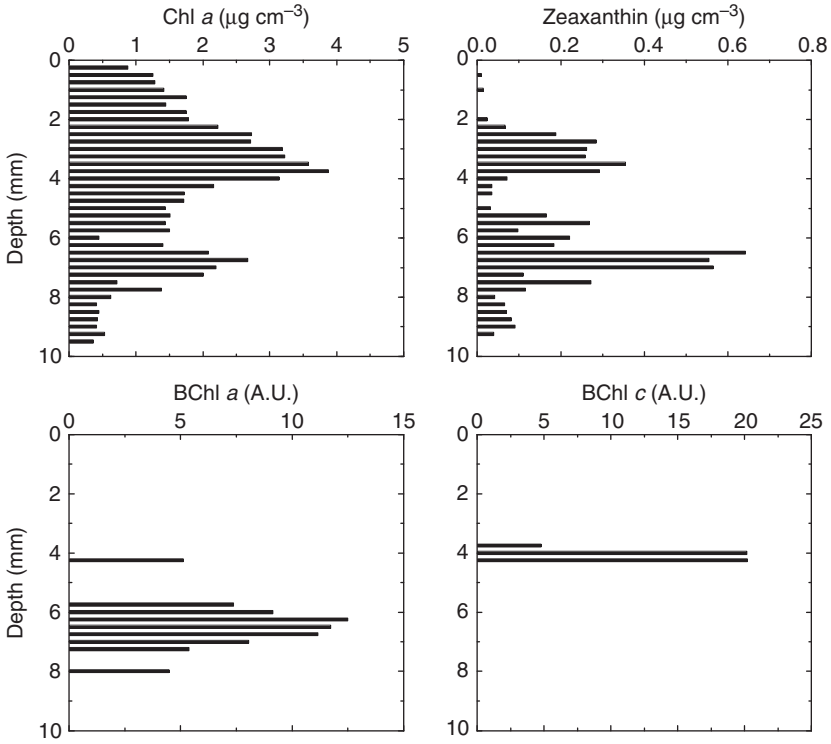

Fig. 5. Vertical profiles of photopigments in the mat, as determined by HPLC analysis of 0.25-mm thin mat sections. Chl *a* and zeaxanthin are presented in μg cm^{-3} of the mat, while the other pigments are in A.U. due to lack of calibration standards.

with pronounced vertical and horizontal heterogeneities (Fig. 6b–d). When horizontally averaged, the vertical pigment distributions matched mostly well with those determined by HPLC (compare Figs 5 and 6g–i). Namely, local Chl *a* maxima due to the presence of algae (diatoms) were observed in the top *c.* 1 mm of the mat, while wide but pronounced peaks of Chl *a* and phycocyanin corresponding to dense cyanobacterial populations were observed at depths of *c.* 3 and 4–5 mm. Local maximum of BChl *c* was detected as a pronounced patch at a depth of 3–4 mm, i.e., in the zone where Chl *a* and phycocyanin exhibited local minimum. Similar complementarities were seen in the HPLC data. However, unlike HPLC analysis, hyperspectral imaging revealed evidence of absorption at 733 nm as well as emission at 756 nm in deeper parts of the mat ($>$ 4 mm, peaking at *c.* 6.5 mm), suggesting abundant presence of BChl *c* also at these zones of the mat. Furthermore, in contrast to the HPLC analysis, which detected BChl *a* only below *c.* 5.5 mm, hyperspectral imaging suggests detectable amounts of BChl *a* throughout the entire mat (0–8 mm), reaching a maximum at depth *c.* 6.5 mm (Fig. 6h).

Hyperspectral analysis of another subsample of the same mat, which was also used for O_2 imaging, revealed a similar degree of patchiness in the pigment distribution, as demonstrated by large variability of colors in the composite RGB image in Fig. 7c–d. Chl *a* was abundant throughout the mat, reaching a wide maximum at *c.* 3 mm depth, while phycocyanin became abundant only at depths below 2 mm. Evidence for the presence of BChl *c* (i.e. pronounced absorption at 733 nm) was found throughout the mat, starting at lower concentrations also at the mat surface and reaching a wide maximum at 3–7 mm (Fig. 7f).

As diatoms (and other algae) produce only Chl *a*, while cyanobacteria produce Chl *a*, in addition to zeaxanthin and phycocyanin, it can be concluded from these profiles that diatoms and other algae are responsible for the upper Chl *a* maximum (0–1.5 mm depth; Chl *a* but insignificant zeaxanthin or phycocyanin present), while at least two apparently different populations of cyanobacteria occur in deeper parts of the mat. BChl *a* and *c*-producing bacteria (purple and green sulfur bacteria and *Chloroflexaceae*; see Discussion) exhibited profound maxima at 6–7 and 3–4+6–7 mm depths, respectively.

Hyperspectral imaging revealed a high degree of horizontal heterogeneity, in addition to vertical stratification, in the distribution of major phototrophic groups of microorganisms in the mat. Particularly striking is the patchy distribution pattern of BChl *c*, depicted by the red channel (i.e. as red, magenta or orange) in the composite images in Figs 6b–c and 7d. It appears that BChl *c*-producing *Chloroflexaceae* are spatially not closely associated with the oxygenic phototrophs (diatoms and/or cyanobacteria) present in the mat, as was hypothesized in this study, but are rather 'sandwiched' in their own specific locations, possibly determined by factors other than excretion of organics by oxygenic phototrophs.

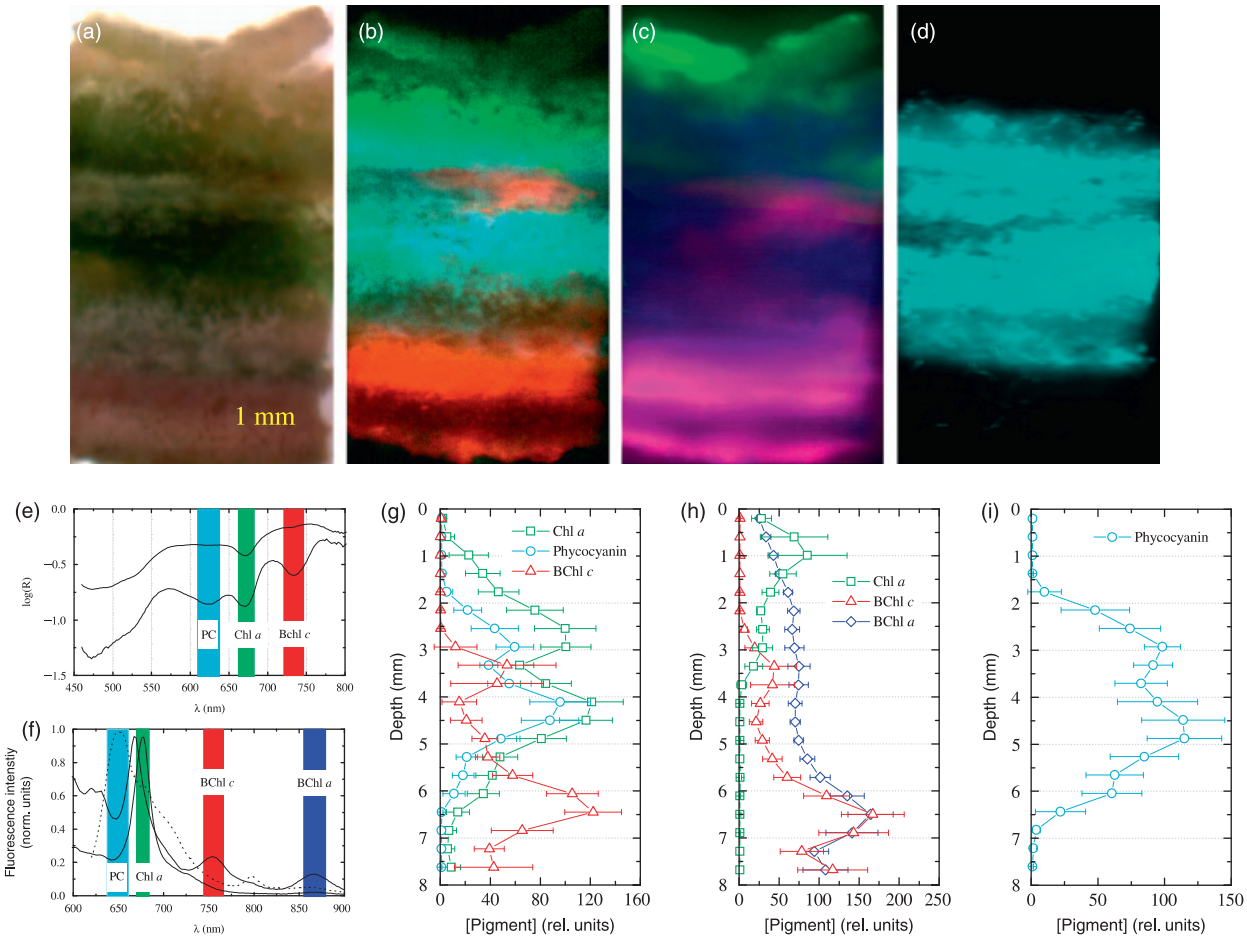

Fig. 6. Hyperspectral imaging of pigments in the microbial mat. (a) True-color image of the mat, as seen by a naked eye under white illumination. (b) Relative concentrations of photopigments Chl *a* (green), phycocyanin (PC, blue) and BChl *c* (red) across a vertical section of the mat, as calculated from the second derivative of the reflectance spectra at specific wavelengths. Examples of the reflectance spectra, together with the spectral features corresponding to the target pigments, are shown in (e). (c–d) Relative concentrations of photopigments across the mat calculated from the magnitudes of the auto-fluorescence peaks emitted when excited by blue (c) and amber (d) lights (Tables 1 and 2). Examples of normalized emission spectra obtained using blue and amber excitation are shown in (f) by solid and dotted lines, respectively. Associations between the emission peaks and the target pigments are also shown. Red, green and blue colors in (c) correspond to photopigments BChl *c*, Chl *a* and BChl *a*, respectively, while cyan color in (d) corresponds to phycocyanin. Note that mix-colored regions represent areas where more than one pigment are concurrently detected (e.g. in B, cyan = blue + green indicates concurrent presence of Chl *a* and phycocyanin; in C, magenta = blue + red indicates the concurrent presence of BChl *a* and *c*). (g), (h) and (i) show the vertical profiles of relative pigment concentrations obtained by horizontal averaging of the corresponding channels in images (b), (c) and (d), respectively.

Chloroflexaceae-related phylotype diversity and depth distribution of selected species

Analysis of the 16S rRNA gene clone library carried out with specific primers revealed the presence of sequences related (58–97%) to characterized members of four of the six known genera of the *Chloroflexaceae* Family (Table 3). Members of three of these genera are known to produce BChl *c* (*Chloroflexus* sp., *Oscillochloris* sp. and '*Candidatus* Chlorothrix halophila'), while members of the fourth genus are known to produce BChl *a* only (*Roseiflexus castenholzii*). By far most of the analyzed unique sequences (22 out of 29, i.e. 76%) appeared to be related to '*Candidatus* Chlorothrix halophila'.

FISH analysis with probes designed to specifically target representatives of the genera *Chloroflexus* and *Roseiflexus* indicated that related phylotypes of both groups were indeed present in the mat. Their distribution, as estimated from the brightness of the FISH probe signal (Fig. 8), appeared to be mainly concentrated in the 2–4 mm depth zone. *Chloroflexus* relatives appeared to be concentrated at a somewhat shallower depth than the *Roseiflexus* relatives. However, the fluorescent signal of both FISH probes was also visible in other mat zones (e.g. at depth *c.* 6 mm). This suggests that

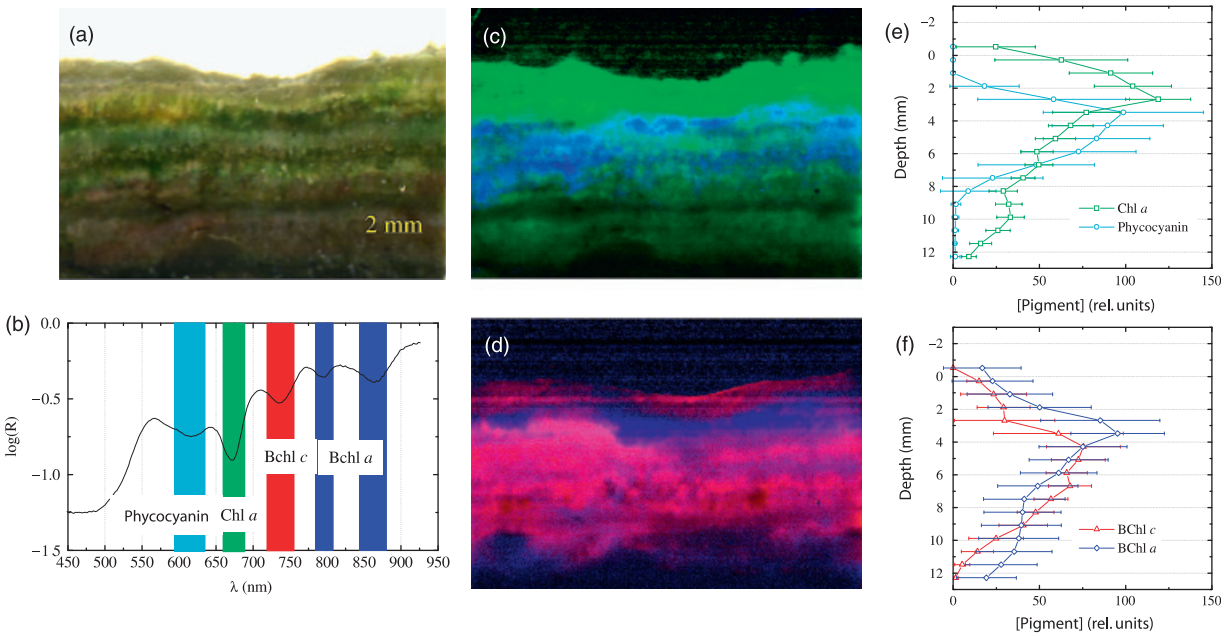

Fig. 7. (a), (b), (c+d) and (e+f) correspond to the same quantities as those displayed in Fig. 6a, b, e and g, respectively, except for the fact that the measurements were conducted on the same mat subsample for which O_2 imaging was carried out (see Figs 3 and 4). Note again mixed colors in (c) and (d): cyan = blue + green, i.e. concurrent occurrence of phycocyanin and Chl *a*, magenta = blue + red, i.e. concurrent occurrence of BChl *a* and BChl *c*.

Table 3. BLAST analysis of 16S rRNA gene sequences obtained from a clone library prepared with *Chloroflexaceae*-specific PCR primers

Number of clones (<97% similarity)	Closest isolate/ % similarity	Closest clone sequence/ % similarity
20	'*Candidatus* Chlorothrix halophila' /90–97% (AY395567)	Uncultured CLB /92–99% (DQ103661)
2	'*Candidatus* Chlorothrix halophila' /93% (AY395567)	Halotolerant bact P4-I-O /93% (AJ308497)
2	*Oscillochloris* sp. /89–90% (AF146832)	Uncultured CLB /92–95% (AJ309642)
2	*Chloroflexus* sp. /89% (AJ308498)	Uncultured CLB /98–99% (DQ329967)
3	*Roseiflexus castenholzii* /58–76% (AB041226)	Uncultured CLB /97–98% (DQ329903)

CLB, *Chloroflexus*-like bacteria.

although the species related to these two genera were concentrated in a specific zone, they were present throughout the entire mat, which is a result similar to that revealed by hyperspectral imaging.

Imaging of oxygen and oxygen production/ consumption rates in the mat

2-D oxygen distributions in the mat showed pronounced horizontal heterogeneity in the upper 2–4 mm of the mat (Fig. 3, top row). Under VIS illumination (light intensity of *c.* 200 μmol photons m^{-2} s^{-1}), peak oxygen concentrations varied between 320 and 420 μM. The top 3–4 mm of the mat were photosynthetically net producing (maximum NP rates ranging between 0.15 and 0.4 mmol m^{-3} s^{-1}), while respiration exceeded photosynthesis at depths below 4–5 mm, reaching maxima of 0.1–0.18 mmol m^{-3} s^{-1} at the oxic/anoxic interface (Fig. 4, top-left). In the dark, the oxic zone was only 2–3 mm thick and the respiration rates in this zone were similar (0.1–0.15 mmol m^{-3} s^{-1}; Fig. 4, top-right).

To estimate the contribution of BChl *c*-producing *Chloroflexaceae* to this respiration, the mat was additionally illuminated by saturating NIR illumination (λ_{max} = 740 nm, corresponding to the specific *in vivo* absorbance of BChl *c*), which was shown to inhibit respiration by *Chloroflexaceae* species (Polerecky *et al.*, 2007). Upon this additional NIR illumination, oxygen penetration depth in the mat significantly increased by 1–2 mm (Fig. 3, middle row). This was accompanied by a dramatic increase in oxygen concentrations in the top mat layers (by 60–140 μM in the VIS light and by 40–60 μM in the dark), most pronounced at depths of 4–6 mm in the VIS light and immediately below the mat surface in the dark (Fig. 3, bottom row). When this change in oxygen concentrations was converted into the respiration rates of BChl *c*-producing *Chloroflexaceae* using the method proposed earlier (Polerecky *et al.*, 2007), it was found that, in the zones where NP was negative, the rates were comparable in magnitude and spatially correlated with the (negative) rates of net photosynthesis in the dark- or

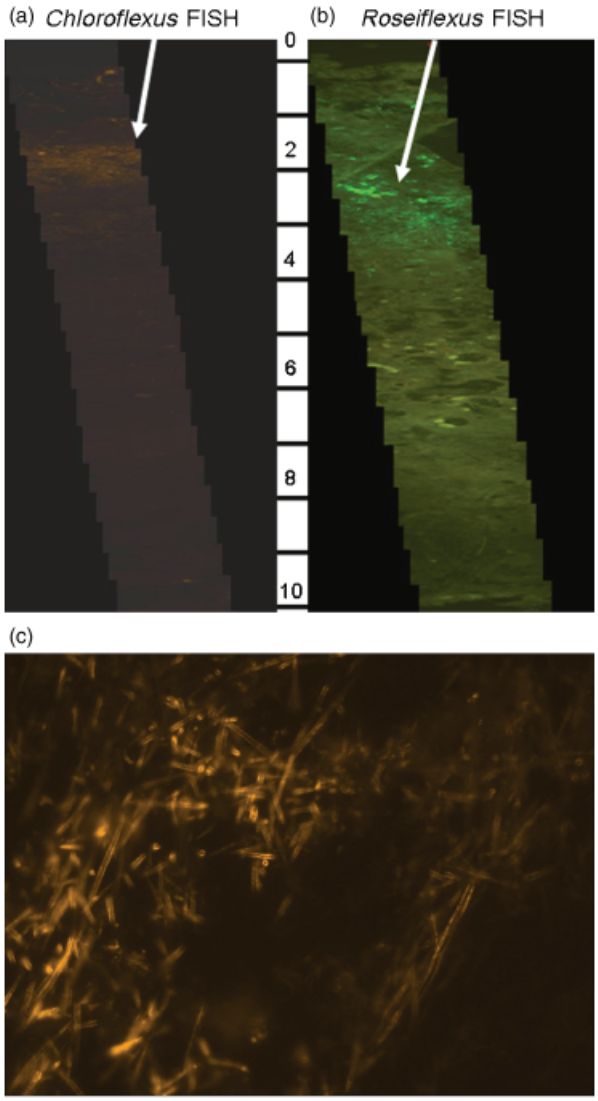

Fig. 8. Images of the microbial mat hybridized with (a) *Chloroflexus* and (b) *Roseiflexus* specific FISH probes. Scale bars indicate depth in millimeters from the mat surface. (c) Close-up of (a) showing positive hybridization of probe CFX1238 with filamentous bacteria.

VIS-light-only illuminated mat (compare the dark-blue-to-magenta patches in the top and bottom rows in Fig. 4). This means that the respiration of BChl *c*-producing *Chloroflexaceae* constituted a significant part of total respiration in the mat's oxic zone.

Discussion

Comparison between HPLC and direct hyperspectral pigment imaging techniques

The most important advantage of the hyperspectral imaging of photopigments (either by detecting their absorption or auto-fluorescence) over the traditional HPLC detection technique is that the structural composition of the sample and thus the spatial organization of the pigmented community members can remain undisturbed. This is because direct imaging does not require pigment extraction before the analysis (Wiggli *et al.*, 1999). The detection limit of the hyperspectral technique appeared to be low (high sensitivity), because pigment concentrations were not diluted as was done in extracts obtained for HPLC analysis in this study, although this could be improved by concentrating the pigment extracts before analysis. Imaging of auto-fluorescence also largely cuts back on the need for pigment separation before analysis, as the combination of specific excitation wavelengths with sophisticated spectral analysis allows detection of individual pigments in a complex mixture (Wiggli *et al.*, 1999).

Although hyperspectral imaging of reflectance spectra combined with the fourth derivative approach for the identification of pigments did provide a valuable insight into the distribution of pigments targeted by this study, hyperspectral imaging in the emission mode appeared to be superior. This was mainly due to a higher degree of specificity, offered by the higher degree of choice of the excitation wavelengths, as well as due to a more direct relationship between the observed fluorescence peak magnitude and the local pigment concentration, which is not to such a large degree as the spectral reflectance measurement affected by the scattering properties of the sample. Another reason for the preferential choice of auto-fluorescence imaging is the fact that the number of identifiable and spectrally separable fluorescence peaks is generally considerably larger than that of specific absorption features.

Important disadvantages of the HPLC analysis are that not all pigments can be readily extracted from the cells, that pigments may be altered during the pigment extraction procedure and that pigments may not be well separated from each other as well as from other interfering compounds present in the mat, which hampers correct identification. One of these factors may have been the reason why the deeper BChl *c* maximum (at 6–7 mm depth) and/or the rather abundant presence of BChl *a* throughout the mat observed by hyperspectral imaging was not detected, or at least not correctly identified, by HPLC. Another possibility could be due to the presence of sulfide in the mat, as this strongly reducing agent may have altered the structure of BChl *a*/*c* during the extraction procedure. Particularly for these reasons we are confident that a further improvement of hyperspectral imaging, for example, by calibrating the method using pigment standards and pure cultures of characterized phototrophic algae and bacteria, may yield a valuable method for pigment analysis in undisturbed complex microbial communities.

Spatial distribution of *Chloroflexaceae* and NIR light-dependent respiratory activity

Previous studies reported that characterized *Chloroflexaceae* species apparently preferentially use organic photosynthates, excreted particularly by cyanobacteria, for photo-heterotrophic growth (Bateson & Ward, 1988; Castenholz, 1988; Hanada & Pierson, 2006; Hanada *et al.*, 2002; van der Meer *et al.*, 2003; Berg *et al.*, 2005). Based on these findings, we hypothesized that the spatial distribution of *Chloroflexaceae* members in the microbial mat would be closely associated with the distribution of oxygenic phototrophs. However, as determined by HPLC and hyperspectral imaging in this study, distributions of the photopigments BChl *c*, which is produced by members of four of the six known *Chloroflexaceae* genera, and Chl *a* and/or phycocyanin, produced by oxygenic phototrophs, were more complementary than similar. Whereas distinct Chl *a* maxima were located in mat zones at depths around 1, 2–3 and 4–5 mm, most of the BChl *c* was found at depths of 3–4 mm and below 5–6 mm. All the pigments investigated exhibited not only pronounced vertical stratification, but were to a large extent, especially BChl *c* and *a*, heterogeneous also in the horizontal direction. Although one part of the BChl *c*-producing population (at 3–4 mm depth) did occur in the oxygen-saturated photic zone of the mat, its patchy rather than a more stratum-like horizontal distribution indicated that the availability of excreted photosynthates was likely not the prime factor determining their spatial distribution.

From studies in which *Chloroflexaceae* members were physiologically characterized, it is known that in addition to photosynthates, most isolates and enrichments can use sulfide as a growth substrate, i.e. as an electron donor for photoautotrophic CO_2 fixation (Pierson & Castenholz, 1974; Klappenbach & Pierson, 2004; van der Meer *et al.*, 2005). This raises a question of whether the availability of sulfide or another potential electron donor for autotrophic growth would influence the occurrence and spatial distribution of BChl *c*-producing *Chloroflexaceae*. Measured sulfide concentration profiles showed that free sulfide occurred at depths $\geq$7 mm, which is too deep for the population present in the 3–4 mm zone, but not for the deeper positioned (6–7 mm) BChl *c*-containing population, which showed a somewhat more homogenous horizontal distribution according to the 2-D hyperspectral pigment analysis. The sulfate reduction rate measurements, however, revealed that this process did occur in all mat zones, including the 0–4 mm zone, although primarily under dark and anoxic conditions. As we determined sulfate reduction rates only in layers that were relatively thick (4 mm), we can only speculate about the 2-D distribution of this process. However, it is plausible that the occurrence of sulfate reduction and its rate may have a patchy distribution, particularly in the upper photic zone of the mat where the oxygen concentration strongly fluctuates during a 24 h light/dark cycle, and thus influence the distribution of the *Chloroflexaceae* members. In several previous studies, sulfate reduction was found to occur in the upper and even fully oxygenated photic zone of mats (Canfield & Desmarais, 1991; Frund & Cohen, 1992; Jørgensen, 1994; Ludwig *et al.*, 2005). Rates in distinct depth zones, however, were found to be highly variable (Ludwig *et al.*, 2005), which may indicate that the process, particularly in the upper, mostly oxygenated, photic zone is highly horizontally heterogeneous. Using a silver foil technique for 2-D mapping of sulfate reduction in lithified modern stromatolites, which can be considered as structural homologues of microbial mats, Visscher found a horizontally heterogeneous sulfate reduction activity (Visscher *et al.*, 2000). The reason why sulfate reduction in oxygenated mat zones may show a heterogeneous rather than a homogenous distribution in the horizontal direction is likely because the process is influenced by a combination of several factors such as differences in the oxygen tolerance of different species of sulfate-reducing bacteria (Cypionka, 2000), availability of suitable organic substrates and success in the competition for those substrates against other microbial community members (Jonkers *et al.*, 2005). Although we did not find significant sulfate-reducing activity in the upper photic zone under light and oxygenated conditions, small pockets may have occurred. Moreover, as significant sulfate reduction in this zone did occur under dark and anoxic conditions, pockets of sulfide, or only partly oxidized sulfur compounds, may have continued to exist in the upper photic zone at least during the initial part of the next light period.

Taking the above-listed considerations into account, i.e. that BChl *c*-containing characterized *Chloroflexaceae* members can use photosynthates excreted by oxygenic phototrophs for (photo)heterotrophic growth as well as sulfide or partly oxidized sulfur compounds for photoautotrophic growth, we hypothesize that their occurrence in the oxygenated upper zone of the mat is maximal in those locations where both photosynthate excretion and sulfate reduction occur during a light/dark cycle. If sulfate reduction had a heterogeneous distribution, which would probably be due to differences in oxygen tolerance of different species, it would primarily influence the horizontal spatial distribution of BChl *c*-containing *Chloroflexaceae* in the upper, often oxygenated photic zone of the mat. The metabolic flexibility of *Chloroflexaceae* would give them, in those locations, a competitive advantage over community members with a more restricted physiology (e.g. either photosynthate or sulfide utilization).

Although in addition to certain *Chloroflexaceae* members some green sulfur bacteria are also known to produce BChl *c*, we assume that species of the former group are responsible

for its occurrence in the oxygenated photic zone (at 3–4 mm depth) of the mat, as all characterized species of the green sulfur bacteria are strict anaerobes (Pfennig & Trüper, 1992). The second and larger BChl *c* maximum found by the hyperspectral analysis in the lower (6–7 mm) part of the photic zone was also likely of *Chloroflexaceae* origin, as oxygen was found to penetrate to a depth of 8 mm in illuminated mats.

BChl *a* maxima were observed by both HPLC and hyperspectral imaging in deeper zones of the mat ($\geq$6 mm), although some BChl *a* was also detected by the spectral imaging technique in other mat zones (0–6 mm). Although this pigment is produced by *Chloroflexaceae* members, most of the BChl *a* in the deeper layer may have originated from oxygen-tolerant purple sulfur bacteria (de Wit & van Gemerden, 1990), as is indicated by the intense purple coloration of this mat zone. The microsensor light measurements showed that NIR light at wavelengths 807+845 and 740 nm, corresponding to the *in vivo* absorbance maxima of BChl *a* and *c*, respectively, was still available in sufficient amounts below 6 mm, which indicates that purple sulfur bacteria and *Chloroflexaceae* could potentially perform anoxygenic photosynthesis, as free sulfide was also detected in this zone.

One of the two FISH probes that were applied in this study targeted *Roseiflexus*-related species. Characterized species of this genus produce BChl *a* but not BChl *c* and were found to be able to grow photoheterotrophically under anaerobic conditions (Hanada *et al.*, 2002). However, as oxygen does not affect bacteriochlorophyll synthesis in *Roseiflexus* (Hanada *et al.*, 2002), it is not surprising that their maximal occurrence in this study was found in the fully oxic upper photic zone. In previous studies, these filamentous bacteria were found to be spatially tightly associated with cyanobacteria, and were in fact found to occur within polysaccharide sheaths of cyanobacterial filament bundles (D'Amelio *et al.*, 1987; Ley *et al.*, 2006). Such a spatial and structural association with filamentous cyanobacteria, which probably supply *Roseiflexus* relatives with organic growth substrates, may in fact have determined the rather shallow depth distribution of these preferentially photoheterotrophic (D'Amelio *et al.*, 1987; Pierson *et al.*, 1994) organisms.

The other FISH probe that was applied in this study targeted *Chloroflexus*-related species, i.e., only one of the four known BChl *c*-producing *Chloroflexaceae* genera. Significant probe signal was observed only in the upper part of the mat at depths 2–4 mm, i.e. in the zone where clear BChl *c* maxima were observed by HPLC and hyperspectral analyses. This result indicates that *Chloroflexus*-related species were responsible for at least a part of the observed upper, but likely not for the deeper BChl *c* maximum. Clone library data revealed that in addition to *Chloroflexus*, *Oscillochloris*- and 'Candidatus *Chlorothrix*'-related sequences also occurred in the mat. As characterized members of the latter two genera are also known to produce BChl *c*, and particularly sequences related to the latter genus dominated the clone library (76%), species related to these genera were most likely responsible for the lower, and possibly for a part of the upper BChl *c* maximum. In line with our hypothesis stated above, we suggest that *Chloroflexus*-related members found (by FISH analysis) in the upper part of the photic zone depend for growth both on the presence of excreted photosynthates and reduced sulfur compounds, while *Chloroflexaceae* members responsible for the lower BChl *c* maximum (*Oscillochloris*- and/or 'Candidatus *Chlorothrix*'-related species) depend for growth less on excreted photosynthates but more on the presence of free sulfide. If the proportion of sequences in the clone library truly reflected the relative abundance of species, the conclusion would be that 'Candidatus *Chlorothrix*'-related species were the dominant *Chloroflexaceae* in this mat. 'Candidatus *Chlorothrix halophila*' is a recently characterized mesophilic and halophilic filamentous anoxygenic phototrophic bacterium that was obtained from a hypersaline microbial mat from Guerrero Negro, Mexico, and cultured in the laboratory in a highly enriched state (Klappenbach & Pierson, 2004). Although sulfide-dependent phototrophic CO_2-fixation was observed in culture (Klappenbach & Pierson, 2004), (photo)heterotrophic growth on organic photosynthates was not determined in that study. In contrast, characterized *Oscillochloris* representatives were shown to use organic compounds as additional carbon sources to CO_2 (Berg *et al.*, 2005). As specific FISH probes for 'Candidatus *Chlorothrix*'- and *Oscillochloris*-related species are not yet available, their spatial distribution and contribution to BChl *c* maxima as observed in the hypersaline mat of this study remains to be quantified.

The second aim of this study was to establish a direct relationship between the presence of BChl *c* and NIR light-dependent respiration occurring in the microbial mat. The NIR light spectrum (715–745 nm, λ_{max} = 740 nm) applied in this study was selected to specifically target BChl *c* and to some extent BChl *d*- and *e*-producing species, as other types of bacteriochlorophyll show maximum *in vivo* absorbance at different wavelengths (BChl *a*: 805+830–890 nm; BChl *b*: 835–850+1020–1040 nm; BChl *g*: 670+788 nm; whereas BChl *c*: 740–755 nm; BChl *d*: 705–740 nm; BChl *e*: 719–726 nm) (Kühl & Fenchel, 2000; Madigan *et al.*, 2000). Comparing Figs 4 (bottom) and 7d, which were measured on the same subsample of the mat, it can be seen that pronounced NIR light-dependent respiration activity of *Chloroflexaceae* determined by planar oxygen optodes is found in locations where abundant concentrations of BChl *c* are found with hyperspectral imaging, and both of these distributions have a very patchy character. Although the

quality of the oxygen data and the noncalibrated character of the hyperspectral data did not allow a more accurate correlation analysis, at least a qualitative match of these two datasets demonstrates that BChl *c*-producing *Chloroflexaceae* are indeed responsible for the respiration in the mat that can be decreased or even completely inhibited by adding specific NIR illumination. Numerical analysis of our oxygen data further suggested that this group is responsible for a major part of respiration in the oxygenated zone in the mat, which is a conclusion similar to that reached in our previous study conducted in a different mat with the same origin (Polerecky *et al*., 2007).

Acknowledgements

A.B. was supported by a grant (DFG JO-412) from the German Research Foundation. The development of the hyperspectral imaging technique was supported by European Commission (project ECODIS, project number 518043). We are grateful to Harald Osmers, Paul Faerber, Alfred Kutsche and Georg Herz for their technical wizardry offered during the development of the spectral imaging system.

References

Bachar A, Omoregie E, de Wit R & Jonkers HM (2007) Diversity and function of *Chloroflexus*-like bacteria in a hypersaline microbial mat: phylogenetic characterization and impact on aerobic respiration. *Appl Environ Microbiol* **73**: 3975–3983.

Barille L, Meleder V, Combe JP, Launeau P, Rince Y, Carrere V & Morancais M (2007) Comparative analysis of field and laboratory spectral reflectances of benthic diatoms with a modified Gaussian model approach. *J Exp Mar Biol Ecol* **343**: 197–209.

Bateson MM & Ward DM (1988) Photoexcretion and fate of glycolate in a hot spring cyanobacterial mat. *Appl Environ Microbiol* **54**: 1738–1743.

Berg IA, Keppen OI, Krasil'nikova EN, Ugol'kova NV & Ivanovsky RN (2005) Carbon metabolism of filamentous anoxygenic phototrophic bacteria of the family *Oscillochloridaceae*. *Microbiology* **74**: 258–264.

Butler WL & Hopkins DW (1970) Analysis of fourth derivative spectra. *Photochem Photobiol* **12**: 451.

Canfield DE & Desmarais DJ (1991) Aerobic sulfate reduction in microbial mats. *Science* **251**: 1471–1473.

Castenholz RW (1988) The green sulfur and nonsulfur bacteria of hot springs. *Green Photosynthetic Bacteria* (Olson JM, ed), pp. 243–255. Plenum Press, New York.

Combe JP, Launeau P, Carrere V, Despan D, Meleder V, Barille L & Sotin C (2005) Mapping microphytobenthos biomass by non-linear inversion of visible-infrared hyperspectral images. *Remote Sensing Environ* **98**: 371–387.

Cypionka H (2000) Oxygen respiration by *Desulfovibrio* species. *Annu Rev Microbiol* **54**: 827–848.

D'Amelio ED, Cohen Y & DesMarais DJ (1987) Association of a new type of gliding, filamentous, purple phototrophic bacterium inside bundles of *Microcoleus chthonoplastes* in hypersaline cyanobacterial mats. *Arch Microbiol* **147**: 213–220.

de Wit R & van Gemerden H (1990) Growth and metabolism of the purple sulfur bacterium *Thiocapsa roseopersicina* under combined light dark and oxic anoxic regimens. *Arch Microbiol* **154**: 459–464.

Fleissner G, Hage W, Hallbrucker A & Mayer E (1996) Improved curve resolution of highly overlapping bands by comparison of fourth-derivative curves. *Appl Spectr* **50**: 1235–1245.

Frund C & Cohen Y (1992) Diurnal cycles of sulfate reduction under oxic conditions in cyanobacterial mats. *Appl Environ Microbiol* **58**: 70–77.

Hanada S & Pierson BK (2006) The family *Chloroflexaceae*. *The Prokaryotes: An Evolving Electronic Resource for the Microbiological Community*, release 3.11 (Dworkin M, ed), pp. 1–41. (http://link.springer-ny.com/link/service/books/10125.). Springer, Heidelberg, Germany.

Hanada S, Takaichi S, Matsuura K & Nakamura K (2002) *Roseiflexus castenholzii* gen. nov., sp. nov., a thermophilic, filamentous, photosynthetic bacterium that lacks chlorosomes. *Int J Syst Evol Microbiol* **52**: 187–193.

Hofstraat JW, van Zeijl WJM, de Vreeze MEJ, Peeters JCH, Peperzak L, Colijn F & Rademaker TWM (1994) Phytoplankton monitoring by flow-cytometry. *J Plankton Res* **16**: 1197–1224.

Holst G & Grunwald B (2001) Luminenscence lifetime imaging with transparent oxygen optodes. *Sensors and Actuators B-Chemical* **74**: 78–90.

Jonkers HM, Ludwig R, de Wit R, Pringault O, Muyzer G, Niemann H, Finke N & de Beer D (2003) Structural and functional analysis of a microbial mat ecosystem from a unique permanent hypersaline inland lake: 'La Salada de Chiprana' (NE Spain). *FEMS Microbiol Ecol* **44**: 175–189.

Jonkers HM, Koh IO, Behrend P, Muyzer G & de Beer D (2005) Aerobic organic carbon mineralization by sulfate-reducing bacteria in the oxygen-saturated photic zone of a hypersaline microbial mat. *Microb Ecol* **49**: 291–300.

Jørgensen BB (1994) Sulfate reduction and thiosulfate transformations in a cyanobacterial mat during a diel oxygen cycle. *FEMS Microbiol Ecol* **13**: 303–312.

Kallmeyer J, Ferdelman TG, Weber A, Fossing H & Jørgensen BB (2004) A cold chromium distillation procedure for radiolabeled sulfide applied to sulfate reduction measurements. *Limnol Oceanogr Meth* **2**: 171–180.

Klappenbach JA & Pierson BK (2004) Phylogenetic and physiological characterization of a filamentous anoxygenic photoautotrophic bacterium '*Candidatus* Chlorothrix halophila' gen. nov., sp. nov. recovered from hypersaline microbial mats. *Arch Microbiol* **181**: 17–25.

Klatt CG, Bryant DA & Ward DM (2007) Comparative genomics provides evidence for the 3-hydroxypropionate autotrophic

pathway in filamentous anoxygenic phototrophic bacteria and in hot spring microbial mats. *Environ Microbiol* **9**: 2067–2078.

Kühl M & Fenchel T (2000) Bio-optical characteristics and the vertical distribution of photosynthetic pigments and photosynthesis in an artificial cyanobacterial mat. *Microb Ecol* **40**: 94–103.

Kühl M & Jørgensen BB (1992) Spectral light measurements in microbenthic phototrophic communities with a fiberoptic microprobe coupled to a sensitive diode-array detector. *Limnol Oceanogr* **37**: 1813–1823.

Kühl M & Jørgensen BB (1994) The light-field of microbenthic communities - radiance distribution and microscale optics of sandy coastal sediments. *Limnol Oceanogr* **39**: 1368–1398.

Kühl M, Steuckart C, Eickert G & Jeroschewski P (1998) A H_2S microsensor for profiling biofilms and sediments: application in an acidic lake sediment. *Aquat Microb Ecol* **15**: 201–220.

Ley RE, Harris JK, Wilcox J, Spear JR, Miller SR, Bebout BM, Maresca JA, Bryant DA, Sogin ML & Pace NR (2006) Unexpected diversity and complexity of the Guerrero Negro hypersaline microbial mat. *Appl Environ Microbiol* **72**: 3685–3695.

Ludwig R, Al-Horani FA, de Beer D & Jonkers HM (2005) Photosynthesis-controlled calcification in a hypersaline microbial mat. *Limnol Oceanogr* **50**: 1836–1843.

Madigan MT, Martinko JM & Parker J (2000) *Brock – Biology of Microorganisms*, 9th edn. Prentice-Hall Inc., Upper Saddle River, NJ.

Nübel U, Bateson MM, Madigan MT, Kühl M & Ward DM (2001) Diversity and distribution in hypersaline microbial mats of bacteria related to *Chloroflexus* spp. *Appl Environ Microbiol* **67**: 4365–4371.

Nübel U, Bateson MM, van Dieken V, Wieland A, Kühl M & Ward DM (2002) Microscopic examination of distribution and phenotypic properties of phylogenetically diverse *Chloroflexaceae*-related bacteria in hot spring microbial mats. *Appl Environ Microbiol* **68**: 4593–4603.

Pfennig N & Trüper HG (1992) The family *Chromatiaceae*. *The Prokaryotes*, 2nd edn (Balows A, Trüper HG, Dworkin M, Harder W & Schleifer KH, eds), pp. 3200–3221. Springer-Verlag, Berlin.

Pierson BK & Castenholz RW (1974) Studies of pigments and growth in *Chloroflexus aurantiacus*, a phototrophic filamentous bacterium. *Arch Microbiol* **100**: 283–305.

Pierson BK, Valdez D, Larsen M, Morgan E & Mack EE (1994) *Chloroflexus*-like organisms from marine and hypersaline environments – distribution and diversity. *Photosynth Res* **41**: 35–52.

Polerecky L, Bachar A, Schoon R, Grinstein M, Jørgensen BB, de Beer D & Jonkers HM (2007) Contribution of *Chloroflexus* respiration to oxygen cycling in a hypersaline microbial mat from Lake Chiprana, Spain. *Environ Microbiol* **9**: 2007–2024.

Precht E, Franke U, Polerecky L & Huettel M (2004) Oxygen dynamics in permeable sediments with wave-driven pore water exchange. *Limnol Oceanogr* **49**: 693–705.

Revsbech NP (1989) An oxygen microsensor with a guard cathode. *Limnol Oceanogr* **34**: 474–478.

Saga Y & Tamiaki H (2004) Fluorescence spectroscopy of single photosynthetic light-harvesting supramolecular systems. *Cell Biochem Biophys* **40**: 149–165.

Strauss G & Fuchs G (1993) Enzymes of a novel autotrophic CO_2 fixation pathway in the phototrophic bacterium *Chloroflexus aurantiacus*, the 3-hydroxypropionate cycle. *Eur J Biochem* **215**: 633–643.

van der Meer MTJ, Schouten S, Damste JSS, de Leeuw JW & Ward DM (2003) Compound-specific isotopic fractionation patterns suggest different carbon metabolisms among *Chloroflexus*-like bacteria in hot-spring microbial mats. *Appl Environ Microbiol* **69**: 6000–6006.

van der Meer MTJ, Schouten S, Bateson MM, Nübel U, Wieland A, Kühl M, de Leeuw JW, Damste JSS & Ward DM (2005) Diel variations in carbon metabolism by green nonsulfur-like bacteria in alkaline siliceous hot spring microbial mats from Yellowstone National Park. *Appl Environ Microbiol* **71**: 3978–3986.

Visscher PT, Reid RP & Bebout BM (2000) Microscale observations of sulfate reduction: correlation of microbial activity with lithified micritic laminae in modern marine stromatolites. *Geology* **28**: 919–922.

Wiggli M, Smallcombe A & Bachofen R (1999) Reflectance spectroscopy and laser confocal microscopy as tools in an ecophysiological study of microbial mats in an alpine bog pond. *J Microbiol Methods* **34**: 173–182.

Chapter V:

A first survey on the Chloroflexaceae Family community structure of four hypersaline microbial mats from three continents

A first survey on the Chloroflexaceae family community structure of four hypersaline microbial mats from three continents

Ami Bachar & Henk M. Jonkers

Abstract

Aims; The aim of this study was to investigate and compare, by 16S rDNA clone library analysis, the community structure of members of the Chloroflexaceae Family from four hypersaline microbial mats from different continents (Chiprana, Spain, Europe; Abu Dhabi, United Arab Emirates, Asia; Guerrero Negro, Mexico, North America; and a mat originating from Chiprana but kept for years in a laboratory based mesocosm system).

Methods; The Chloroflexi phylum, which accommodates, among others, filamentous anoxygenic phototrophic bacteria of the Family Chloroflexaceae, roots deeply in the tree of life. Although only few isolates of this Family have been characterized to date, a high diversity of related 16S rDNA sequences has been found in clone libraries of hot spring and hypersaline microbial mats. As the characterized isolates appear metabolically and therefore also likely functionally different, closely related 16S rRNA gene sequences from environmental samples may reflect the occurrence of related functional groups in their natural habitat. Using previously designed specific Chloroflexaceae 16S primers, three clone libraries were constructed from Chiprana, Abu-Dhabi and the Mesocosm mats and phylogenetically compared with the previously described North American one.

Results; we observed a number of unique environmental sequences (< 97% homology) in each mat; however, in all four mats clone libraries, the majority of retrieved sequences were most closely related to the previously isolated species '*Candidatus* Chlorothrix halophila'

Main Conclusions: it is concluded that both a relatively high and endemic local diversity is present and that '*Candidatus* Chlorothrix halophila', a bacteriochlorophyll *c*-producing species, and/or close relatives are pandemic and dominates the Chloroflexaceae community in hypersaline mats. We hope that this initial comparative study will stimulate further investigations on the biogeography, physiology and phylogeny of this ancient and metabolically diverse group of Chloroflexaceae.

Keywords: Chloroflexaceae, cloning, microbial-mats, hypersaline

Introduction

The Chloroflexaceae Family is composed of filamentous anoxygenic phototrophic bacteria and is a division of the Chloroflexi phylum which additionally harbors non-phototrophic genera (Fig. 1).

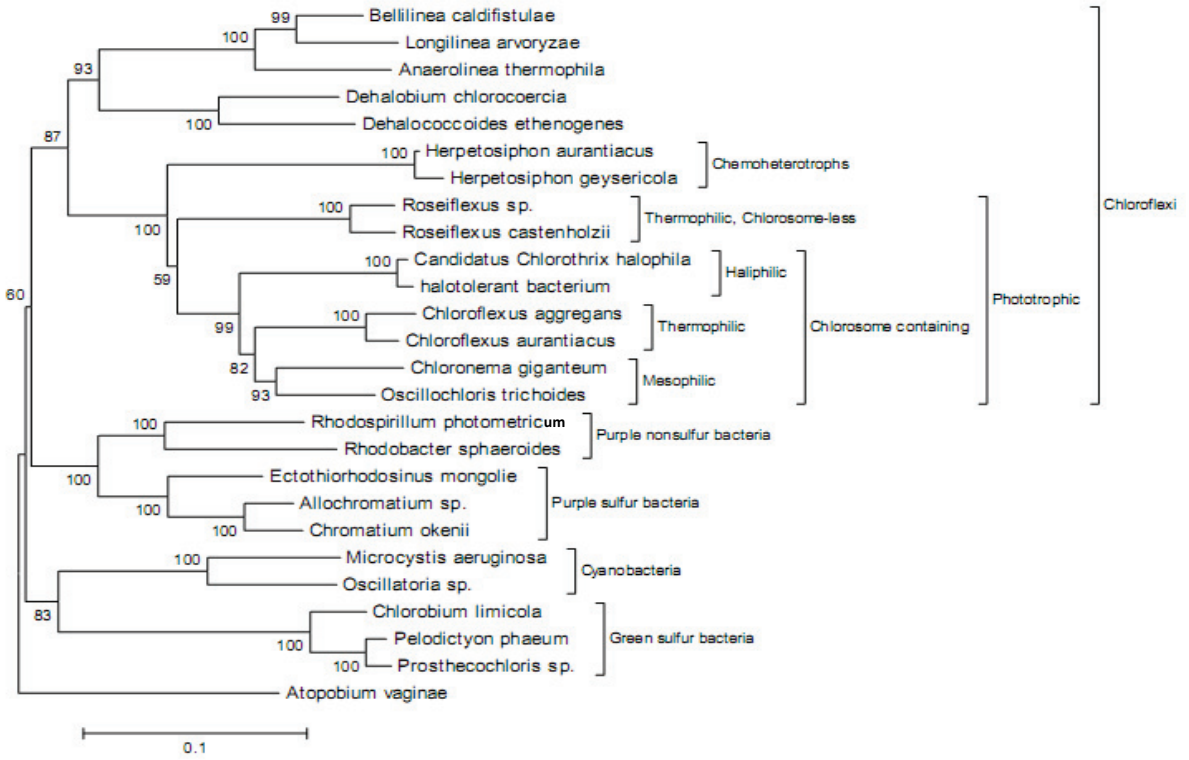

Fig 1: Evolutionary history of the Chloroflexi Phylum and representative isolates form major phototrophic groups inferred using the Minimum Evolution method (bootstrap test 1000 replicates): available isolates (26 taxa total) represent the evolutionary history of this group (Eck & Dayhoff, 1966). The tree is drawn to scale; Heliothrix oregonensis is not included as only a partial sequence is available in database. Members of the Chloroflexaceae Family are indicated as 'Phototrophic' in the tree (10 taxa). The tree is drawn to scale.

The Chloroflexi phylum is a deeply branching root of the tree of life, what may indicate that members are direct descendents of ancient bacteria. Several members of the Chloroflexaceae Family have been previously isolated and resembling morpho- and genotypes occurring in various microbial mats have been reported ever since it's first and foremost studied member, *Chloroflexus aurantiacus*, was discovered (Pierson & Castenholz, 1971). This organism, as well as the rest of the so-far isolated members of the Chloroflexaceae, is an anoxygenic phototrophic filamentous bacterium with gliding motility and bacteriochlorophyll (BChl) *a* as its principle reaction centre-based photosynthetic pigment. Members of some of the Chloroflexaceae genera, i.e. *Chloroflexus*, *Oscillochloris*, *Chloronema* and *Candidatus*

Chlorothrix, feature chlorosomes which are specialized compartments that constitute their main light harvesting system harboring, like the green sulfur bacteria (Fig. 1), BChl *c* in addition to BChl *a* as primary pigments. Isolates of the other two described Chloroflexaceae genera (*Roseiflexus* and *Heliothrix*) lack chromosomes and possess, like members of the purple sulfur bacteria (Fig. 1), only BChl *a* as sole bacteriochlorophyll (Hanada et al., 2002, Pierson et al., 1985). The photosynthetic system of the chlorosome-carrying Chloroflexaceae thus appears 'chimeric' as these have a pheophytine-quinone PSII-type reaction center like the purple sulfur bacteria which do not carry chlorosomes, but not the iron-sulfur PSI-type reaction center of the chlorosome-carrying green sulfur bacteria. This phenomenon makes members of the Chloroflexaceae even more intriguing from an evolutionary viewpoint, particularly in light of the fact that the three phototrophic groups are phylogenetically very distant from one another (Fig. 1). Besides bacteriochlorophyll composition, other functional differences occur between Chloroflexaceae members. While some may use inorganic carbon sources for photoautotrophic growth (e.g. *Oscillochloris* spp.), others might depend on organic carbon via photoheterotrophy (e.g. the chlorosome-less Chloroflexaceae). Furthermore, while some are able to respire with oxygen e.g. *Chloroflexus* spp. (Pierson & Castenholz, 1974, Hanada et al., 1995), others are not e.g. *Oscillochloris trichoides* (Keppen et al., 2000). These highly variable metabolic abilities among isolates from different genera could indicate that within the Chloroflexaceae family, phylogenetic position and functionality may be linked at the genus level. Thus, phylogenetic clusters at the genus level may represent groups of species with a specific functionality and, hence, a specific ecological role in their environment. It furthermore appears from the phylogenetic tree (Fig. 1), that isolated and characterized strains with or without chlorosomes from different environments, form different phylogenic clusters (<85% similarity): chlorosome-carrying thermophilic (*Chloroflexus*), mesophilic (*Chloronema* & *Oscillochloris*), halophilic (*Candidatus* Chlorothrix) and chlorosome-less thermophiles (*Roseiflexus* & *Heliothrix*) (Hanada & Pierson, 2006). However, this is not likely a distinctive feature, as several studies reported non-closely related Chloroflexaceae sequences originating from one particular environment (Pierson et al., 1994, Nübel et al., 2001, Bachar et al., 2007). The diversity within the Chloroflexaceae Family is also much greater then what can be inferred from isolated strains alone. The latter studies revealed furthermore the occurrence of high within-genus diversity in specific environments.

Studies on hypersaline environments report observations of filamentous olive-colored Chloroflexaceae related species, occasionally spatially associated with other bacteria e.g. *Beggiatoa*, cyanobacteria, purple sulfur bacteria (Mack & Pierson, 1988, D'Amelio et al., 1989, Stolz, 1990, Venetskaya & Gerasimenko, 1988, Sorensen et al., 2005, Lefebvre et al., 2006, Ley et al., 2006). These associations are considered

mutually beneficial. For example, in Chloroflexaceae-cyanobacteria associations Chloroflexaceae use organic excretions of cyanobacteria, while vice versa the cyanobacteria may benefit from sulfide removal by its reciprocal associate since sulfides are inhibitory for most cyanobacteria. Chloroflexaceae species may also benefit from being located near sulfate-reducing bacteria. While the latter provide the former with reduced sulfur compounds which can be used as electron donors for anoxygenic photosynthesis, Chloroflexaceae species reduce by aerobic respiration oxygen that may be inhibitory for sulfate-reducing bacteria (Bachar *et al.*, 2008). In one study, Chloroflexi-related sequences dominated the clone library of a phototrophic microbial mat, challenging the general belief that cyanobacteria are numerically the most important community members (Ley et al., 2006). That study at least confirmed findings of another study (Bachar *et al.*, 2007) in which it was found that Chloroflexaceae representatives are important members in hypersaline sedimentary environments.

In this study we compared 16S rDNA gene clone libraries obtained from four hypersaline microbial mats from three continents (Asia, Europe and America) to find out whether distant but environmentally similar hypersaline microbial mats support analogous or rather completely different Chloroflexaceae communities. Specific aim of the study was to establish whether the dominant members of the respective mat communities are closely related and thus represent cosmopolitan species.

Methods

Mat sampling and clone library preparation

In order to compare Chloroflexaceae community structure from different locations, clone libraries from 4 distinct hypersaline microbial mats were examined. Primers which were previously designed to specifically target members of the Chloroflexaceae Family, i.e. CCR344F (ACGGGAGGCAGCAGCAAG) and CCR1338R (ACGCGGTTACTAGCAACT), (Nübel *et al.*, 2001) and with which a hypersaline mat from Guerrero Negro (GN; California, Mexico) was previously analyzed was also used in this study. To enable phylogenetic analysis and comparison of respective mat communities, we analyzed mats from Lake Chiprana (LC; NE Spain, Europe) (Bachar et al., 2007, Jonkers et al., 2003), Sabkha of Abu-Dhabi (AD; United Arab Emirates, Asia) (Abed et al., 2007, Abed et al., 2008) and a mesocosm-based microbial mat (MM) which originated from Lake Chiprana but was incubated for years in our institute (Bachar et al., 2008). Samples from LC, AD and MM were taken on October 2004, December 2004 and March 2006 respectively and were immediately frozen in liquid nitrogen and kept at -80ºC until analysis. DNA was extracted from samples using the Phenol-Chloroform procedure and was subjected to direct PCR

amplification with the above-mentioned primers. The reaction was performed in a Mastercycler thermocycler (Eppendorf, Hamburg, Germany) according to the protocol described in (Nübel *et al.*, 2001). The product was visualized on an agarose gel, excised and subsequently cleaned using a DNA purification kit (QIAGEN, Hilden, Germany). Two microliters of purified product was then ligated into the pGEM-T Easy vector (Promega, Madison, WI) and transformed into *Escherichia coli* TOP10 cells (Invitrogen, Carlsbad, CA) according to the manufacturer's recommendations. Overnight cultures were prepared from positive transformations in a 2-ml 96-well culture plate. Purified plasmids were sequenced in one direction with the M13F primer, using a BigDye Terminator v3.0 cycle sequencing kit (Applied Biosystems, Foster City, CA). Samples were run on an Applied Biosystems 3100 genetic analyzer (Foster City, CA). Sequences were submitted to the GenBank (Accession number: EU979419 to EU979471).

Phylogenetic analysis of 16S rRNA gene sequences

Phylogenetic analyses of obtained sequences were conducted in MEGA4 (Tamura *et al.*, 2007). First, the retrieved and amplified partial sequences from the mats were grouped into phylotypes based on the criterion that sequences of the same phylotype share more than 97% similarity (Rossello-Mora & Amann, 2001). Chosen representatives were fully sequenced from both directions and compared to available Chloroflexaceae related sequences that were >1000 bp long, using the RDP II database (Cole *et al.*, 2007). In order to select which phylogenetic model best describes obtained data, alignment was analyzed by "Find-model" (http://hcv.lanl.gov/content/sequence/findmodel/findmodel.html) using the full set of 28 possible models from which Jukes-Cantor was found best fitting (Posada & Crandall, 1998). Phylogenetic trees were constructed based on 10000-fold bootstrap analysis runs, using maximum likelihood, maximum parsimony, and neighbor joining methods, which all showed similar patterns.

The evolutionary relationships of 112 Chloroflexaceae-related sequences obtained were inferred using the Minimum Evolution method (Rzhetsky & Nei, 1992). The evolutionary distances were computed using the Maximum Composite Likelihood method (Tamura *et al.*, 2004) and are given in the units of the number of base substitutions per site. The Minimum Evolution tree was searched using the Close-Neighbor-Interchange (CNI) algorithm (Nei & Kumar, 2000) at a search level of 1. The Neighbor-joining algorithm (Saitou & Nei, 1987) was used to generate the initial tree. Codon positions included were 1st+2nd+3rd+Noncoding. All positions containing gaps and missing data were eliminated from the dataset (Complete deletion option).

A survey over available Chloroflexaceae Family related sequences from the RDPII database revealed several dozens of unique groups with 85-97% rDNA sequence similarity. For this study we considered a similarity of 97-100% representative for the species level, or at least for the minimal molecular operational taxonomic unit; 93-96% for the genus-level, and 86-92% as related, but above the genus, i.e. the Family level (Stackebrandt & Goebel, 1994).

Results

The phylogenic tree constructed from our considerate environmental samples and available isolates from the GenBank is presented in Fig 2. Different annotations represent different origin: sequences originated from the mesocosm mat are labeled MM and numbered 1-96; sequences originated from Abu-Dhabi are labeled AD and numbered 101-196; sequences originated from Lake Chiprana are labeled LC and numbered 201-296; sequences originated from Guerrero Negro (Ley et al., 2006, Nübel et al., 2001), are labeled GN and accession number, as acquired from the RDPII database. The numbers of unique clones (groups of sequences which share ≥97% homology) from each environment are presented in Table 1. The 'level' section indicates, within a cluster, how far away the two most dissimilar sequences are from each other. Two clusters represent sequence relatedness on the species level (≤3% difference), i.e. 'Chlorothrix cluster' and IV; four on the genus level (II, III, VI and VII) and two on higher than genus level (I and V).

	Chlorothrix cluster	Cluster I	Cluster II	Cluster III	Cluster IV	Cluster V	Cluster VI	Cluster VII
GN	1	2	4	-	2	4	8	1
MM	4	4	3	2	-	-	2	3
AD	1	-	3	-	4	1	6	-
LC	-	3	2	4	-	-	1	-
CR	-	-	2	-	1	-	-	-
Level	≤3% (Specie)	<15%	≤6% (Genus)	≤6% (Genus)	≤3% (Specie)	<13%	≤6% (Genus)	≤6% (Genus)

Table 1: cluster analysis of unique sequences from the different 4 mats considered + 3 more sequences from Cabo Rojo saltern mats.

GN = Guerrero negro (22 unique Chloroflexaceae sequences) (Ley et al., 2006, Nübel et al., 2001)
MM = Mesocosm mat (20 unique Chloroflexaceae sequences, 8 unique clusters)
AD = Abu-Dhabi (17 unique Chloroflexaceae sequences, 7 unique clusters)
LC = Lake Chiprana (11 unique Chloroflexaceae sequences, 5 unique clusters)
CR = Cabo Rojo saltern mats (Isenbarger et al., 2008)

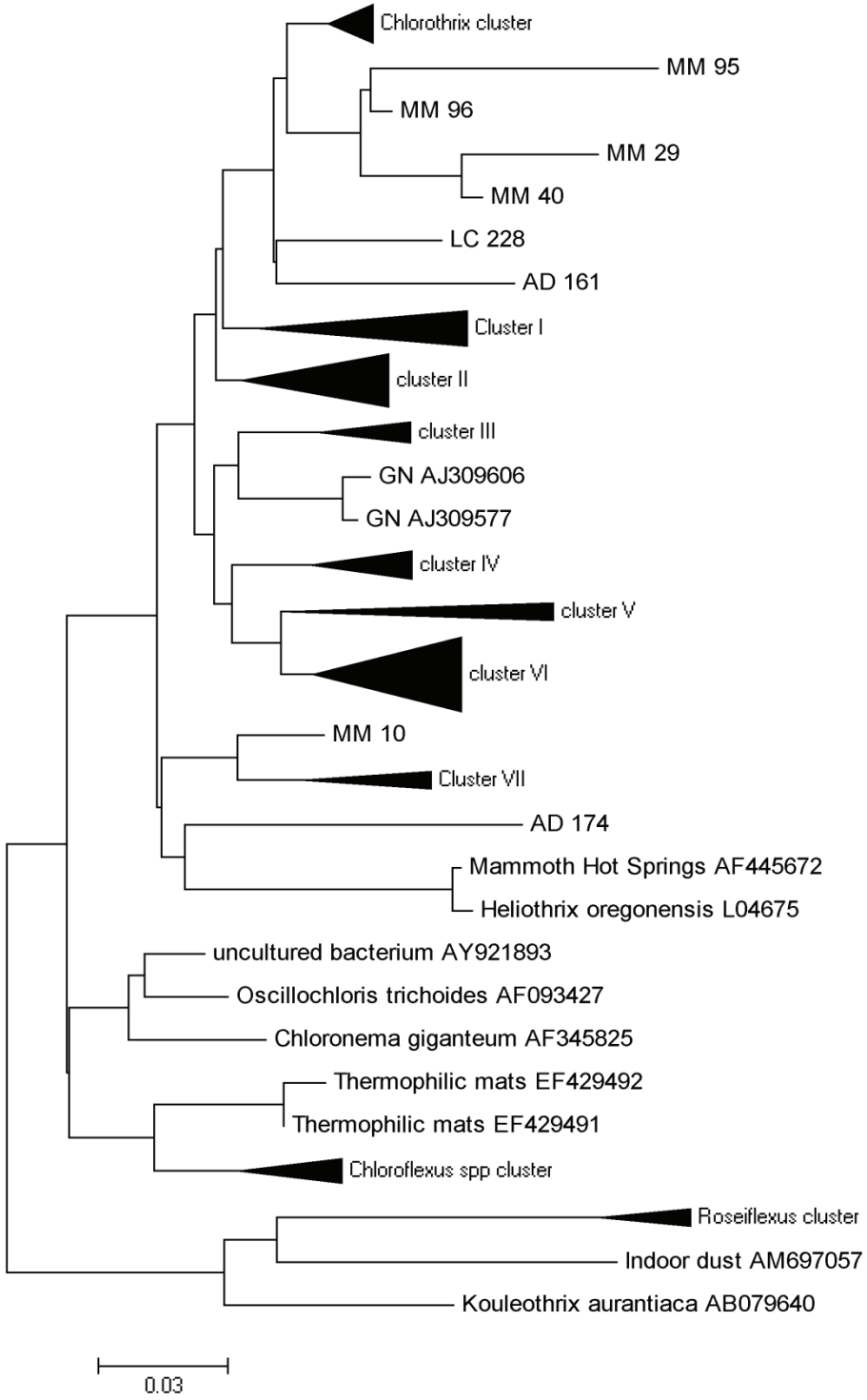

Fig 2: The evolutionary relationships of Chloroflexaceae-related taxa inferred using the Minimum Evolution method (a 10,000-bootstrap consensus tree is depicted). Sequences acquired in this study are in bold. Chloroflexus spp cluster has C. aurantiacus and C. aggregans isolates + some environmental clones not from our clone libraries. The Roseiflexus cluster has Roseiflexus isolates (non from our libraries). Cluster III is composed from sequences originated in LC and MM only. Clusters IV and V are the only ones that have neither LC nor MM originated representatives. Branch lengths larger than 0.03 are presented and in the same units (number of base substitutions per site) as those of the evolutionary distances used to infer the phylogenetic tree

From the four mats considered, six unique sequences clustered on the species level with the previously isolated and characterized '*Candidatus* Chlorothrix halophila'. Strikingly, except for these sequences, all other unique sequences did not closely relate to any of the previously isolated and characterized Chloroflexaceae members (Fig 2). Based on isolated and characterized Chloroflexaceae members it would be reasonable considering 6% sequence variation as a threshold for different functional groups (see discussion below). On that base we attempted to assess which environment represented the highest functional diversity.

GN sequences conformed into 6 clusters + clone GN_AJ309606 or GN_AJ309577 (seven possible functional groups); AD has five clusters + clones AD161 and AD174 (seven possible functional groups); MM has six clusters + clones MM95, MM10 & MM29 (nine possible functional groups); LC has four clusters + clone LC228 (five possible functional groups). If we conceptually pull the oceanic mats (i.e. GN/AD/RC) and the Lake Chiprana originated mats (LC/MM) together, the functional diversity is as follows: oceanic mats conform into seven clusters + three unique exterior sequences; Lake Chiprana conforms into six clusters + four unique exterior sequences. At least 10 phylogenetic groups are representing the oceanic and the hypersaline environments, each. The overall functional diversity in our entire dataset is eight clusters + six solitaire sequences. The cluster III seems endemic to the Hypersaline Lake while no relatives from strictly oceanic clusters IV & V were detected in that environment.

GN, where cloning effort was highest, represents by all means the highest diversity both in numbers of Chloroflexaceae related unique sequences (34) and in their phylogenetic distribution over seven possible functional groups. LC original mat however, seemed to be the least diverse among the tested environments with only 11 unique Chloroflexaceae related sequences that conform into five possible functional groups. Interestingly, the diversity in the MM was much greater than LC, the mat it originated from. With 25 unique sequences from nine possible functional groups, the MM diversity seems roughly equivalent to that of GN. Possible reasons for this unexpected phenomenon are suggested below (discussion). A clear example of a sequence that was detected in MM but not in LC is the *Candidatus* Chlorothrix halophila related one. Nevertheless, all sequences acquired in this study were more phylogenetically related to this sole hypersaline isolate in the Chloroflexaceae Family then to any of the other available Chloroflexaceae isolates.

Clusters IV and V are exceptional in the sense that all their sequences are from an open water system (i.e. hypersaline environments with connection to the sea), while Cluster III appears to represent sequences endemic to the Lake Chiprana. In contrast,

the “pandemic” cluster II accommodates representatives from all the considered environments.

Discussion

For the past century microbiologists have considered a basic principle of microbial ecology to be that microorganisms are not subject to geographical boundaries, but instead are dispersed globally and thrive wherever they find a hospitable environment (de Wit & Bouvier, 2006). The Dutch biologist Lourens Baas-Becking postulated that "everything is everywhere: the environment selects", meaning that most bacterial species are widely distributed, while different ecosystems select for the bacteria that are best adapted, consequently leading to relatively greater abundance of these bacteria. There is some evidence supporting the perception that different ecosystems harbor unique microbial populations, i.e. that bacterial populations can exhibit biogeographic distribution (Whitfield, 2005, Martiny et al., 2006).

Members of the phylum Chloroflexi and the Chloroflexaceae Family in particular have previously shown to be dominant in various microbial mats, both quantitatively (Ley et al., 2006, Bachar et al., 2007, Abed et al., 2007) and functionally, as Chloroflexaceae respiration showed significant contribution to oxygen and carbon cycling in the Lake Chiprana microbial mat (Polerecky et al., 2007). Two-dimensional mapping of pigments distribution and activity of Chloroflexaceae in the hypersaline mesocosm mat MM, derived from Lake Chiprana, indicated that these organisms are mainly located in the upper photic zone, in layers or patches (Bachar et al., 2008). The number of unique sequences from clone-libraries obtained with a set of Chloroflexaceae-specific primers previously developed (Nübel *et al.*, 2001) indicated that Chloroflexaceae may be phylogenetically much more diverse then it seem from available cultivated and partly physiologically-characterized strains. In particularly the latter study at GN, few dozen unique Chloroflexaceae sequences (with ≤97% similarity) were reported suggesting a high diversity of this Family.

The sequencing efforts done in this study increased the number of unique Chloroflexaceae sequences known from Lake Chiprana derived mats from 3 (Bachar *et al.*, 2007) to 36. These sequences, 11 from LC and 25 from MM, designate the presence of a large number of candidate new species. It is nowadays frequent to consider a 97% sequence similarity of the 16S rRNA gene as the threshold to differentiate between unique species, although this rather artificial threshold is questionably arbitrary and may not be indicative of functional differences. Within the Chloroflexaceae Family, as far as we know from isolated strains, a much larger,

over 6% 16S rRNA gene difference is observed between functionally different strains. Therefore it seems doubtful that (Chloroflexacean) environmental sequences with more than 93% similarity represent species with a significantly different metabolism, although it may be the case for sequences of larger differences. However, except for the strain *Candidatus* Chlorothrix halophila all other so far isolated and characterized Chloroflexaceae members originate from non-hypersaline environments, we cannot be certain that this would also apply to hypersaline species. It would be very interesting to physiologically characterize future isolates closely related to *Candidatus* Chlorothrix halophila as well as to other clusters accommodating sequences derived from hypersaline environments in order to clarify this. Therefore, characterization of more isolates related to hypersaline clusters is urgently needed as this could shed more light on potential metabolic and thus functional differences.

Besides the Lake Chiprana mat, we further investigated in this study the diversity and phylogenic community-composition of 2 additional hypersaline mats and found 17 and 25 unique Chloroflexaceae sequences in the respective mats from AD (United Arab Emirates) (Abed *et al.*, 2007) and an artificial microbial mat grown in a mesocosm at the Max-Plank Institute for marine microbiology, Bremen (Germany). The latter mat was obtained from an inoculum derived from the original LC mat (Bachar *et al.*, 2008). Therefore a possibly lower, but not higher diversity was expected, since species could be lost while new ones are not expected to evolve quickly or invade the mat from the non-hypersaline laboratory environment. Several reasons may explain the obtained result, foremost, as clone numbers were limited, full biodiversity was not covered. A higher cloning effort would have indisputably improved species richness and decreased species divergence of both mats. Secondly, MM environmental conditions, although tried to mimic the original lake conditions, were different (e.g. constant temperature, light quantity and quality, presence of possible grazers) which could potentially have resulted in the numeric dominance of different populations of the Chloroflexaceae community in both mats. This may have affected the PCR potentially biased method and elucidate higher diversity in an artificial mat then its original mat. Thirdly, as the mesocosm mat was incubated under non-sterile conditions, we cannot fully exclude introduction of contaminant Chloroflexaceae members from the laboratory environment, although this seems rather improbable.

A combination of the mentioned reasons likely contributed to this probably-only-apparent higher diversity in the mesocosm-kept mat. For these reasons we must refer to the number of unique species as a minimum value for the local Chloroflexaceae community rather than an absolute community composition structure.

The GN showed highest diversity of representatives in all but one clusters. It may be that other examined environments of this study are as diverse as GN and only lower cloning effort (i.e. 96 clones per site) is responsible for seemingly poorer biodiversity. On the other hand, LC showed lowest biodiversity of dominant Chloroflexaceae species – a mat where chemical composition of the water is significantly different from GN and AD (Jonkers *et al.*, 2003). This may have restricted succession of air-born and/or anthropogenic introduction of additional Chloroflexaceae members to the lake. The fact that the lake is isolated and geographically remote from other water bodies may as well have contributed to its lower Chloroflexaceae diversity. In contrast, at GN and AD occasional flooding with seawater or wind-carried droplets from the sea could potentially have introduced additional Chloroflexaceae members from more remote regions. It may consequently be that geographical isolation is responsible for the lower diversity found in LC, and geographical inclusion is perhaps the reason, sequences from GN are more dispersed throughout the phylogenic tree.

Furthermore, albeit all mats were situated in a hypersaline environment, other environmental differences may have caused variations in Chloroflexaceae diversity. While the LC mat is characterized by a 1-mm thick compact green-dark layer covering the surface, the MM surface layer was 1-cm thick and consisted of differently colored layers. This difference was likely caused by variations in dynamics of physico-chemical gradients, e.g. oxygen and sulfide gradients influenced respectively by light intensity and (internal) carbon cycling.

A striking outcome of this study is that all sequences acquired in this study were most closely related to *Candidatus* Chlorothrix halophila. The high diversity amongst *Candidatus* Chlorothrix relatives indicates that the Chloroflexaceae hypersaline lineage is under-represented with a single isolated species. According to previous (e.g. Nübel et al 2001) and our study, it seems that environmental sequences from hypersaline mats around the world are most closely related to the genus *Candidatus* Chlorothrix.

Local species assemblages can be interpreted as the consequence of successive filters acting on the regional species pool. These filters, represented by climatic conditions, disturbance regime (e.g. bio-turbulence) and biotic interactions, result in a specific local assemblage that is a non-random, quantitative and qualitative, subset of species from the regional pool (Schmid *et al.*, 2002). For this reason, larger sequencing effort would probably reveal presence of more species that are less dominant and thus invisible in our experimental setup. Eventually, perhaps everything will be everywhere, but it may possibly take a bacterium to cross the sea from the North Pole to the South Pole, faster than it would take it to get into a secluded lake on land. Transfer rate from one location to the other and from one

geographically "isolated" ecosystem to another (e.g. Lake Chiprana vs. Guerrero Negro and Dubai) is hard to predict.

Acknowledgements

A. Bachar was supported by a grant (DFG JO-412) from the German Research Foundation.

References

ABED, R. M., KOHLS, K. & DE BEER, D. (2007) Effect of salinity changes on the bacterial diversity, photosynthesis and oxygen consumption of cyanobacterial mats from an intertidal flat of the Arabian Gulf. *Environmental Microbiology,* **9,** 1384-92.

ABED, R. M., KOHLS, K., SCHOON, R., SCHERF, A. K., SCHACHT, M., PALINSKA, K. A., AL-HASSANI, H., HAMZA, W., RULLKOTTER, J. & GOLUBIC, S. (2008) Lipid biomarkers, pigments and cyanobacterial diversity of microbial mats across intertidal flats of the arid coast of the Arabian Gulf (Abu Dhabi, UAE). *FEMS Microbiol Ecology*.

BACHAR, A., OMOREGIE, E., DE WIT, R. & JONKERS, H. M. (2007) Diversity and function of *Chloroflexus*-like bacteria in a hypersaline microbial mat: phylogenetic characterization and impact on aerobic respiration. *Applied and Environmental Microbiology,* **73,** 3975-83.

BACHAR, A., POLERECKY, L., FISCHER, J. P., VAMVAKOPOULOS, K., DE BEER, D. & JONKERS, H. M. (2008) Two-dimensional mapping of photopigment distribution and activity of Chloroflexus-like bacteria in a hypersaline microbial mat. *FEMS Microbial Ecology*.

COLE, J. R., CHAI, B., FARRIS, R. J., WANG, Q., KULAM-SYED-MOHIDEEN, A. S., MCGARRELL, D. M., BANDELA, A. M., CARDENAS, E., GARRITY, G. M. & TIEDJE, J. M. (2007) The ribosomal database project (RDP-II): introducing myRDP space and quality controlled public data. *Nucleic Acids Research,* **35,** D169-D172.

D'AMELIO, E. D., Y. COHEN & DES MARAIS, D. J. (1989) Comparative functional ultrastructure of two hypersaline submerged cyanobacterial mats: Guerrero Negro, Baja California Sur, Mexico, and Solar Lake, Sinai, Egypt. *Microbial mats physiological ecology of benthic microbial communities.* (ed. by Y. COHEN & E. ROSENBERG), pp.97-103. American Society for Microbiology, Washington, D.C.

DE WIT, R. & BOUVIER, T. (2006) 'Everything is everywhere, but, the environment selects'; what did Baas Becking and Beijerinck really say? *Environmental Microbiology,* **8,** 755-758.

ECK, R. V. & DAYHOFF, M. O. (1966) *Atlas of Protein Sequence and Structure*. National Biomedical Research Foundation, Silver Springs, Maryland.

HANADA, S., HIRAISHI, A., SHIMADA, K. & MATSUURA, K. (1995) *Chloroflexus aggregans* sp. nov., a filamentous phototrophic bacterium which forms dense cell aggregates by active gliding movement. *International Journal of Systematic Bacteriology,* **45,** 676-81.

HANADA, S. & PIERSON, B. K. (2006) The Family Chloroflexaceae. *The Prokaryotes: an evolving electronic resource for the microbiology community.* (ed. by S. F. MARTIN DWORKIN, EUGENE ROSENBERG, KARL-HEINZ SCHLEIFER AND ERKO STACKEBRANDT), pp.815-842. Springer-Verlag, New York.

HANADA, S., TAKAICHI, S., MATSUURA, K. & NAKAMURA, K. (2002) Roseiflexus castenholzii gen. nov., sp nov., a thermophilic, filamentous, photosynthetic bacterium that lacks chlorosomes. *International Journal of Systematic and Evolutionary Microbiology,* **52,** 187-193.

ISENBARGER, T. A., FINNEY, M., RIOS-VELAZQUEZ, C., HANDELSMAN, J. & RUVKUN, G. (2008) Miniprimer PCR, a new lens for viewing the microbial world. *Applied and Environmental Microbiology,* **74,** 840-849.

JONKERS, H. M., LUDWIG, R., DE WIT, R., PRINGAULT, O., MUYZER, G., NIEMANN, H., FINKE, N. & DE BEER, D. (2003) Structural and functional analysis of a microbial mat ecosystem from a unique permanent hypersaline inland lake: 'La Salada de Chiprana' (NE Spain). *FEMS Microbiology Ecology,* **44,** 175-189.

KEPPEN, O. I., TOUROVA, T. P., KUZNETSOV, B. B., IVANOVSKY, R. N. & GORLENKO, V. M. (2000) Proposal of Oscillochloridaceae fam. nov, on the basis of a phylogenetic analysis of the filamentous anoxygenic phototrophic bacteria, and emended description of Oscillochloris and Oscillochloris trichoides in comparison with further new isolates. *International Journal of Systematic and Evolutionary Microbiology,* **50,** 1529-1537.

LEFEBVRE, O., VASUDEVAN, N., THANASEKARAN, K., MOLETTA, R. & GODON, J. J. (2006) Microbial diversity in hypersaline wastewater: the example of tanneries. *Extremophiles*, **10**, 505-513.

LEY, R. E., HARRIS, J. K., WILCOX, J., SPEAR, J. R., MILLER, S. R., BEBOUT, B. M., MARESCA, J. A., BRYANT, D. A., SOGIN, M. L. & PACE, N. R. (2006) Unexpected diversity and complexity of the Guerrero Negro hypersaline microbial mat. *Applied and Environmental Microbiology,* **72,** 3685-95.

MACK, E. E. & PIERSON, B. K. (1988) Preliminary characterization of a temperate marine member of the Chloroflexaceae. *Green Photosynthetic Bacteria.* (ed. by J. M. OLSON, J. G. ORMEROD, J. AMESZ, E. STACKEBRANDT & H. G. TRÜPER), pp.237–241. Plenum Publishing, New York, NY.

MARTINY, J. B. H., BOHANNAN, B. J. M., BROWN, J. H., COLWELL, R. K., FUHRMAN, J. A., GREEN, J. L., HORNER-DEVINE, M. C., KANE, M., KRUMINS, J. A., KUSKE, C. R., MORIN, P. J., NAEEM, S., OVREAS, L., REYSENBACH, A. L., SMITH, V. H. & STALEY, J. T. (2006) Microbial biogeography: putting microorganisms on the map. *Nature Reviews Microbiology,* **4,** 102-112.

NEI, M. & KUMAR, S. (2000) *Molecular Evolution and Phylogenetics*. Oxford University Press, New York.

NÜBEL, U., BATESON, M. M., MADIGAN, M. T., KUHL, M. & WARD, D. M. (2001) Diversity and distribution in hypersaline microbial mats of bacteria related to Chloroflexus spp. *Applied and Environmental Microbiology,* **67,** 4365-71.

PIERSON, B. K. & CASTENHOLZ, R. W. (1971) Bacteriochlorophylls in gliding filamentous prokaryotes from hot springs. *Nature New Biology,* **233,** 25-7.

PIERSON, B. K. & CASTENHOLZ, R. W. (1974) A phototrophic gliding filamentous bacterium of hot springs, Chloroflexus aurantiacus, gen. and sp. nov. *Archives of Microbiology,* **100,** 5-24.

PIERSON, B. K., GIOVANNONI, S. J., STAHL, D. A. & CASTENHOLZ, R. W. (1985) Heliothrix-Oregonensis, Gen-Nov, Sp-Nov, a Phototrophic Filamentous Gliding Bacterium Containing Bacteriochlorophyll-A. *Archives of Microbiology,* **142,** 164-167.

PIERSON, B. K., VALDEZ, D., LARSEN, M., MORGAN, E. & MACK, E. E. (1994) Chloroflexus-like organisms from marine and hypersaline environments: distribution and diversity. *Photosynthesis Research***,** 35-52.

POLERECKY, L., BACHAR, A., SCHOON, R., GRINSTEIN, M., JORGENSEN, B. B., DE BEER, D. & JONKERS, H. M. (2007) Contribution of Chloroflexus respiration to oxygen cycling in a hypersaline microbial mat from Lake Chiprana, Spain. *Environmental Microbiology,* **9,** 2007-2024.

POSADA, D. & CRANDALL, K. A. (1998) MODELTEST: testing the model of DNA substitution. *Bioinformatics,* **14,** 817-8.

ROSSELLO-MORA, R. & AMANN, R. (2001) The species concept for prokaryotes. *FEMS Microbiology Reviews,* **25,** 39-67.

RZHETSKY, A. & NEI, M. (1992) A simple method for estimating and testing minimum evolution trees. *Molecular Biology and Evolution,* **9,** 945-967.

SAITOU, N. & NEI, M. (1987) The neighbor-joining method: a new method for reconstructing phylogenetic trees. *Molecular Biology and Evolution,* **4,** 406-25.

SCHMID, B., J. JOSHI & SCHLAPFER, F. (2002) Empirical evidence for biodiversity-ecosystem functioning relationships. *The Functional Consequences of Biodiversity: Empirical Progress and Theoretical Extensions. Monographs in Population Biology.* (ed. by A. P. KINZIG, S. W. PACALA & D. TILMAN), pp.120-150. Princeton University, Princeton, NJ.

SORENSEN, K. B., CANFIELD, D. E., TESKE, A. P. & OREN, A. (2005) Community composition of a hypersaline endoevaporitic microbial mat. *Applied and Environmental Microbiology,* **71,** 7352-65.

STACKEBRANDT, E. & GOEBEL, B. M. (1994) Taxonomic note: a place for DNA-DNA reassociation and 16S rRNA sequence analysis in the present species definition in bacteriology. *International Journal of Systematic Bacteriology***,** 846-849.

STOLZ, J. F. (1990) Distribution of phototrophic microbes in the flat laminated microbial mat at Laguna Figueroa, Baja California, Mexico. *Biosystems,* **23,** 345-57.

TAMURA, K., DUDLEY, J., NEI, M. & KUMAR, S. (2007) MEGA4: Molecular Evolutionary Genetics Analysis (MEGA) software version 4.0. *Molecular Biology and Evolution,* **24,** 1596-9.

TAMURA, K., NEI, M. & KUMAR, S. (2004) Prospects for inferring very large phylogenies by using the neighbor-joining method. *Proceedings of the National Academy of Sciences,* **101,** 11030-11035.

VENETSKAYA, S. L. & GERASIMENKO, L. M. (1988) Electron microscopic study of microorganisms in a halophilic cyanobacterial community. *Microbiology,* **57,** 377-383.

WHITFIELD, J. (2005) BIOGEOGRAPHY: Is Everything Everywhere? *Science,* **310,** 960-961.

Chapter VI:

Discussion, conclusions and perspectives

Discussion, conclusions and perspectives

Photosynthetic microbial mats are interesting subjects for study due to several reasons: it is a common believe that such bacterial communities covered the planet and played significant roles in the development of ancient oceanic and atmospheric conditions, particularly development of atmospheric oxygen concentrations. Studies of modern mats may shed light on the impact of ancient microbial communities on biogeochemical cycles which affected ancient and still affect present environments. The harsh environmental conditions under which microbial mats are nowadays (due to the rise of predatory organisms) usually established are distinctive habitats for extremophyles – in a way such extreme organisms/conditions are expected to be found on e.g. Mars or Titan moon. The study and development of scientific tools and ideas regarding such environments may therefore also be crucial for the further investigation and understanding of extraterrestrial habitats. Furthermore, mats may be used for technological purposes such as bioremediation of contaminated soils and/or water bodies (Lovley, 2003). Microbial complex communities are often used in land farming, bioreactors, composting, bioaugmentation, rhizofiltration, biostimulation and more. Other applicable aspects of microbial community studies, except for sheer scientific knowledge acquisition, are energy conservation and medical compound research. For these reasons and more it is important to further develop scientific tools for microbial community investigation.

Indeed, during the research presented in this thesis, at which *Chloroflexus*-like bacteria (CLB), the phototrophic members of the Chloroflexi phylum i.e. Chloroflexaceae Family, the dual aim was to further develop advanced scientific techniques and to apply these to unravel eco-physiological impacts of CLB on microbial community processes and on the environment. This resulted in the publication and submission of the following manuscripts: (Bachar, Jonkers, submitted; Bachar *et al.*, 2007; Bachar *et al.*, 2008; Polerecky *et al.*, 2007). This research program aimed to continue investigations on the mats of Lake Chiprana following the study of Jonkers et al. 2003 which established some general structural and functional analysis of the microbial mat ecosystem of the lake. In chapter II (Bachar *et al.*, 2007) we established the functionality and diversity of CLB in the

Chiprana mats: in this study some of the phylogenetic variation and the impact of CLB aerobic respiration on total community respiration were reported. We encountered four different phylotypes (sharing less than 96% 16S rRNA sequence similarity) apparently related to filamentous anoxygenic phototrophic CLB. In chapter V the CLB community diversity of the lake was further established, and here it was discovered that the CLB community of this, but also other distinct hypersaline microbial mats was dominated by a specific group of phylotypes closely related to the previously proposed new species '*Candidatus* Chlorothrix halophila' (Bachar, Jonkers, submitted). Besides the established high diversity of Chloroflexaceae phylotypes, also the major proportion of CLB related pigments Bacteriochlorophyll c and γ-carotene found in the mat, pointed to the light harvesting importance and hence ecological significance of the Chloroflexaceae Family in the Chiprana mats. The demonstrated near infrared (NIR) light dependent shift of the microbial community from photosynthesis to aerobic respiration could be attributed to CLB. In that study we pointed out, for the first time, that application of non-oxygenic NIR light (e.g. 740nm) drastically increased oxygen concentrations in the mat due to CLB ability to switch between aerobic respiration in the absence of NIR light to anoxygenic photosynthesis in its presence. We concluded that CLB play a significant role in the cycling of carbon in the studied mat and demonstrated a microsensor based methodology for rapid establishment of the presence and significance of CLB in environmental samples.

In a follow-up study the NIR light dependent physiology of CLB was further investigated and quantified (Polerecky *et al.*, 2007). I developed an idea based on the light-dark shift method (Revsbech, Jørgensen, 1983) to measure the *initial* oxygen uptake by CLB due to the shift from NIR presence to its absence: when NIR light is available, CLB would use it for photosynthesis as their "preferable" energy acquisition system, rather than respiration. When NIR light is shut off, anoxygenic photosynthesis stops and oxygen is immediately being uptake. In other words , if NIR light is absent, CLB could respire oxygen; when NIR light is added they will stop or reduce their oxygen uptake for respiration and use the light for photosynthesis (see Chapter II, Fig 4a). This rapid and simple method may be considered as an *In situ* measurement of CLB activity in mats: it indicates how much of the oxygen is consumed by CLB under dark conditions and reflect the *In situ* "preference" of CLB to photosynthesis over respiration. With no available hypersaline CLB culture, this

method is highly valuable in measuring respiration and photosynthetic rate of the CLB community, and hence it's ecological importance. By the good help of Dr. Polerecky, a mathematical model was designed for the conceptual and principal observations measured (see "basic theory" section in Chapter III).

In order to have an independent reference measurement of oxygen demand of the mat under different light conditions, further investigation of the relationship between photosynthesis, light and respiration was measured using membrane inlet mass spectrometry which basically showed a similar inhibition of respiration due to light quality. We concluded that, under the used experimental conditions, CLB were potentially responsible for almost all respiration in the studied mats upper few millimeters. It is not suggested that in practice all oxygen is consumed by CLB in the upper photic zone; other oxygen-consuming organisms/processes are present and contribute as well to oxygen consumption: in nature, ambient light intensities are 1-2 orders of magnitude higher than those we used (due to method limitations), which allow much higher oxygen production levels during daytime and hence CLB can/do not consume it all. Other present aerobes may have lower affinities for oxygen and will only start to contribute significantly to community aerobic respiration at higher oxygen concentrations (practically conditions of supersaturating oxygen levels during mid daytime,) at which we do not really know how CLB behave. We know that CLB would "prefer" photosynthesis over respiration and that the two processes may compete on the same electron transfer chain, hence blocking one of the processes while allowing the other to proceed (see introduction). On the other hand during high light levels, when oxygen is saturating, free sulfides, the common electron donors for photosynthesis, may not be available for CLB. Conditions used in the experimental setup may best mimic early morning or evening conditions, times that were suggested before at which CLB may be most active at.

This observation is of major importance for past and future studies employing the traditional light-dark shift method since significant overestimation of photosynthesis may be caused by CLB community, depending on the used light source: if full sunlight spectra is used (from ultra violet to infrared) CLB, if present, may cause severe overestimation of community oxygenic photosynthetic rate. This stresses the need of using 400-700nm light for more accurate oxygenic photosynthesis measurements using the light-dark shift method.

It is still not fully clear which physiological process is employed by CLB during mid day in the mat. Some suggestions were made in Chapter IV where spatial characterization of CLB was explored: it seems that CLB distribution is arranged in patches (see e.g. Chapter IV Fig. 6b), maybe congruent with the distribution of sulfide pockets produced by dense aggregates of sulfate-reducing bacteria. Both functional groups of bacteria could benefit from such a spatial organization. Sulfate-reducing bacteria produce sulfides providing CLB with a preferred electron donor while simultaneously CLB could scavenge oxygen what would otherwise be inhibitory to sulfate-reducing bacteria. In order to better understand the In-situ physiology of CLB during a 24 hour cycle, I suggest future examination of this topic to consider radioisotopes and FISH (MAR-FISH) as possible testing method: with this method direct carbon fixation (organic or inorganic) can be attributed to CLB in a quantitative manner – what may indicate the actual metabolism of this group during daytime. Isolation of hypersaline CLB strains will help significantly in understanding metabolic rates of this group and in particular the relation between oxygen consumption to photosynthetic production under different light regimes.

In a complex system characterized by steep biogeochemical gradients (oxygen, sulfide, light, pH etc') elucidation of the spatial distribution of bacteria could contribute to the clarification of their in situ physiology. Organisms are expected to dominate niches where the combined set of environmental conditions is close to their optimal physiological requirements. My colleagues and I combined several independent methods and elucidated for the first time that CLB aggregate or settle in particular patches or layers in the upper photosynthetic mat. The straight-forward FISH and two-dimensional oxygen distribution showed spatial distribution of CLB in the intact mat, using specific genetic markers and light conditions, respectively. The distinct and ordered spatial distribution of different CLB species was further supported by spatial pigment distribution. From the second chapter of this thesis (Bachar *et al.*, 2007) we already knew that CLB related pigments are relatively highly abundant in our examined hypersaline mat, and now we discovered that most of it is concentrated in discrete locations at the upper photic/oxic zone of the mat (Bachar *et al.*, 2008). We further noticed some species-specific depth distributions of the Chloroflexi Phylum in the studied mat, using denaturing gradient gel electrophoresis (DGGE, unpublished data). The latter observation of species specific depth

distribution of Chloroflexi, the diversity of phylotypes acquired in a clone library (Chapter II), and the different and non overlapping FISH signals of 2 Chloroflexaceae members in the mat (Chapter IV) indicate that besides *Candidatus* Chlorothrix halophila other oxygen-respiring CLB are present in hypersaline mats.

Throughout the entire work microsensors were of major importance as they provided rapid and accurate measurements of the chemistry of the mat as well as characterized biogeochemical processes in the different mat layers. The latter study (Chapter IV) in which the spatial distribution of CLB and oxygen producing bacteria in a microbial mat was investigated, demonstrated the importance of high resolution tools as microsensors. The advantages and shortcomings of this tool were previously discussed e.g. (Santegoeds *et al.*, 1998) and one conclusion is that the combination of molecular and microsensor techniques enable *In situ*, localization and determination of the abundance and activity of present microorganisms. The individual methods bear high potential but it is particularly the combination of techniques that allows clarification of the structure and function of microbial communities in their natural environment (Amann, Kuhl, 1998). I learned to appreciate as well as suspect this wonderful tool and glad I had the opportunity to experiment with it during my time in the MPI.

Chapter V describes the construction of clone libraries of three geographically remote hypersaline microbial mats and the comparison of these with a fourth, previously characterized mat (Bachar, Jonkers, submitted). We discovered that Lake Chiprana harbors several dozens of unique CLB phylotypes, questioning whether these represent different species, each with a specific functional role in the mat. In this first biogeographic study concerning Chloroflexaceae members we showed that hypersaline CLB form a clad phylogenetically separated from previously characterized non-hypersaline species. The obtained phylotypes from different hypersaline mats (Spain, Germany, United Arab Emirates and Mexico) appeared phylogenetically closer related to the previously characterized chlorosome-bearing and hypersaline strain *'Candidatus* Chlorothrix halophila' than any other isolated bacterium. These results thus indicate that hypersaline mats are dominated by a specific phylogenetic group of Chloroflexaceae. Future studies should focus on the isolation and physiological characterization of members from this specific group to clarify possible functional similarities or differences with dominant CLB members in

non-hypersaline mats. It was an interesting observation to find that some hypersaline CLB are apparently cosmopolitan as they were found in distinct mats located on three continents, while others appear endemic to specific locations, although the latter observation needs further studies (cloning effort) to substantiate this conclusion. I would also recommend using Lake Chiprana as a case study for evolutionary question since it is a unique isolated hypersaline ecosystem with unique chemical composition. It is highly interesting to compare species and genes that may be endemic for this lake to other environments. Our CLB phylogenetic study shows the potential of the secluded lake and we hope it will attract further bioinformatics studies of CLB and other bacteria as well.

I conclude that the Chloroflexaceae Family is an interesting group of organisms, and that particularly of its hypersaline members many eco-physiological features remain to be clarified. Isolation of more members of this family will further clarify the relation between phylogeny and functionality, as suggested in Chapter V. *In situ* study of CLB carbon uptake, using radioisotopes and FISH may be applied in order to directly measure CLB donation to carbon turnover in the mat. Furthermore, quantitative analysis of 16S gene copy using specific CLB primers can give real numbers of present (DNA-qPCR) or active (RNA/cDNA-qPCR) and "*per capita*" calculations of e.g. O_2 or C uptake, what would allow comparison to other mat members. Future eco-physiological characterization of CLB in non-aquatic or non-illuminated environments such as soil- and deep sea habitats respectively, will enable comparison with photosynthetic mat species, what could provide better insights into biogeographic-, phylogenetic- and evolutionary aspects and relationships. With respect to Lake Chiprana I regret not having the time of applying CLB specific DGGE and terminal restriction fragment length polymorphism (TRFLP), two independent methods that will better support our knowledge of CLB biodiversity in the lake. I recommend a follow-up study of the one described in Chapter V following three directions: (1) TRFLP/DGGE examination of CLB in the 4 mats considerate, for a better view of CLB biodiversity and comparison of their biogeography; (2) quantitative analysis using CLB specific primers to measure both presence and activity, both as a biogeographic study in remote hypersaline environments and within a single mat under different depths; (3) a general estimation of biodiversity (bacteria,

Archaea and Eukarya) in Lake Chiprana, in addition to what was already done by Jonkers et al. (2003).

This ancient and ubiquitous phototroph should and needs to be investigated for it is both a window to antique times and a valuable objective for the days to come We hope that the above studies will continue the traditional isolation and cultivation, characterization studies of CLB, that started at the early 1970's, and reinforce the basis of future studies. The study of extremophiles and especially CLB that are close to the root of the tree of life, may lead us closer to understanding the origin of life on earth since these life forms deal today with an environment all life had to deal with in the beginning of life on earth. The used term "living fossils" well represent organisms that live in extreme environment and struggle, in addition to competition on natural resources, also harsh physical/chemical conditions. Scientific methods developed and applied for extreme environments are probably most relevant for life expeditions on March and Titan in which extreme temperatures and chemical compositions are reported: it was only this year (August 2008) proven that water is present in the soil of March's north pole, where temperatures are constantly below zero (Celsius), the atmosphere is thin and no sign of life is detected by chemical analysis nor microscopic observations of the soil. In such extreme conditions we will probably find life forms, if present, with similar adaptations as those of our poles. The Titan moon has methane lakes and rivers that may support life in a similar manner as in methane seeps in the bottom of our oceans. These and more indications of possible life supporting conditions are present naturally here on earth and biogeochemical studies of such, may contribute significantly when life will be discovered out of earth. High temperatures, very high or very low pH, hypersalinity, extreme pressures and extreme low energy receiving ecosystems are typical environmental properties of other planets and may mimic the conditions on ancient earth at times when life was assumedly formed. If we will know how to study and understand extreme environments and organisms that live in them we will get a glimpse of the past and tools for the future.

REFERENCE

Amann R, Kuhl M (1998) *In situ* methods for assessment of microorganisms and their activities. *Current Opinion in Microbiology* **1**, 352-358.

Bachar A, Jonkers HM (submitted) A first survey on the *Chloroflexaceae* Family community structure of four hypersaline microbial mats from three continents. *Journal of Biogeography*.

Bachar A, Omoregie E, de Wit R, Jonkers HM (2007) Diversity and function of *chloroflexus*-like bacteria in a hypersaline microbial mat: phylogenetic characterization and impact on aerobic respiration. *Applied and Environmental Microbiology* **73**, 3975-3983.

Bachar A, Polerecky L, Fischer JP, Vamvacopoulos K, de Beer D, Jonkers HM (2008) Two dimensional mapping of photopigment distribution and activity of Chloroflexus like bacteria in a hypersaline microbial mat. *FEMS Microbiology and Ecology.*

Lovley DR (2003) Cleaning up with genomics: applying molecular biology to bioremediation. *Nature Reviews in Microbiology* **1**, 35-44.

Polerecky L, Bachar A, Schoon R, Grinstein M, Jorgensen BB, de Beer D, Jonkers HM (2007) Contribution of Chloroflexus respiration to Oxygen cycling in a hypersaline microbial mat from Lake Chiprana, Spain. *Environmental Microbiology* **in press**

Revsbech NP, Jørgensen BB (1983) Photosynthesis of Benthic Microflora Measured with High Spatial-Resolution by the Oxygen Microprofile Method - Capabilities and Limitations of the Method. *Limnology and Oceanography* **28**, 749-756.

Santegoeds CM, Schramm A, de Beer D (1998) Microsensors as a tool to determine chemical microgradients and bacterial activity in wastewater biofilms and flocs. *Biodegradation* **9**, 159-167.

Ami Bachar's List of publications:

1) **Bachar, A**.; Omoregie, E.; de Wit, R.; Jonkers, H. M. (2007) Diversity and function of *Chloroflexus*-like bacteria in a hypersaline microbial mat: Phylogenetic characterization and impact on aerobic respiration. 73 (12), 3975-3983 Applied and Environmental Microbiology.
2) Polerecky, L.; **Bachar, A**.; Schoon, R.; Grinstein, M.; Jorgensen, B. B.; de Beer, D.; Jonkers, H. M. (2007) Contribution of *Chloroflexus* respiration to oxygen cycling in a hypersaline microbial mat from Lake Chiprana, Spain. 9 (8), 2007-2024 Environmental Microbiology.
3) **Bachar, A**.; Polerecky, L.; Fischer, J. P.; Vamvakopoulos, K.; de Beer, D.; Jonkers, H. M. (2008) Two-dimensional mapping of photopigment distribution and activity of *Chloroflexus*-like bacteria in a hypersaline microbial mat. 65 (3), 434-448 FEMS Microbiology Ecology.

Submitted manuscripts:

4) **Bachar, A** and Jonkers H. M. (submitted) A first survey on the community structure of Chloroflexaceae Family from four hypersaline microbial mats located on three continents. Journal of Biogeography.